Function of YjeE and Ribosome Assembly Factors

A STUDY OF THE *ESCHERICHIA COLI* YJEE PROTEIN AND RIBOSOME ASSEMBLY FACTORS

BY

CHAND SINGH MANGAT, B.SC.

A Thesis
Submitted to the School of Graduate Studies
in Partial Fulfillment of the Requirements
for the Degree
Doctor of Philosophy

McMaster University

© by Chand Singh Mangat, July 2012

DOCTOR OF PHILOSOPHY (2012) McMaster University
(Biochemistry and Biomedical Sciences) Hamilton, Ontario

TITLE: **A Study of the *Escherichia coli* YjeE Protein and Ribosome Assembly Factors**

AUTHOR: Chand Singh Mangat, B.Sc. (McMaster University)

SUPERVISOR: Professor E.D. Brown

NUMBER OF PAGES: ix, 116

ABSTRACT

Antibiotic resistance in bacterial pathogens is reducing the efficacy of current antibacterials; thus, the identification of novel antibacterial targets and inhibitors is crucial. Using the model organism *Escherichia coli*, we discuss herein two novel antimicrobial targets: namely, the protein YjeE and the process of ribosome assembly.

YjeE is essential for viability in bacteria, widely conserved amongst bacterial pathogens and has no human homologue. We searched for a small molecule probe of the function of YjeE to help circumvent the inadequate genetic tools that are available for studying this protein. Sensitive methods for detecting ligand binding were optimized; however, this effort yielded no inhibitors. A second approach to studying the function of YjeE was the development of a reporter using a promoter that is directly upstream of *yjeE* in *E. coli*. The activity of this promoter was tested in the presence of small molecules of known function and in diverse gene deletion backgrounds. We found that YjeE was linked to the inhibition of DNA and protein translation as well as central metabolism and respiration. These interactions prompted experiments that revealed YjeE to be dispensable under anaerobic conditions.

Many antibiotics target the ability of the ribosome to carry out protein synthesis; however, no current antibiotics target the process of ribosome biogenesis. In order to identify new biogenesis factors, the non-essential fraction of the *E. coli* genome was screened for deletions that gave rise to cold-sensitive growth. We found that genes associated with ribosome function were the most represented cold sensitive factors amongst the genes of known function. We identified and present here two new putative ribosome biogenesis factors, *prfC* and *ychF*, which had phenotypes associated with ribosome assembly defects.

ACKNOWLEDGMENTS

I thank Dr. Eric Brown for his steadfast support and advice throughout my graduate career. I thank my Committee Members for their guidance of this work and valuable career advice. I am deeply indebted to my family for their encouragement. To my labmates, I thank you for cleaning up hazardous materials.

Finally, I thank my wife Amrita for her constant support and confidence in my abilities. This work and my sanity would not have been possible without her love and patience.

Table of Contents

LIST OF FIGURES

LIST OF TABLES

LIST OF ABBREVIATIONS AND SYMBOLS

A-site	amino acyl-tRNA binding site
ADP	adenosine-5`-diphosphate
ATP	adenosine-5`-triphosphate
Amp	ampicillin
ASMS	affinity selection mass spectrometry
BODIPY	4,4-difluoro-4-bora-3a-4a-diaza-*s*-indacene
BSA	bovine serum albumin
DHFR	dihydrofolate reductase
DTT	dithiothreitol
E-site	exit-tRNA binding site
EDTA	ethylenediaminetetraacetic acid
FP	fluorescence polarization
GDP	guanosine-5`-diphosphate
GTP	guanosine-5`triphosphate
IPTG	isopropyl β-D 1-thiogalactopyranoside
Kan	kanamycin
K_D	dissociation constant
K_M	Michaelis-Menten constant
LB	Luria-Bertani
LPS	Lipopolysaccharide
MANT	2′/3′-O-N-methylanthraniloyl
Nt	nucleotides
NTP	nucleotide triphosphate
iNTP	initiator nucleotide triphosphate
mP	millipolarization
P-loop	phosphate-binding loop
P-site	peptidyltransferase-tRNA binding site
PBS	phosphate buffered saline
ppGpp	guanosine-5`-diphosphate-3`-diphosphate
RP	reverse phase
RF	Release factor
r-protein	ribosomal protein
rRNA	ribosomal RNA
SEC	size exclusion column chromatography
SDS-PAGE	sodium dodecyl sulphate polyacrylamide gel electrophoresis
Spec	spectinomycin
Tet	tetracycline
TRAFAC	translation factor associated class
Tris	2-amino-2-hydroxymethyl-propane-1,3-diol
TR	Texas red
UF	ultrafiltration

1 CHAPTER ONE INTRODUCTION

1.1 THE NEED FOR NEW ANTIBIOTICS

The human body is a habitat for communities of bacteria that outnumber human cells by ten to one [1]. Modern sequencing techniques have enabled us to survey the great variety of organisms that we share our bodies with. The skin is colonized by a mixture of *Propionibacterineae*, *Corynebacterineae*, *Staphylococci* and other bacteria in proportions that are exquisitely unique to the sampling site. The one to two kilograms of bacteria that reside in the gut consist of a dense population of *Streptococci*, *Bacteroides* and many other species whose collective genomic content is greater than our own [1-3].

Among the many benign bacterial species that colonize humans are also those that cause disease. Robert Koch discovered the relationship between bacteria and disease when he observed that the injection of anthrax-contaminated blood caused sepsis and death in mice [4]. Koch's later work with tuberculosis formalized the causal relationship between disease and bacteria with his now famous postulates. This work was awarded the Nobel Prize in medicine in 1905 [5-7]. Koch studied acute bacterial infections that caused strong symptoms. Bacteria are now known or suspected to be the cause of a growing list of chronic conditions, such as psoriasis [8], obesity [9], multiple sclerosis [10], peptic ulcers and other inflammatory diseases [11]. The unexpected discovery that *Helicobacter pylori* was the causative agent of peptic ulcers was awarded the 2005 Nobel prize in medicine, 100 years after Koch was awarded his prize [12].

While Koch established the cause of infectious diseases, his contemporary Paul Ehrlich worked on identifying therapies. Ehrlich proposed that "chemoreceptors" had a specific relationship or "avidity" with small molecules, which separated them from non-specific antiseptics [13]. He was a proponent of a paradigm of drug discovery that is followed to this day, which is to screen many molecules for a desired bioactivity and refine the structure of the inhibitor to increase potency. Ehrlich's insights ushered in the age of antibiotics beginning with the discovery of the first broadly acting and commercially availably chemotherapy against bacteria, the sulphanilamide Prontosil [14]. The majority of currently used antibiotics were discovered in the following decades, the so-called "golden age" of antibiotic discovery. Antibiotics discovered during this time targeted one of four pathways: RNA, DNA, cell wall and protein synthesis [15].

1.1.1 The demise of antibiotics

The widespread use of antibiotics has led to the rise of antibiotic-resistant pathogens. Bacteria are able to circumvent the action of antibiotics in one of three major ways: degradation of the antibiotic, efflux of the antibiotic out the cell or genetic alteration of the cellular target to reduce affinity [15]. It has recently been found that antibiotic resistance is an ancient phenomenon that predates antibiotics

clinical use [16]. The rise of antibiotic resistance in clinical pathogens has caused an increasing burden on the health-care system. A survey of Canadian hospitals found that colonizations by methicillin-resistant *Staphylococcus aureus* (MRSA), a strain responsible for skin and blood infections, rose 17 fold from the year 1995 to 2007 [17]. In the United States, 18,000 deaths were attributed to MRSA in 2005, a mortality rate that is even higher than that of HIV infections [18]. Over the past decade, half of the countries in Europe observed that 20% of *E. coli* isolates were resistant to fluoroquinolone antibiotics [19].

New antibiotics are one strategy to combat the rise of antibiotic resistant pathogens; however, drug discovery efforts from large pharmaceutical companies are becoming less fruitful in this regard. A well documented "innovation gap" in antibiotic development refers to the period from the early 1960's to the 2000's when no new classes of antibiotics were introduced into the clinic [20]. The innovation problem is further exacerbated by the failure to discover new chemical scaffolds for antibiotics, since most new antibiotics are derivatives of older ones [21]. Twenty antibiotics were released for clinical use since 2000 and 18 of these were derivatives of previously known classes of antibiotics [22]. Hence, new antibacterial compounds with novel chemical scaffolds are of utmost urgency.

1.1.2 Novel antibiotics from novel biology

Most currently used antibiotics inhibit well-studied pathways. Certain aspects of bacterial physiology that are less studied may contain novel targets for antibiotics, which would help combat antibiotic resistance. These targets have been largely avoided by pharmaceutical companies, since scant knowledge of the target can slow development of the inhibitor [23]. In a target validation effort by GlaxoSmithKline (GSK), 350 genes were found to be common to *H. influenzae*, *Streptococcus pneumoniae* and *S. aureus* and a full third of those genes were of unknown function [23]. From 1995 to 2001, GSK performed 67 high-throughput screens but poorly characterized genes were avoided [23]. Despite these drawbacks, some inhibitors with novel mechanisms of action are being pursued in clinical trials. For example, molecules that target peptide deformylation, fatty acid biosynthesis, membrane disruption, ATP synthesis and amino-acyl tRNA synthesis are currently in development [22]. A better understanding of bacterial physiology and biochemistry will fuel the development of future antibiotics as it has for HIV research [24]; academic labs can play an important role in this area.

The overarching goal of this thesis is to extend our knowledge of poorly characterized aspects of bacterial physiology, which show promise as antibacterial drug targets. We studied two promising new antibacterial targets in the model organism *E. coli*. The first is the ATPase YjeE and the second is the process of ribosome assembly. An overview of the structure and function of YjeE, an enigmatic and poorly characterized protein, is provided. We also review what is known about

the synthesis of ribosomal components and the process by which they are assembled into a functioning ribosome. These processes are described for *E. coli* and all gene names are those of *E. coli*, unless otherwise specified.

1.2 YjeE AS A NOVEL ANTIBACTERIAL DRUG TARGET

Poorly characterized and essential genes that are widely distributed amongst pathogens and absent in humans are promising antimicrobial drug targets [25-27]. One such gene is *yjeE*, which is well-conserved amongst Gram-positive and Gram-negative bacteria [28]. The *yjeE* gene was found to be essential for growth and viability in genome-scale studies of several species of bacteria [29-33]. The essentiality of *E. coli yjeE* has also been demonstrated through targeted deletion on the chromosome and complementation by an ectopic copy [34]. The broad conservation, essentiality and lack of a human homologue of *yjeE* are features of an attractive antimicrobial drug target, however, its limited characterization hampers further development as such. The structure and function of YjeE are reviewed below.

1.2.1 The YjeE protein

The 1.7 Å crystal structure of *H. influenzae* YjeE was published by Teplyakov and co-workers in 2002. The structure shows that the protein has the fold of a phosphate binding loop ATPase [35]. YjeE contains canonical Walker A (G-X_4-G-K-S/T) and Walker B (R/K-$X_{(7/8)}$-Hy_4-D-X_2-G) nucleotide binding motifs, where X represents any amino acid and Hy represents any hydrophobic amino acid [36]. A protein sequence alignment of YjeE orthologues of pathogenic bacteria is presented in Figure 1-1. The Walker A and Walker B motifs are outlined. These motifs bind and position the triphosphate moiety, Mg^{2+} and H_2O in the active site. This is demonstrated in Figure 1-2A, where the conserved Walker A (red) and Walker B (green) residues are highlighted on a surface rendering of the protein. The Walker A residues are found proximal to the α and β phosphates of ADP and the Walker B residues co-ordinate the Mg^{2+} ion and the nucleophilic water.

YjeE is a mixed α / β protein with seven β-sheets in the centre, which are connected by six α -helices (Figure 1-2B). YjeE was first identified as a RecA type fold based on a similar strand order and sequence. The authors noted, however, that a single protein fold does not fully describe its architecture. The fold of YjeE is reminiscent of conserved GTPases that are involved in translation (ribosome biogenesis, maturation and translation), also known as the TRAFAC class of GTPases [37]. YjeE shares three characteristic features with this class: an absolutely conserved threonine N-terminal to β2 (Figure 1-1, marked "T"), a short linking sequence between strands β2 and β3 and antiparallel strands β3 and β4 within the conserved central domain (Figure 1-2B) [38]. Thus, YjeE is a unique hybrid protein

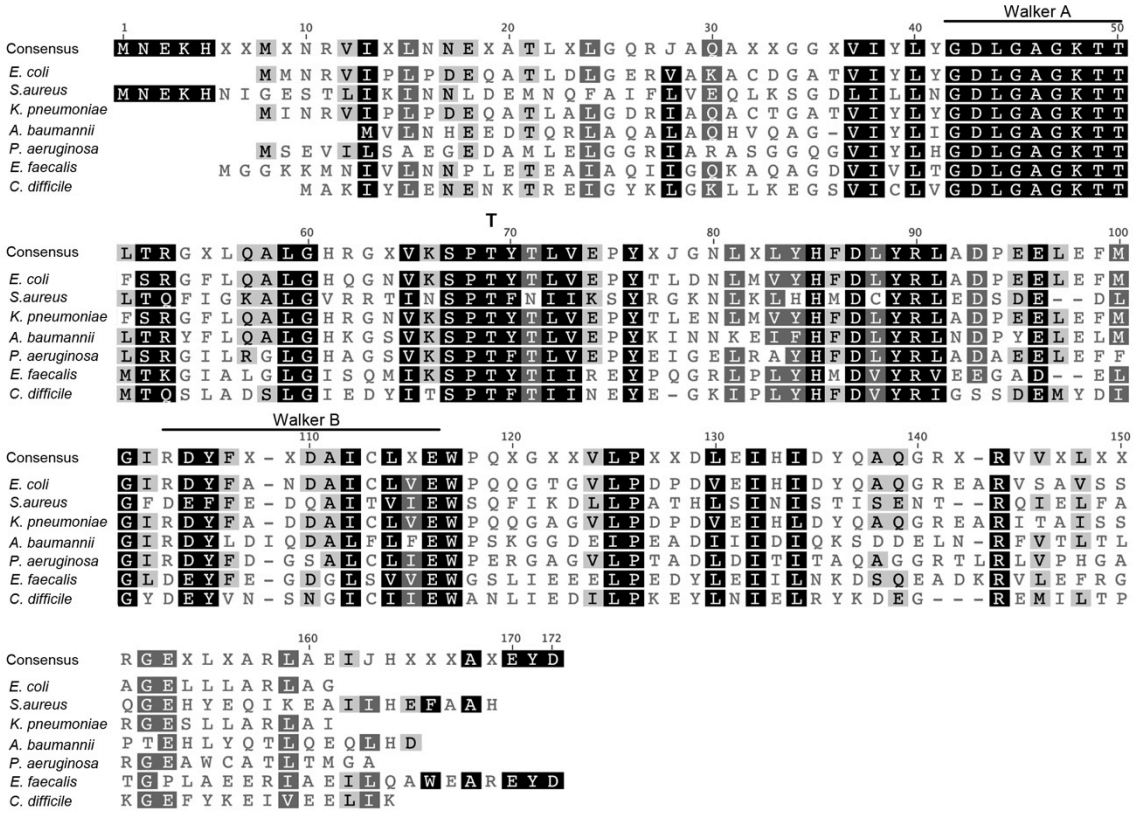

Figure 1-1. Protein sequence alignment of YjeE orthologues of pathogenic bacteria.

Conserved Walker A and B sequence motifs are indicated. Black (100%), dark grey (> 80%), light grey (> 60%) and white shading (< 60%) indicate the degree of similarity amongst sequences. The alignment was created with the Geneious version 5.5 software [39].

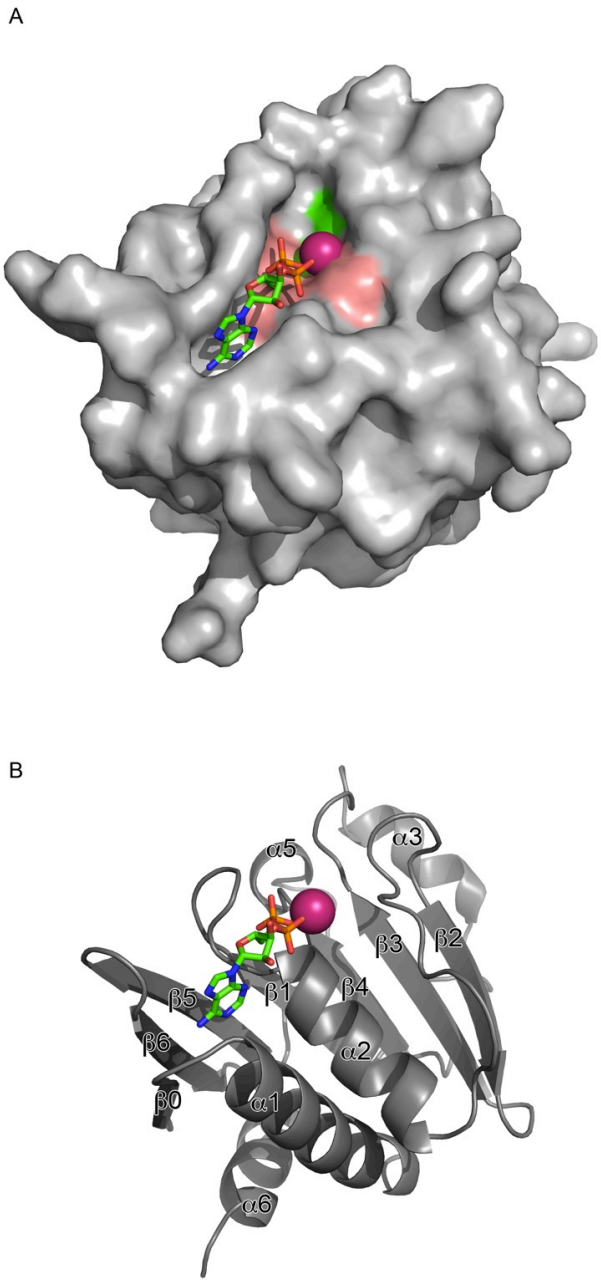

Figure 1-2. The 1.7 Å crystal structure of the *H. influenzae* orthologue (HI0065) of the YjeE protein.

ADP is shown in stick representation and the Mg^{2+} ion is shown as a magenta sphere. **(A)** Surface representation. Walker A and B motifs are indicated on the surface in red and green, respectively. **(B)** Ribbon representation. Helices and beta sheets are indicated. The figure was created with MacPymol version 1.5 software [40] using the structure solved by Teplyakov et al. [35].

that displays features of both RecA–type ATPases and translation associated GTPases.

YjeE is a P-loop NTPase [34]. An ATPase assay performed with crystallized, ultra-pure *H. influenzae* YjeE demonstrated an extremely slow ATPase activity (k_{cat} of 1 h^{-1}) [34]. Site directed mutants in the Walker A (Thr42Ala) and Walker B (Asp80Gln) motifs of the *E. coli* protein were unable to complement a conditional deletion of *yjeE* (strain EB-445, [34]). Nucleotide binding experiments have shown 8 fold and 10 fold reduction in the affinity for ADP for the Thr42Ala and Asp80Gln variants, respectively [34]. None of the variants tested were able to completely abolish the ATPase activity of the YjeE protein.

1.2.2 The cellular function(s) of YjeE

When this project began, various disparate lines of evidence implicated YjeE in stress response or adaptation to adverse environmental conditions. In a proteomic survey of *H. influenzae* grown under aerobic and anaerobic conditions, YjeE (HI0065) was found in abundance only in the aerobic condition [41]. The photosynthetic cyanobacteria *Anabaena* sp. pcc 7120 regulates cell morphology in response to nitrogen concentrations. In nitrogen deplete conditions, a fraction of cells differentiate into heterocysts, which have the ability to fix nitrogen and enrich their environment. When *hetY* (a homologue of *yjeE*) was over-expressed, differentiation was partially suppressed and when it was deleted, heterocyst morphology was abnormal [42]. Interestingly, the local concentration of oxygen is a governing factor in heterocyst development, which partially unifies observations in *Haemophilus* and *Anabaena*. This publication is also interesting because it is the only report where a homologue of *yjeE* has been deleted in the absence of complementation. Further, the lethality associated with YjeE depletion can be partially suppressed by over-expression of RstA, a two component response regulator [43]. RstA has been implicated in the regulation of anaerobic respiration, iron scavenging and nutrient responses, amongst others [44]. Furthermore, YjeE was significantly up-regulated when *E. coli* MG1655 was grown under low nutrient conditions, which mimic those found in the mouse intestinal lumen [45]. Finally, work performed in our laboratory by Dr. Ranjana Pathania revealed that over-expression of YjeE conferred up to four-fold resistance to antibiotics with diverse mechanisms of action, namely, spectinomycin, fosmidomycin, phosphomycin, cycloserine [46].

1.2.3 A newly discovered role for YjeE in tRNA modification

Recent work has implicated YjeE in a universal modification of tRNAs. YjeE, along with three other enzymes, YrdC, YdjD and YeaZ, was shown to be required for the addition of a threonylcarbamoyl moiety at the N6 position of adenine 37 of tRNA ($t6A_{37}$). This occurs for tRNAs that carry isoleucine, threonine, lysine, methionine

(not fMet-tRNA), asparagine, arginine, serine and leucine [47]. With the exception of leucine, all the codons for the above amino acids begin with an adenine nucleotide. The studies that implicated *yjeE* in tRNA modification are described below.

In *Saccharomyces cerevisiae*, Sua5 (YrdC) and Kae1 (YdjD) were implicated in $t6A_{37}$ modification through two studies. A bioinformatic analysis suggested that Sua5 might be involved in the $t6A_{37}$ modification and it was shown to bind to $tRNA^{thr}$ lacking $t6A_{37}$ [48]. Kae1 was subsequently suggested to function in the $t6A_{37}$ modification by its sequence similarity and phylogenetic distribution similarity with YrdC [49]. This was confirmed *in vivo* in *S. cerevisiae* by deletion of Kae1, which resulted in the loss of tRNA bearing the $t6A_{37}$ modification. Kae1 complemented the loss of t6A37 tRNA *in trans* [49].

YjeE formed an interaction complex with YeaZ and YgjD in *E. coli* [50]. Since YdjD and YrdC were suggested to function in $t6A_{37}$ modification, the other two components of the interaction complex were tested for this activity as well. *In vitro* synthesis of $t6A_{37}$ was observed using purified YjeE, YgjD, YeaZ and YrdC [51]. The omission of any one of the proteins resulted in the loss of $t6A_{37}$ synthetic activity, suggesting that each protein is essential for $t6A_{37}$ formation. The exact role of each enzyme in modification of $t6A_{37}$ is yet to be determined.

1.2.4 Research directions for the YjeE project

At the outset of this project, the function of *yjeE* in tRNA modification was not known. We employed two strategies to understand the function of YjeE. Chapter Two describes the follow-up from a primary screen for a small molecule inhibitor of YjeE. Such a molecule could circumvent the inadequate genetic tools we use to study this essential gene. In Chapter Three, we developed a transcriptional reporter of *yjeE*. We then monitored its response to bioactive compounds and gene deletions and found functional associations with diverse areas of cellular metabolism. In Chapter Five, future considerations for YjeE as an antimicrobial drug target are discussed.

1.3 RIBOSOME ASSEMBLY AS A NOVEL ANTIBACTERIAL DRUG TARGET

The ribosome is composed of both RNA (rRNA) and proteins (r-proteins). The process by which these two components are synthesized, chemically modified and assembled into a functional ribosome is known as ribosome assembly. The ribosome is responsible for the synthesis of proteins. Indeed, the ribosome is a celebrated target of antibacterial drug discovery and a chemical inhibitor exists for nearly each step of protein synthesis [52]; however, a clinical antibiotic targeting the ribosome assembly process is lacking. A number of recent studies have shown that mutants in ribosome assembly are unable to colonize higher organisms, namely *rsgA*, *bipA* and *rimP* [53-55]. A further four ribosome assembly factors are essential

for viability, widely distributed and represent potential novel antimicrobial drug targets, namely *engA*, *yihA*, *obgE* and *era*. These features suggest that there is potential usefulness in ribosome assembly as an antimicrobial drug target. The structure of the ribosome and the synthesis and assembly of its components are reviewed below.

1.3.1 The structure of the ribosome

In the year 2000, three crystal structures of the prokaryotic ribosome were published, where the researchers who made this landmark discovery were subsequently awarded the 2009 Nobel Prize in Chemistry [56-59]. Below is a description of the *E. coli* ribosome using the published structure of the 70S ribosome at 3.5 Å [60]. The ribosome consists of two subunits of unequal size, termed the small 30S and large 50S subunit. These associate to form the functional 70S ribosome. The inter-subunit interface is the surface where the two subunits meet. A view of this surface is presented in Figure 1-3A and Figure 1-3D for the 30S and 50S, respectively. The surface of the subunit that is opposite to the inter-subunit interface is known as the solvent face. This is presented in Figure 1-3B and 1-3E for the 30S and 50S subunit, respectively.

The core of the ribosome is comprised of rRNA. The large subunit contains two rRNAs, which are called the 23S and 5S, and are 2904 nt and 120 nt in length, respectively. The 30S subunit contains a single 16S rRNA of 1542 nt. The formation of helices in the rRNA pinches off sub-domains that further divide the 23S and 16S sequence (Figure 1-3). The 16S rRNA contains three sub-domains: the 5' or body domain, the platform or central domain, and the 3' head domain. The first three domains form around a central RNA pseudoknot and the final 3' minor domain drapes over the body domain (Figure 1-3A-C). The 16S rRNA sub-domains are compact, distinct globular structures that can individually self-assemble *in vitro* [61-63]. This domain structure is thought to facilitate large conformational movements of the 30S subunit during protein translation [64-66]. The 50S subunit contains seven domains, six of which are encoded within the 23S rRNA and are numbered one to six, where a seventh domain encoded within the 5S rRNA [67] (Figure 1-3D & 3E). The 50S rRNA domains are interlocking and form a rigid semi-spherical structure that is strikingly distinct from the independent globular domains of the 30S.

The 30S and 50S subunits contain 21 and 34 proteins, respectively. Their structures reveal an RNA core with ribosomal proteins around the periphery (Figure 1-4). With the exception of the peptide exit tunnel, the functionally important centres of the ribosome are located on the inter-subunit interface. They are noted for being relatively devoid of protein and emphasize that the core of the protein synthetic machinery is comprised of RNA, i.e. the ribosome is a ribozyme [68].

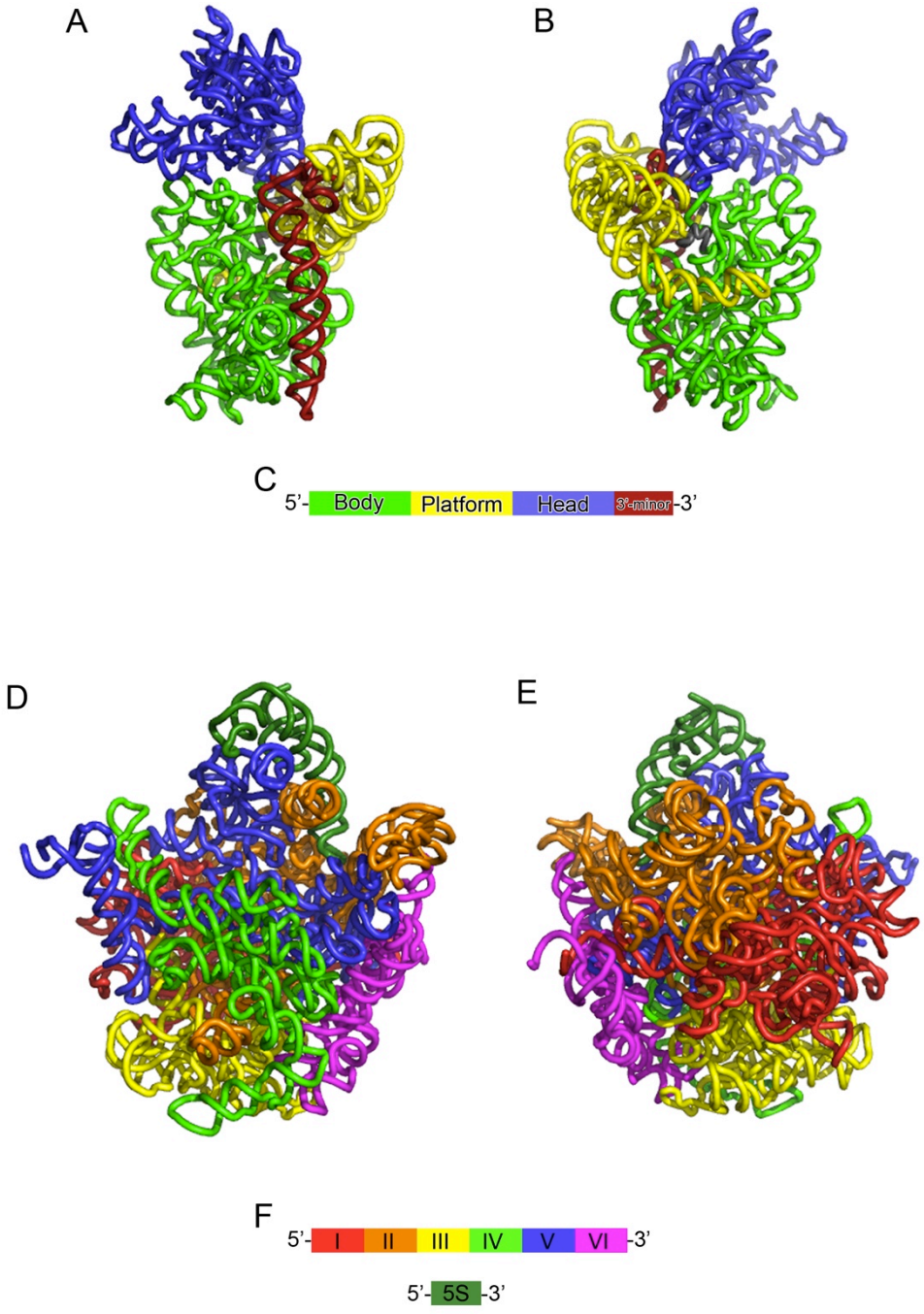

Figure 1-3. rRNA Domains of the *E. coli* ribosomal subunits.

For the 30S subunit, the **(A)** interface view and **(B)** solvent view are shown and the colors correspond to the domains in **(C)**. For the 50S subunit, the **(D)** interface view and **(E)** solvent view are shown and the colors correspond to the domains in **(F)**. The figure was created with MacPymol version 1.5 software [40] using the *E. coli* 70S ribosome solved by Schurwirth *et al* [60] .

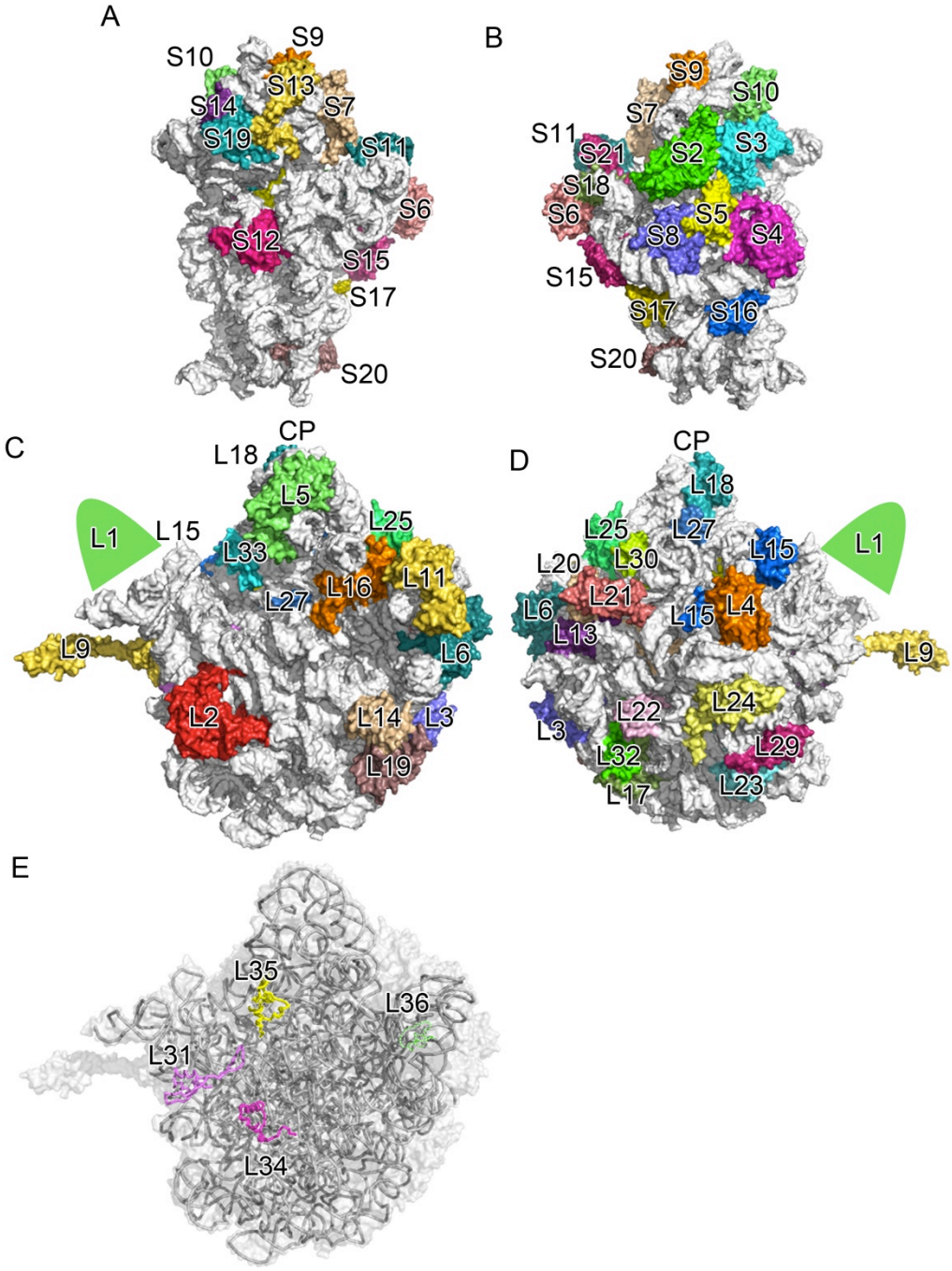

Figure 1-4. Ribosomal proteins of the 30S and 50S subunits.

Interface view of the **(A)** 30S and **(C)** 50S ribosome. Solvent view of the **(B)** 30S and **(D)** 50S ribosome. **(E)** Buried proteins of the 50S subunit are shown in a ribbon representation of the solvent view. The rRNA is grey and proteins are depicted in color. The figure was created with MacPymol version 1.5 software [40] using *E. coli* 70S solved by Schurwirth *et al* [60].

The E,P and A sites of the 30S are generally located between the head and body domains in a region that begins from the cleft between protein S7 and S11 and extends downwards at a 45 degree angle to just above protein S12 (Figure 1-4A). The top of the 3' minor domain is the region where the decoding site is located (Figure 1-3A, red). Its outline is visible in the surface rendering of the 30S (Figure 1-4B). The peptidyl-transferase center is located on the 50S ribosome in the region between L16 and L5 in the inter-subunit view (Figure 1-4C). The above-mentioned regions are incidentally where many ribosome biogenesis factors have been mapped as discussed below.

When viewed from the interface, three appendages project from the body of the 50S: on the left is the L1 stalk, in the top centre the central protuberance (CP) and to the right is the L7/L11 stalk (Figure 1-4C & 4D). The L1 protein is highly flexible and does not resolve well in crystal structures its position is indicated in Figures 1-4D & 4E. The central protuberance contains the 5S rRNA and protein L18 and L17. To the right is the L7/L11 stalk which contains the unresolved L10 protein. L31, L34, L35 and L36 are buried and not visible in a surface rendering of the ribosome, their positions are outlined in Figure 1-4E.

1.3.2 The ribosome assembly maps

R-proteins are generally small and positively charged. Nearly half of the r-proteins have basic extensions that push into the rRNA core of the subunits and are thought to stabilize the negative charges at the centre of the ribosome [60]. How r-proteins and rRNA come together was the subject of intense research in the 1960's and 1970's, which is reviewed below.

Nomura discovered that functional 30S subunits could be reconstituted *in vitro* by using only r-proteins and naked rRNA [69, 70]. These results were later verified by using purified components [70, 71]. These experiments demonstrated that all the information required for the assembly of the ribosome was intrinsic to its components. Reconstitution experiments led to the discovery of a co-operative and hierarchical relationship in the binding of 30S r-proteins to 16S rRNA [71-73]. Nomura found that six proteins were able to bind directly to rRNA, which are termed primary binders. Each of the six primary binding r-proteins in complex with 16S rRNA was then incubated with each of the remaining r-proteins. Proteins that bound the primary binding complexes were termed secondary binders and so on for tertiary binders. The resultant assembly map is depicted as a network of arrows connecting proteins that bind cooperatively.

30S primary binding proteins tend to bind near the 5' end of the 16S rRNA. This predicted a cascade of rRNA binding that proceeds from 5' to 3' [74, 75]. Recent reconstitution experiments have provided further resolution of 30S assembly by measuring the folding of rRNA [76]. These experiments revealed that the primary binding r-proteins facilitate rRNA folding, which nucleates assembly

independently on each of the rRNA domains. These local changes promote the subsequent binding of secondary r-proteins [77-79].

The 50S reconstitution conditions were discovered by Nierhaus and were found to be harsher and more complicated compared to the 30S reconstitution [80]. Depending on the method employed, the 50S reconstitution can yield up to three intermediates of increasing maturity. Nierhaus and his co-workers described the assembly map of 50S subunit over the course of several studies [81-84]. Some similarities exist between the 30S and 50S assembly processes. Like 30S r-proteins, 50S r-protein binding is cooperative whereby primary binding proteins potentiate the binding of secondary binding proteins and so on. 50S assembly has a general 5' to 3' polarity whereby nearly all the proteins essential for the formation of the first reconstitution intermediate bind near the 5' end of the 23S rRNA [84]. The 50S assembly map is more complicated; for instance, many proteins in the 50S subunit are quaternary binders so the 50S assembly map contains a denser network of interactions. The complex assembly of the 50S is attributed to the larger number of components (Figure 1-4) and more complicated domain architecture (See Figure 1-3) compared to the 30S subunit [85]. Unlike the 30S, where assembly has been studied on a minute timescale, detailed dissection of the 50S assembly process is lacking.

1.3.3 RNA folding in ribosome assembly

One of the major steps of ribosome assembly is RNA folding, which is streamlined because rRNA adopts simple secondary structures [86]. Further, all 30S r-protein activation energies are similar to avoid bottlenecks in assembly, and there are multiple paths to the mature form [87]. Problems in assembly arise when RNA forms misfolded structures that are either kinetically or thermodynamically trapped [88]. Kinetic traps form when alternative non-native structures are stably formed but cannot complete the assembly process. An input of energy is required for them to continue maturation. Thermodynamic traps form when a ribosomal intermediate switches between conformations that are energetically equivalent but only one form can go on to maturity. A number of conformations must be "searched" before the correct one is formed. For large RNA molecules, kinetic trapping is the dominant problem encountered during maturation [89]. Half of the 5' 30S sub-domain is kinetically trapped at the outset of a reconstitution experiment [63]. So, while ribosome assembly can proceed down multiple paths, these paths are dotted with many stable intermediates that proceed very slowly to maturity.

R-proteins can promote the formation of the ribosome by disrupting non-native conformations of rRNA, promoting or stabilizing native conformations and stabilizing the tertiary structure of the ribosome through long-range interactions. One-third of large ribosomal proteins and protein S12 act as general RNA chaperones in an *in vitro* assay of intron splicing [90, 91]. The proposed mechanism

is that, due to their charged nature, some r-proteins can act as a non-specific denaturant that disrupt non-native structures and promote re-folding [89, 92]. Whether this property of r-proteins is pertinent to ribosome assembly is not known. Rather than disrupting a non-native structure, protein L20 was recently found to stabilize the mature form of its binding site on the ribosome [93]. Similarly, the small subunit protein S16 was found to promote folding of the 30S 5' sub-domain by reducing the population of non-native intermediates [75, 79]. Finally, small subunit proteins have been demonstrated to stabilize long-range interactions outside of their binding sites [78]. Thus, r-proteins promote rRNA folding by stabilizing the ribosome or promoting folding to avoid pitfalls such as kinetic and thermodynamic traps.

1.3.4 The synthesis of rRNA and r-proteins

Ribosome assembly *in vivo* begins with the production of r-proteins and rRNA. Ribosomes constitute 50% of the dry mass of the bacterial cell; thus, poor regulation of ribosome synthesis could incur a great fitness cost.

E. coli has seven nearly identical copies of the rRNA operon on its chromosome. The general structure of each rRNA operon is 5' - 16S – tRNA – 23S – 5S – tRNA, where the tRNA sequences can vary and there is always least one present. A pair of upstream promoters, P1 and P2, controls transcription of the rRNA operons. Transcription originates from both promoters, however, P1 activity is stronger during high growth rates (See [94] for a review). The strength of promoter P2 is higher than P1 at low growth rates and is less subject to regulation [95, 96]. A number of proteins and transcription factors exert control over rRNA transcription but two small molecules are at the core of this control; namely initiator NTPs (iNTP) and guanosine penta / tetraphosphate ((p)ppGpp) [97, 98]. iNTP has authority over rRNA transcription at low growth rates when NTP concentrations are limiting. During periods of rapid growth (p)ppGpp has authority over rRNA transcription. RelA and SpoT produce and degrade (p)ppGpp in response to amino acid availability. As amino acid concentrations fall, (p)ppGpp concentrations increase [98]. The result of these control systems is very tight regulation of the synthesis of ribosomes.

The three species of rRNA are transcribed as a single, immature transcript that is trimmed in successive steps by a set of endonucleases and exonucleases (RNAses). The endonuclease RNase III acts first by liberating pre-16S, pre-23S and pre-5S rRNA [99, 100]. The 5' and 3' ends of pre-16S rRNA have an extra 115 and 33 nt, respectively. RNase E cuts at a site 66 nt upstream of the mature 5' end of 16S rRNA and RNase G produces the mature 5' end [101, 102]. The surplus 33 nt at the 3' end of the 16S rRNA are cut by an unknown RNase [103]. The pre-23S rRNA is functionally mature [104] but contains an extra three or seven nt at its 5' end and seven or nine extra nt at the 3' end following RNAse III cleavage [105]. The nuclease

that trims the final pre-23S 5' end to maturity is not known. RNase T processes the 3' end of pre-23S rRNA [106]. The pre-5S rRNA, also referred to as 9S rRNA, is more than twice the size of the mature product with an extra 84 and 42 nt at the 5' and 3' ends, respectively [105]. RNase E processes 9S rRNA leaving 3 nucleotides at both the 5' and 3' ends [107]. Final maturation of pre-5S is carried out by an unknown enzyme at the 5' end and RNase T at the 3' end [108].

The 55 r-proteins are encoded on the *E. coli* chromosome within 21 operons ranging in size from one to eleven cistrons (See [109] for a review). A single r-protein can control synthesis of its own operon by binding a control sequence encoded within the mRNA and attenuating translation. When there is an abundance of free rRNA, r-proteins bind rRNA instead and enter the assembly process thereby relieving repression of r-protein translation. Conversely, when rRNA levels are low, free r-proteins accumulate and certain ones bind to their control sequences resulting in inhibition of r-protein translation. This method of control is termed translational coupling. The control site is usually within the second or third cistron of the transcript, which means that translation can be initiated but the ribosome stalls early on the transcript. Translational coupling has been demonstrated for 11 of the 21 r-protein operons, which encode 70% of the r-proteins. The free concentration of r-proteins is dictated by the amount of available rRNA, thus rRNA transcription controls ribosome synthesis. R-protein synthesis is further controlled by either regulating the stability or elongation of mRNA, however, these methods do not appear to be as widespread as translational coupling [109]. Recent work has found that (p)ppGpp directly regulates the transcription of a significant fraction of r-protein operons, adding another level of coordination between rRNA and r-protein synthesis [110].

1.3.5 Participation of immature rRNA and transcription in ribosome assembly

Ribosome assembly occurs as the rRNA is being transcribed so r-proteins bind immature rRNA before it undergoes nucleolytic processing. There is evidence that the immature rRNAs act as chaperones in ribosome assembly. The region upstream of the mature 16S 5' termini contain a highly conserved sequence that interacts with the 16S 5'-domain [111, 112]. Mutations in this region can lead to a cold-sensitive phenotype and altered 16S folding and 30S assembly [113, 114]. In the *rrn* operon, the presence of an intervening tRNA sequence between 16S rDNA and 23S rDNA influences the maturation of the 3' end of 16S rRNA [115, 116]. The intervening sequence between the 16S rRNA and 23S rRNA also influences the formation of 50S ribosomes [117]. Lastly, deletions of extra-ribosomal assembly factors nearly universally lead to the accumulation of pre-16S and pre-23S rRNAs. Thus, ribosome rRNA maturation is a critical step in the ribosome assembly process.

Transcription of rRNA may directly regulate ribosome assembly. Ribosome biogenesis is co-transcriptional. As rRNA emerges from RNA polymerase r-proteins bind [118]. Ribosomal intermediates have been observed on nascent rRNA [118]. , As judged by pulse labeling, the entire process of maturation takes approximately 2 minutes [119], which is approximately the time it takes to transcribe the entire rRNA operon [120]. Interestingly, the highly processive phage T7 RNA polymerase cannot substitute for the native polymerase in ribosome assembly *in vivo* [121]. Further, the host RNA polymerase was observed to undergo a 3 fold change in rate while transcribing the rRNA operon [120]. These observations suggest that transcription may be an active participant in regulation of the assembly process.

1.3.6 The ribosome assembly factors

The synthesis and assembly of 54 ribosomal proteins and 3 ribosomal RNAs as well as 46 known enzymatic modifications in *E. coli* are necessary to produce a mature ribosome in the cell [122, 123]. Biochemical reconstitution experiments occur at conditions that are far from physiological [71, 80, 123, 124]. In the cell a set of *trans*-acting factors, termed ribosome assembly factors, are thought to be critical for the assembly of ribosomal subunits to occur at a rate that meets the protein synthesis demands of the cell.

The role of ribosome biogenesis factors are to promote the binding of r-proteins to the rRNA, to alter rRNA or r-proteins covalently and they are hypothesized to serve as check-points to co-ordinate the process of biogenesis. Ribosome biogenesis factors fall into the following groups: RNA helicases, chaperones, rRNA nucleases, rRNA chemical modifications, r-protein modifications and RNA binding proteins - with or without GTPase domains (See Table A-1 for a list of biogenesis factors). The rRNA or r-protein modification factors make covalent modifications, which may serve as checkpoints to co-ordinate assembly or to fine-tune the structure of the ribosome. For RNA helicases and RNA binding proteins, the exact changes to the ribosome that they facilitate have been more elusive. RNA helicases and RNA binding proteins form transient and context-dependent interactions with the ribosome that are difficult to capture. Cells depleted of ribosome assembly factors commonly exhibit the following phenotypes: accumulation of precursor rRNA, immature ribosomal subunits, temperature sensitive growth and antibiotic sensitivity (see [125] for a recent review).

1.3.7 Helicases

A family of enzymes known as the DEAD–box RNA helicases couple the hydrolysis of ATP to the local unwinding of RNA [126]. DEAD–box proteins are thought to facilitate ribosome assembly by disrupting stable non-native RNA conformations [127]. In *E. coli,* there are 5 DEAD-box helicases and four are

implicated in ribosome assembly: SrmB, RhlE, CsdA/DeaD and DbpA. Depletion of these factors led to many of the hallmark phenotypes of ribosome assembly factors. Ribosome assembly defects were observed to varying degrees but were most dramatic in the *csdA* and *srmB* null strains. Deletions of *csdA* or *srmB* led to an increase in doubling time at 25°C and accumulation of 50S precursors that do not have the full complement of r-proteins [128-130]. Both the *csdA* and *srmB* deletion strains had elevated amounts of precursor 23S rRNA but precursor 16S rRNA was only seen in the *srmB* deletion [129, 130]. The deletion of *dpbA* or *rhlE* did not lead to alterations in the concentration of free ribosomal subunits or cold-sensitive growth [128, 131]. Current data suggests that all the helicases act in 50S assembly, where perhaps the complicated, interlocking domain structure of the 50S requires more supervision during assembly.

1.3.8 Chaperones

The Hsp70 system of proteins (DnaK - DnaJ - GrpE) and the GroEL/ES chaperone are involved in the folding of nascent and incorrectly folded proteins, respectively [132, 133]. Experiments with temperature sensitive mutants of *dnaK* [134] and later experiments with deletions of *dnaK* and *dnaJ* indicated that under prolonged heat stress, 30S and 50S precursors are formed [135]. Similarly, a temperature sensitive mutation in *groEL* produced 50S precursor particles and *groEL* over-expression can partially suppress the deletion of *dnaK*, suggesting an overlap in functions [136]. The Culver group has suggested that the Hsp70 chaperones directly bind to pre-30S particles and assist in the incorporation of late stage r-proteins [137, 138] but these results have been contested [139]. Recently, a model has been suggested whereby heat stress overwhelms the heat shock response and unfolded and inactive proteins accumulate, including ribosome assembly factors [140]. Irrespective of the mechanism, heat stress does produce late stage ribosomal intermediates.

1.3.9 Small subunit assembly factors

The are seven known small subunit maturation factors in *E. coli* can be divided into two groups (See [125] for a review): those that contain only an RNA binding domain (RbfA, RimM, RimP, RimJ and YibL) and those that combine an RNA binding domain with a GTPase domain (Era and RsgA). (see [141, 142] for reviews of prokaryotic GTPases). All small subunit factors bind the 30S subunit and RsgA was found to bind the 70S ribosome as well [143]. Small subunit assembly factors are all dispensable for growth, with the exception of Era [144]. Additionally, all small subunit biogenesis factors displayed cold-sensitive growth upon deletion or mutation, with the exception of *rimJ*.

Relatively little is known about RimJ and YibL. RimJ is an S5 acetyl-transferase, which is suggested to have a role in ribosome assembly that is independent of its acetyl-transferase activity [145]. RimJ was identified as a high copy suppressor of a cold-sensitive mutant of S5 and it binds the 30S precursors that this mutant produces. YibL bound free 30S ribosomes and a *yibL* deletion displayed cold-sensitive growth [146]. For the rest of the small subunit factors (*era*, *rimP*, *rimM*, *rsgA* and *rbfA*) there is a growing body of evidence that these proteins are critical for the assembly of the 3' or head domain and that most act late in the assembly process. The Era protein, however, seems to have wide-ranging effects on 30S assembly.

The binding sites of Era, RsgA and RbfA are known through cryo-electron co-structures while the binding site of RimM is implied through biochemical and genetic evidence. A cryo-electron microscopy derived structure of Era revealed that it binds the 30S subunit between the head and platform in a cleft formed by S7, S11 and S2 [147]. Two recent cryo-EM structures of the RsgA:30S complex differed slightly in the placement of RsgA on the 30S, but there was consensus that RsgA interacted with the 3' minor domain and helix 24 of the central domain [148, 149]. Interestingly, the RsgA and RbfA binding sites on the 30S subunit have significant overlap and are centered over the 3' minor domain and the decoding center of the 30S subunit [150, 151]. Indeed, RsgA promoted the release of RbfA from the ribosome and was hypothesized to act as a check-point in late stage assembly [152]. Genetic and biochemical evidence suggests that RimM binds a narrow region on the interface side of the 30S between the head and body domains [153]. The trend among 30S assembly factors is that they bind at the interface of the 3' or head domain, which is the last to sub-domain form.

Two approaches have addressed the extent to which small subunit assembly factors promote the incorporation of r-proteins into the 30S subunits. The first is the time-resolved measurement of r-protein binding to the immature 30S subunit during *in vitro* reconstitution, which was carried out for Era, RimP and RimM. Addition of Era to a 30S reconstitution reaction increased r-protein incorporation in the 5' domain (S5 and S12), central domain (S11) and 3' domain (S19) with smaller effects on the incorporation of 3' domain protein S7, S10, S13, S14 and S19 [154]. RimP accelerated the binding of r-proteins to the 5'domain (S5 and S12) and the 3' domain (five of eight proteins) [154]. RimM increased the binding of r-proteins to the 3' domain (S3, S9, S10 and S19) and decreased the binding of S12 and S13 [154]. The second approach to determine the extent to which 30S assembly factors facilitate the incorporation of r-proteins was the quantification of r-proteins bound to immature 30S subunits isolated from deletions. This approach was used for Δ*rsgA*, which exhibited decreased levels of S21, S1 and S2, all late stage r-proteins [155]. In summary, Era influenced the binding of both early and late r-proteins while RimP acted primarily in late assembly and RimM and RsgA acted exclusively in late assembly.

1.3.10 Large subunit assembly factors

Like the 30S factors, the 50S assembly factors can be split into two groups (see [125] for a review); those that contain only RNA binding domains (*yhbY and yihI*) and those that combine RNA binding domains with a GTPase domain (*engA*, *ogbE* / $cgtA_E$, and *yihA*). Only the 50S GTPases are essential for viability [156-160]. 50S assembly factors exhibit many of the same phenotypes that 30S assembly factors do, such as accumulation of ribosomal precursors, subunit binding and cold-sensitive growth upon depletion. Compared to the 30S assembly factors, there is less biochemical data on the roles of 50S factors but they are also suggested to act in late in the process.

Large subunit factors preferentially bind the 50S subunit and their depletion from the cell led to an accumulation of ribosomal subunits. An *yhbY* null accumulated free 30S and 50S subunits at the expense of the 70S ribosome and polysomes. YhbY bound 30S, 50S and 70S ribosomes with a strong preference for the 50S subunit. [146]. When YihI was overexpressed, it produced a ribosome subunit profile similar to the *yhbY* null and an increase in 16S and 23S rRNA precursors [161]. Depletion of EngA also caused an increase in free ribosomal subunits and the protein was found to bind the 30S and 50S subunits [156, 157]. Much of the information about the YihA protein came from studies of its orthologues in Gram-positive organisms, where it is known as YsxC; it interacted with total ribosomes and the 50S subunit in *B. subtilis* and *S. aureus,* respectively [162, 163]. An ObgE temperature sensitive mutant accumulated both free 30S and 50S subunits at the expense of the 70S ribosome [164, 165]. ObgE binds to both the 30S and 50S subunits as well as 16S and 23S rRNA [164]. Two ObgE temperature sensitive strains accumulated pre-16S and pre-23S rRNA [164, 165]. The distinguishing feature of 50S factors is they also bind the 30S subunit, while 30S factors almost exclusively bind the small subunit.

The influence of 50S assembly factors on *in vitro* reconstitution or co-structures of 50S factors and the ribosome have not been reported. We can infer the roles of 50S factors and their binding sites on the ribosome by the 50S r-proteins that are missing when the factor is depleted from the cell. Depletion of *E. coli* EngA led to the production of a pre-50S particle that was depleted of r-proteins L2, L6, L9, and L18. These proteins are scattered along the subunit interface and it was suggested that EngA functions in this location as well [157]. On the other hand, depletion of the *B. subtilis* EngA orthologue, YphC led to reduced L16, L27 and L36 [162]. These proteins are found closer to the peptidyl transferase center. Interestingly, depletion of the YihA orthologue in *B. subtilis*, YsxC and YphC / EngA led to reduction of some of the same proteins (L16, L27 and L36) [162]. YihI was found to increase the GTPase activity of EngA by 2-fold [161]. 50S subunits purified from strains harboring the ObgE temperature sensitive allele showed a deficiency of

proteins L16 and L33, which are found at the interface near the PTC [165]. With the exception of L2, all of the r-proteins mentioned above are predicted to be late assembly proteins based on the Nierhaus assembly map. Further, most of the above proteins are found at the interface near the functional important center, the PTC.

1.3.11 rRNA modifications

In *E. coli* there are 11 modified nucleosides on the 16S rRNA and 25 on the 23S. They are modified in three ways: methylation at the nucleobase or ribose, isomerization of uridine (pseudouridylation) and reduction of uridine to dihydrouridine (See [166] for a review). When rRNA modification genes were deleted there were rarely strong phenotypes observed and most modifications are not conserved across species [166]. On the other hand, rRNA modifications are concentrated around the important functional centers of the ribosome and are believed to fine-tune the structure and stability of the ribosome [167]. In *E. coli*, reconstitution reactions of the 30S ribosomes using unmodified rRNA show only a slight decrease in functionality [168], while reconstituted 50S subunits using unmodified rRNA are non-functional [169]. Three modification enzymes are most important to ribosome assembly: *ksgA*, *rluD* and *rrmJ*. The roles of these three enzymes in ribosome assembly are discussed below.

KsgA methylates A1518 and A1519 on the final helix of the 16S rRNA in the 3' minor domain [170]. These residues are conserved throughout all kingdoms of life and are found in the decoding center of the ribosome on helix 45 (See [171] and references therein). Deletion of *ksgA* led to cold-sensitive growth, accumulation of free ribosomal subunits and pre-16S rRNA [171]. When overexpressed, a methyltransferase-deficient KsgA variant caused an even stronger phenotype and greater accumulation of free 30S subunit than the complete deletion. Catalytically inactive KsgA bound strongly to the ribosome, thus, it was hypothesized that methylation triggers release of KsgA from the ribosome [171]. The methylation activity of KsgA was dispensable. It was hypothesized that methylation of A1518 / A1519 and subsequent release of KsgA is a checkpoint in late stage assembly. KsgA has a genetic interaction with RsgA, which acts late in assembly, further suggesting a role in coordinating the final steps of ribosome biogenesis [172].

Pseudouridylation of U1911, U1915 and U1917 of the 23S rRNA are conserved throughout all orders of life [173]. These modifications are carried out by the enzyme RluD in *E. coli* [174]. RluD is the only pseudouridine synthase in *E. coli* whose deletion caused a very slow growth phenotype and accumulation of ribosomal subunits [172, 175, 176]. Ribosomes isolated from *csdA* deletion mutants are devoid of the pseudouridylations catalyzed by RluD, suggesting that RluD acts after CsdA [177]. An *rluD* and *rsgA* double deletion enhances the slow growth phenotype of the *rsgA* single deletion, which further supports the hypothesis that RluD acts late in assembly [172].

RrmJ / RlmE catalyzes the methylation of U2552 in the 23S rRNA at a loop that contributes to tRNA binding at the A-site [178]. Deletion of *rrmJ* led to a severe slow growth phenotype and the accumulation of free 30S and 50S subunits [179, 180]. When ribosomes were isolated in low Mg^{2+} conditions, a precursor 50S subspecies was found [180]. The subunit that migrated with mature 50S was a substrate for methylation but the immature species was not. This suggested that RrmJ might serve as a checkpoint protein that marks only mature ribosomes. Overexpression of *engA* or *obgE* suppressed the growth defect and the ribosome profile defects of a *rrmJ* null strain [181].

1.3.12 R-protein modifications

Eleven ribosomal proteins can be modified by the addition of acetyl, glutamyl methyl and methylthiol moieties (reviewed in [122]). Very little phenotypic data has been generated for these proteins and a slow growth phenotype has only been reported in two cases. The first case was acetylation of protein S5 by RimJ, where a mutant exhibited sensitivity to growth at 42 °C [182]. The second case was loss of methylation of L3 caused by a mutant allele of *prmB.* This strain had a moderate growth defect at 22°C and an increase in 50S precursors [183]. For the five r-protein modifications for which we know the cognate enzymes, there are no growth defects in the mutants. These genes are *rimK* (S6 glutamination), *rimO* (S12 methylthiolation), *rimI* (S18 acetylation), *rimL* (L7/L12 acetylation) and *prmA* (L11 methylation) [146, 184-186]. There are an additional four r-protein modifications for which the enzymes are not known. These are methylations of S11, L16 and L33 and acetylation of L33.

1.3.13 Research directions for the ribosome assembly project

Amongst the various ribosome assembly factors, it is unclear which would be the most fruitful for antimicrobial drug discovery. Further, it is possible that all the assembly factors have not been identified. To find new factors we made use of two qualities of known assembly factors: most ribosome assembly factors are non-essential for viability and cold-sensitivity is a common phenotype amongst ribosome assembly factors. Chapter Four describes a systematic search for ribosome assembly factors by testing for cold sensitivity in a library of non-essential gene deletions in *E. coli*. In Chapter Five I discuss the future of ribosome assembly factors as drug targets.

2 CHAPTER TWO -CHARACTERIZATION OF ACTIVE MOLECULES FROM A HIGH-THROUGHPUT SCREEN FOR INHIBITORS OF YJEE

2.1 CHAPTER TWO PREFACE

Abdellah Allali-Hasani purified YjeE and synthesized mADP for the primary screen. Nadine Elowe performed the primary screen. Jonathan Cechetto and Nadine Elowe analyzed the data from the primary screen.

I carried out all the experiments described in this chapter.

2.2 INTRODUCTION

One way to understand gene function is to observe the phenotypes that arise when the gene is deleted. Essential genes are difficult to study in this way because of inefficient genetic tools. To deplete the essential gene *yjeE* from the cell, a strain was constructed where the native copy was replaced with a drug-resistance marker and an ectopic copy was placed under the control of an arabinose-inducible promoter at the *araBAD* locus (*yjeE::kan; araBAD::yjeE-cat*) [34]. In the absence of arabinose, death ensues because of depletion of this essential gene. Cell death did not occur, however, until after three rounds growth in the absence of arabinose, which took 36 hours. A lengthy depletion time could allow downstream effects and second-site mutations to obscure the true function of YjeE. Others have shown that the *araBAD* promoter has a low level of transcriptional activity in the absence of inducer and there is a stochastic response. Thus, the *araBAD* promoter is inadequate to study stable low abundance proteins such as YjeE even though it is one of the best genetic tools available [187, 188].

An alternate method to traditional genetic techniques for resolving gene function is chemical genetics, recently reviewed in [189, 190]. In chemical genetics, a cell-permeable small molecule inhibitor, rather than a gene deletion, is used to modulate gene function. The most well-known small molecule probes are antibiotics, which allow inhibition of specific steps of essential cellular processes [191]. Indeed, nearly every step of protein translation has an antibiotic inhibitor [52]. Small molecules produce protein inhibition with rapid onset, on the timescale of minutes to seconds, and can be as quickly reversed. Genetic methods may take hours to days to produce the same effect and reversal is slower. Further, the concentration of small molecule inhibitors can be tuned to produce a dose-responsive phenotype.

We took a reverse chemical genetics approach to study YjeE by searching for a specific small molecule inhibitor. The ATPase activity of YjeE was the natural target for high-throughput screening (HTS), however, YjeE has an extremely slow catalytic turnover of 1 h^{-1}, which can easily be obscured by the presence of highly active ATPases that sporadically contaminate protein preparations [34]. A fluorescence polarization assay was used to measure the binding of YjeE to ADP that was modified with a fluorophore at the 2’ / 3’ position of the ribose ring. The McMaster High-throughput screening laboratory (MAC-HTS) screened *E. coli* YjeE against 51,000 compounds for their ability to displace 2'-/3'-O-(N-methylanthraniloyl) adenosine 5'-O-diphosphate (mADP) from the YjeE protein. Some 954 molecules were selected that had activities below three standard deviations of the average activity of controls lacking compound. To remove highly fluorescent molecules, those that had fluorescence intensities above three standard deviations from the average of controls containing only mADP were removed. Compounds were also eliminated to reduce redundancy based on structural

similarity and those that could not be re-supplied were also eliminated. This yielded 134 active compounds that were characterized in this work.

Fluorescence polarization (FP), which was used in the primary screen, was also used here in the secondary screen to confirm the active molecules. FP and its use in HTS are reviewed in [192-200]. When a fluorophore in solution is excited by plane polarized light, the emitted light is polarized. Rotation of the fluorophore causes depolarization of the emission, whereby the degree of depolarization is related to the rate of rotation. The rate of rotation is determined by the size of the molecule and the viscosity and temperature of the solution. A fluorophore that is bound to a protein will rotate much slower, due to its large apparent size. Displacement of the fluorophore from the protein, thus, increases the rate of tumbling and decreases polarization, which is measured by a fluorometer. FP assays use a single label in a homogenous assay. The output is ratiometric so the assay is largely insensitive to contaminating proteins.

We used affinity selection mass spectrometry (ASMS) to study the affinity of YjeE for putative inhibitors. For general reviews of this method see [201, 202]. ASMS is based on the principle that at equilibrium, ligands will bind their targets according to their characteristic dissociation constant (K_D). The ligand:protein complex can be quickly separated from free ligand and free protein by either ultrafiltration (UF) or size exclusion chromatography (SEC) before a new equilibrium is established. The amount of ligand in the ligand:protein complex is measured by mass spectrometry, to infer the strength of binding. Although this method was used in medium throughput here, it requires little protein and can be used in much higher throughput.

We characterized 134 molecules from two rounds of selection from the primary screen. The ATPase activity and mADP binding of YjeE were both tested in follow-up assays. The first round of molecules tested were potent in both of these assays but were ultimately found to be reactive false-positives. The second round of molecules, which were less potent, were active in the FP assay but not the ATPase assay. These were later found to interfere with the FP assay due to their intrinsic fluorescence. We developed the ASMS assay using previously described inhibitors of *E. coli* dihydrofolate reductase (DHFR) [203]. Although the assay could detect ligands that bound with low micro-molar affinity, no compounds were found that bound YjeE.

2.3 Materials and Methods

General Methods

Tris, HEPES, isopropyl β-D-thiogalactoside (IPTG) and dithiothreitol (DTT) were obtained from Bioshop Canada (Burlington, ON). Luria-Bertani (LB) growth media was obtained from BD Biosciences (Mississauga, ON). Ampicillin was obtained from Sigma Aldrich (Oakville, ON). Triethylamine (99%) was obtained

from Anachemia Canada (Montreal, PQ). BODIPY-TR labeled ADP (bADP) was obtained from Invitrogen Canada (Burlington, ON). Mant-ADP was synthesized according to previously published methods [204]. Preparation of competent cells and transformation was performed according to manufacturer's protocols (Bio-rad, Hercules, CA).

YjeE Purification

YjeE that was used for the secondary screen was purified using the following method. *E. coli* BL21 (DE3) harboring plasmid pDEST17-*yjeE* [34] was grown at 37°C in LB media supplemented with 50 μg/mL ampicillin. At OD_{600} of 0.6, cultures were induced with 1 mM IPTG, grown for an additional 3 hours, then harvested. Cell pellets were washed with 0.85% NaCl and re-suspended in Buffer A (20 mM HEPES, 500 mM NaCl, 15 mM imidazole, 30% glycerol, EDTA-free protease inhibitor cocktail (Roche, Laval, PQ), 0.05 mg/mL RNase and 0.05 mg/mL DNase (Fermentas, Burlington, ON)). Cells were lysed by three passes through a French press at 19,000 psi. Lysate was clarified by centrifugation at 50,000 x g for 1 hour. Clarified lysate was loaded onto a 1 mL HisTrap Ni-NTA affinity column (Amersham Biosciences, Baie d'Urfe, QC). YjeE was resolved over a linear gradient of 15 mM - 300 mM imidazole and fractions determined to contain YjeE by SDS-PAGE analysis were pooled. Pooled YjeE was diluted 10 fold with Buffer B (20 mM HEPES, pH 7.5 and 1 mM DTT) and loaded onto a Q-Sepharose Fast Flow anion-exchange column (2.6 cm × 10 cm) (Amersham Biosciences). The column was washed with 100 mL of Buffer B and proteins were resolved with a linear gradient of 0 – 1M NaCl. Fractions determined to contain YjeE by SDS-PAGE analysis were pooled. Glycerol was added to a final concentration of 15 % (v/v) and stored at -80°C.

Fluorescence Assays

For assays using mADP, fluorescence was measured on an LJL Analyst HT (Molecular Devices, Sunnyvale, CA) fitted with 360/35 band-pass excitation and 530/25 band-pass emission filters. For assays using bADP, fluorescence was measured on a PTI fluorometer (Photon Technology International, London, ON), fitted with dual emission monochromators (λex = 580 nm, λem = 620 nm). Measurements on the LJL Analyst HT were taken from black low profile 96-well plates (Costar) while measurements on the PTI fluorometer were taken from low volume (500 μL) cuvettes. Typical assay volumes were 50 μL for 96 well plates and 150 μL for cuvette based measurements. Fluorescence intensities (I) were measured in the parallel ($I_{\parallel}$) and perpendicular orientation ($I_{\perp}$) and polarization (P) was calculated according to equation 1 [205].

$$P = \frac{I_{\parallel} - I_{\perp}}{I_{\parallel} + 2I_{\perp}} \quad (1)$$

The data for dose-response assays were fit to a four parameter logistic equation using SigmaPlot v. 11.0 (SPSS Science, Chicago, IL, U.S.A) with equation 2, where max and min are the maximal and minimal asymptotes, hillslope is the slope at the midpoint and EC_{50} is the concentration of compound that produced 50% displacement of the ligand.

$$\Delta\text{mP} = \text{min} + \frac{(\text{max} - \text{min})}{1 + \frac{[\text{compound}]^{-Hillslope}}{\text{EC50}}} \quad (2)$$

ATPase Assays

10 μM YjeE was added to 100 μM inhibitor in assay buffer (20 mM HEPES, 10 mM $MgCl_2$) and 1 mM DTT when indicated. Samples were incubated for one minute before the reaction was initiated with 1 mM (final) ATP. Reactions proceeded at room temperature for four hours before being quenched with 6 M (final) urea and filtered through microfuge centrifugal filters that had a 5 kDa molecular weight cutoff (Millipore, Bedford). ATP and ADP were resolved by anion exchange chromatography on an HPLC as described previously [34].

ASMS General Methods

C^{14} - trimethoprim (Roche, Laval, PQ) (25 μM) was incubated with or without DHFR (50 μM) or bovine serum albumin (BSA) (50 μM) in a total volume of 50 μL. Samples were incubated in either phosphate buffered saline (PBS), 50 mM HEPES or 1 mM HEPES, pH 7.5. PBS or HEPES were used when scintillation counting or mass spectrometry were used for quantitation, respectively. Reactions were allowed to come to equilibrium for 1 hour and split into equal 25 μL aliquots. The first aliquot (25 μL) was applied to a fast SEC mini-column in a 96-well format (Millipore Multiscreen –HV) using Sephadex G-25 and G-50 resin (Amersham Biosciences, Baie d'Urfe, PQ). The second aliquot was used as a control for ligand detection. Mock selections that used buffer in place of protein were used to determine background signal. Column volumes were approximately 200 μL and columns were equilibrated with binding buffer for at least 3 hours prior to use. Elution was performed at 1000 x g for three minutes and ^{14}C - trimethoprim was quantified by scintillation counting or mass spectrometry (described below).

Electrospray ionization mass spectrometric (ESI-MS) detection of ligands

Ligand detection was performed by ESI-MS. An MDS Sciex Q Trap triple quadrupole ESI mass spectrometer fitted with a TurboIon source was used for this purpose. The instrument was set to enhanced MS in positive mode, scan range 50-1700 m/z, q3 fill time 20.00 msec, scan rate 4000 amu/s and pause time 5.007 msec. Components of the recovered protein:ligand complex were resolved by reverse phase chromatography on an HPLC. A C_{18} column (150 mm X 4.6 mm i.d., Zorbax stable bond 3 μm) was used with solvent A (0.04% formic acid in water) and solvent B (0.04% formic acid in acetonitrile). The program consisted of a 9 min gradient from 5% B to 100% B at a flow rate of 1.0 mL/min and a total run time of 14 min. A T-splitter was used to reduce flow into the mass spectrometer to 100 μL/min. Samples for ESI-MS were filtered through a 5 kDa filter (Millipore) and lyophilized overnight. Samples were dissolved in 20 μL solvent A and 10 μL was analyzed by MS.

2.4 RESULTS

2.4.1 First round of compound selection

An overview of the secondary screen of putative inhibitors of YjeE is presented in Figure 2-1. Each of the 134 compounds identified in the primary screen were tested in dose-response ADP binding assays. Of these, 29 compounds were deemed potent (IC_{50} < 50 μM), picked from the library plates and tested in ATPase assays (Figure 2-2A). High control reactions, lacking inhibitor, produced 12.0 ± 1.1 μM ADP. Compounds were selected that reduced the ATPase activity of YjeE to less than 80%, which corresponded to 3 standard deviations below the high controls of this assay. This yielded 9 compounds: MAC-0016889, MAC-0017254, MAC-0022267, MAC-0022879, MAC-0022881, MAC-0023440, MAC-0041717, MAC-151227 and MAC-151283.

The 9 compounds that were active in the ATPase assay were re-ordered from suppliers and retested in the ATPase assay. Five re-ordered compounds were less inhibitory in the ATPase assay compared to initial tests using compounds that were obtained from library plates. These were MAC-0022267, MAC-0022281, MAC-0041717, MAC-151227 and MAC-151283 (Figure 2-2B – grey bars). Reactive electrophilic compounds that are promiscuous are known to produce false positives in HTS [206, 207]. Nucleophilic compounds, such as DTT, at high concentration preferentially react with promiscuous compounds rendering them inactive.

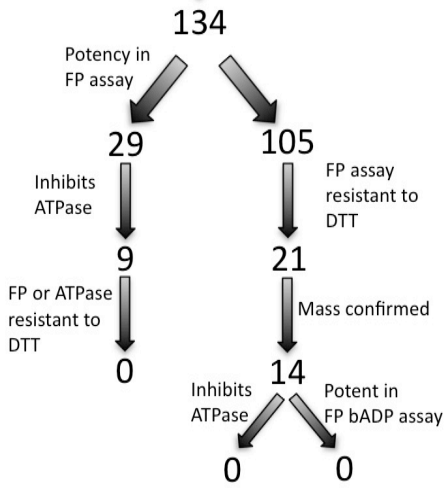

Figure 2-1. Overview of the secondary screen of YjeE.

(Left branch) Of the 134 compounds that were selected from the primary screen, the 29 most potent compounds were tested in an ATPase activity assay. Nine inhibitors were identified and the sensitivity of inhibition to DTT was tested in the activity assay and the FP binding assay. All compounds were sensitive to DTT in the ATPase assay. (Right branch) The 105 compounds that were not selected in the first round were tested for sensitivity of the inhibition to DTT in the FP assay. Some 21 DTT-resistant compounds were found and the identities of 14 were confirmed by mass spectrometry. None of the DTT resistant compounds were active in either the ATPase assay or in the FP assay when a red-shifted fluorophore (bADP) was substituted for mADP.

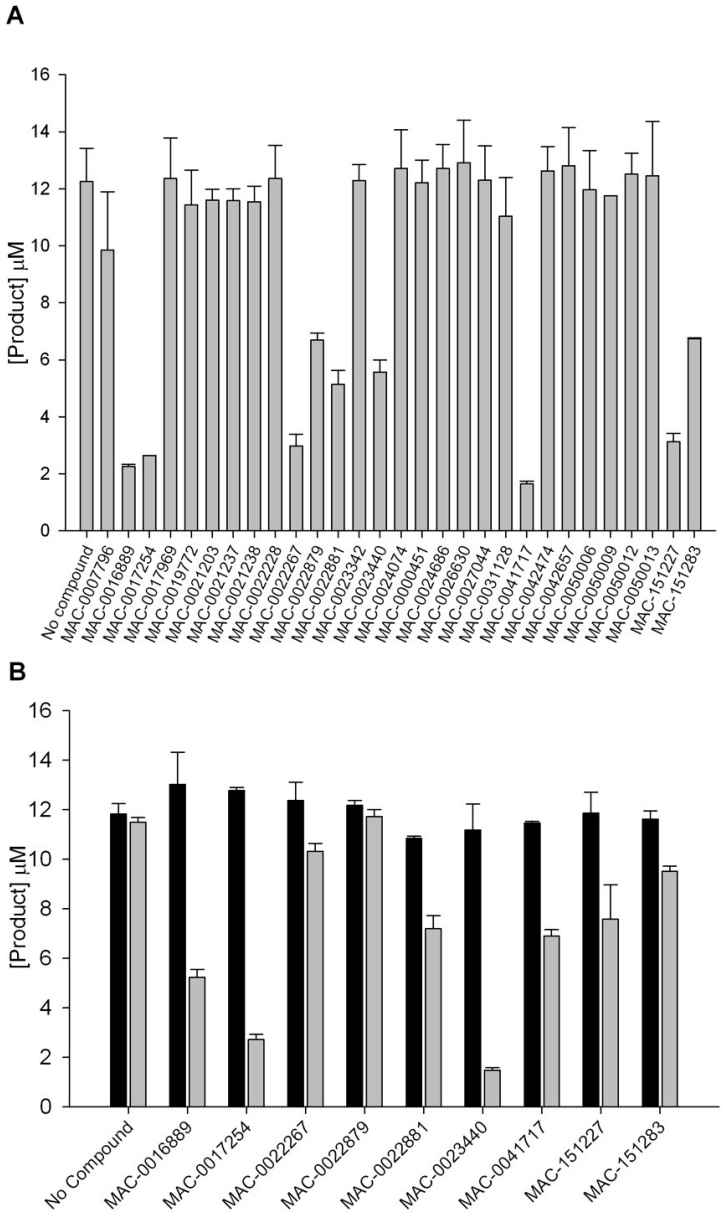

Figure 2-2. ATPase activity of YjeE in the presence of the 29 most potent compounds from the primary screen.

(A) The hydrolysis of 1 mM ATP by 10 μM YjeE was tested in the presence of 29 compounds that were obtained from the library compound plates. **(B)** Nine compounds that showed inhibition in the initial assay were re-ordered and tested in the ATPase assay in the presence (black bars) or absence (grey bars) of 1 mM DTT. Data represent the average of triplicates and error bars represent one standard deviation.

All 9 compounds lost activity in both the ATPase assay and the FP assay in the presence of 1 mM DTT (Figure 2-2B, black bars; Figure 2-3, A-I). DTT did not affect the ability of YjeE to hydrolyze ATP or bind mADP (Figure 2-2B and Figure 2-3, J).

2.4.2 Second round of compound selection

All of the compounds in the first round of selection were found to be reactive so the remaining 105 active molecules from the primary screen were revisited. Sensitivity of binding to DTT was used as a filter for reactive compounds. Each of the 105 compounds was tested in dose-response FP assays for activity in the presence of DTT and 21 DTT-resistant compounds were identified. Of these, the identities of 14 compounds were confirmed by mass spectrometry.

The dose-response curves of the 14 compounds with confirmed masses are shown in the appendix Figure A-1. The activity of one such compound (MAC-0000451) and a control (ADP) are shown in Figure 2-4A and 2-4B, respectively. MAC-0000451 had IC_{50} constants in the presence and absence of DTT of 54 μM and 68 μM, respectively. In the control assay, unlabeled ADP was used to displace mADP. ADP produced similar results as MAC-0000451, with IC_{50}s of 59 μM and 78 μM in the presence and absence of DTT, respectively (Figure 2-4B). The fluorescence intensity of each well is overlaid in Figure 2-4 and Figure A-1, open triangles. In most cases, a two to five fold increase in fluorescence intensity was observed with increasing compound (Figure A-1), suggesting that the compounds themselves were fluorescent. Three compounds exhibited only 1.5 fold increase in fluorescence but these compounds were only poor or partial inhibitors (Figure A-1 I-J). None of the 14 mass-confirmed compounds were found to significantly inhibit the ATPase activity of YjeE (Table 2-1).

2.4.3 bADP FP assay

The high fluorescence of the 14 mass confirmed compounds suggested that the high fluorescence might be confounding to the FP measurement of mADP. To test this hypothesis, a red-shifted BODIPY-TR labeled ADP (bADP) was used in place of the mADP in the binding assay. First, the K_D constant of bADP for YjeE was determined by measuring the FP of a solution of fixed bADP concentration (0.5 μM) and increasing concentrations of YjeE (2.6 μM – 140 μM) (Figure 2-5A). The resultant data was fit to a single-site hyperbolic binding function, which produced a K_D of 26 ± 4 μM. This is in agreement with previously published affinity for the unlabeled nucleotide [34]. Single point binding assays were performed using both mADP and bADP at a high compound concentration (125 μM) (Figure 2-5B). High and low

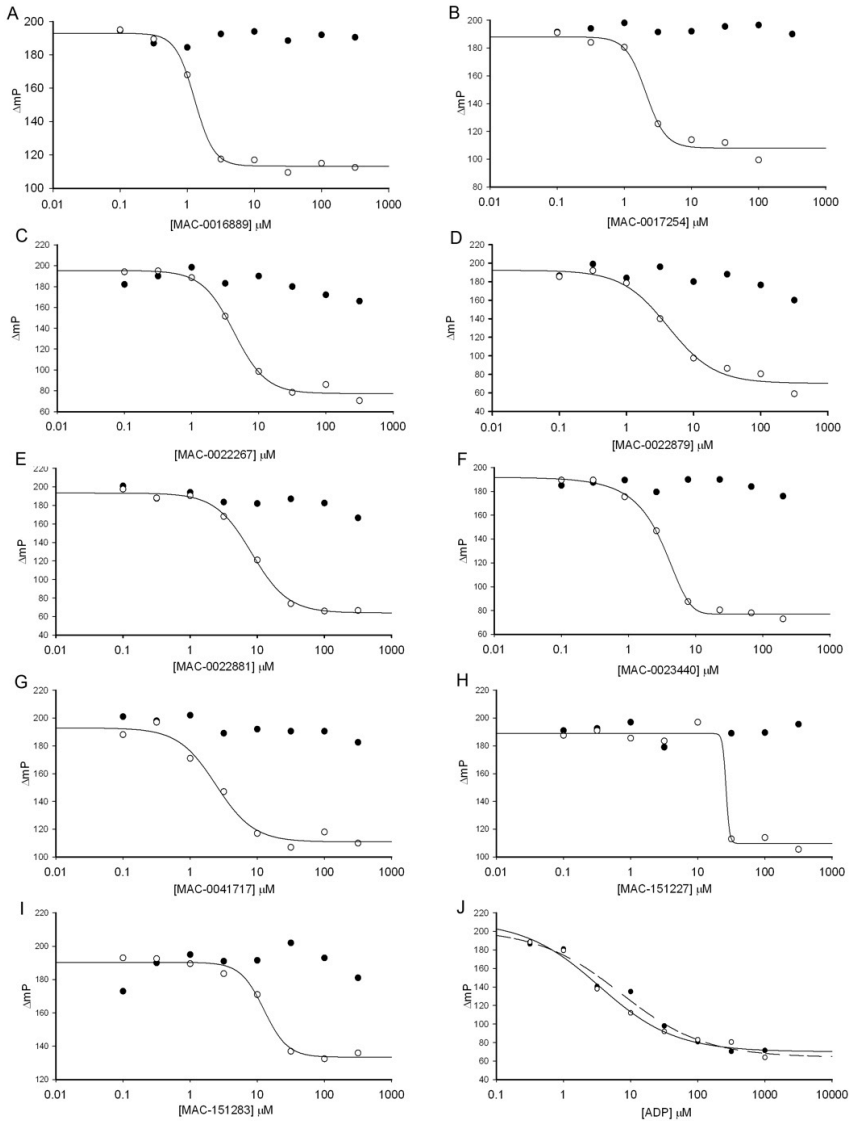

Figure 2-3. Dose-responses of binding and sensitivity to DTT of 9 YjeE active molecules.

Increasing amounts of **(A-I)** compound or **(J)** ADP were incubated with 10 μM YjeE and 2 μM mADP in the presence (closed circles) or absence (open circles) of DTT. Fitted curves are drawn with solid or dashed lines when assays were performed in the absence or presence of DTT, respectively. Data are the average of duplicates.

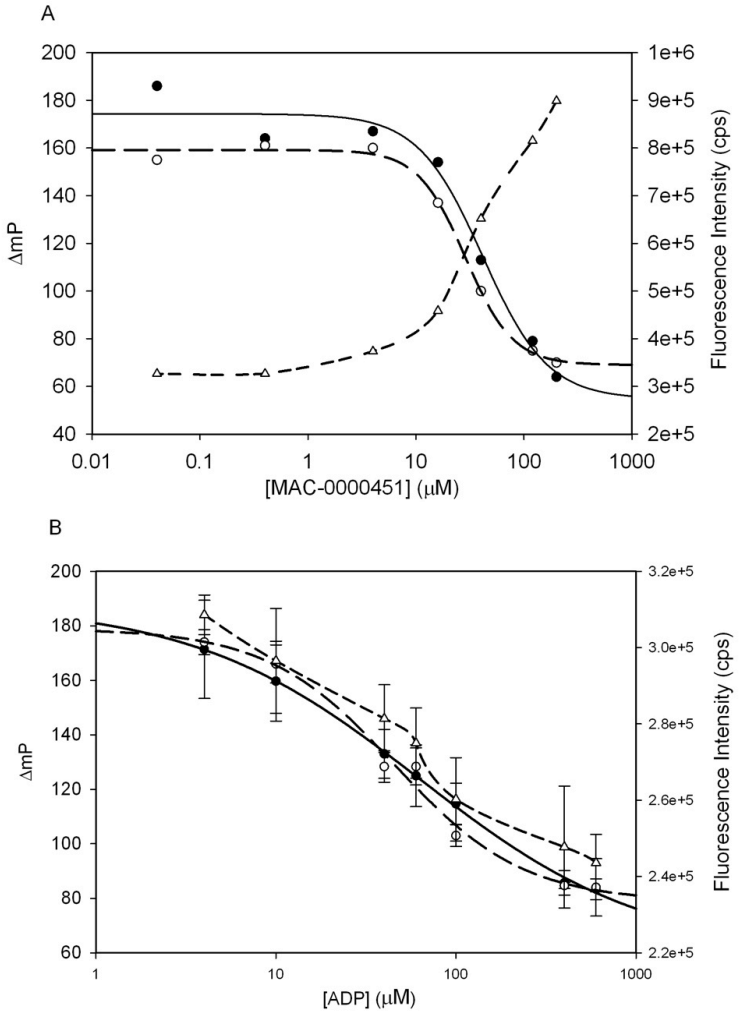

Figure 2-4. Dose-responses to binding of one of the 14 DTT-resistant compound and ADP in the fluorescence polarization assay.

Dose-response curves of YjeE bound to mADP with increasing concentrations of **(A)** MAC-0000451 or **(B)** ADP in the presence (closed circles, solid lines) or absence (open circles, long dashed lines) of DTT. Data were collected and processed as in Figure 2-3. Data for MAC-0000451 and ADP represent the average of duplicates and triplicates, respectively. Errors bars represent one standard deviation. Fluorescence intensity (triangles, short dashed line) is presented on the secondary y-axis.

Table 2-1. The ATPase activity of YjeE in the presence of DTT-resistant compounds.

Compound	ADP [a] (μM)		σ
None	13.0	±	0.2
MAC-0000451	10.9	±	0.1
MAC-0000886	13.3	±	0.4
MAC-0010953	10.8	±	0.1
MAC-0020594	11.4	±	0.6
MAC-0022228	11.3	±	0.7
MAC-0023342	10.8	±	0.0
MAC-0024686	11.1	±	0.5
MAC-0027045	12.8	±	0.2
MAC-0043879	12.6	±	0.5
MAC-0050012	14.6	±	1.1
MAC-0050014	11.6	±	0.7
MAC-0050889	14.4	±	0.2
MAC-0050927	14.3	±	2.1

[a]-10 μM YjeE was incubated with 1 mM ATP in the presence of DMSO or 100 μM compound for four hours at RT. The reaction was quenched with 6 M urea and the products were quantified by HPLC.

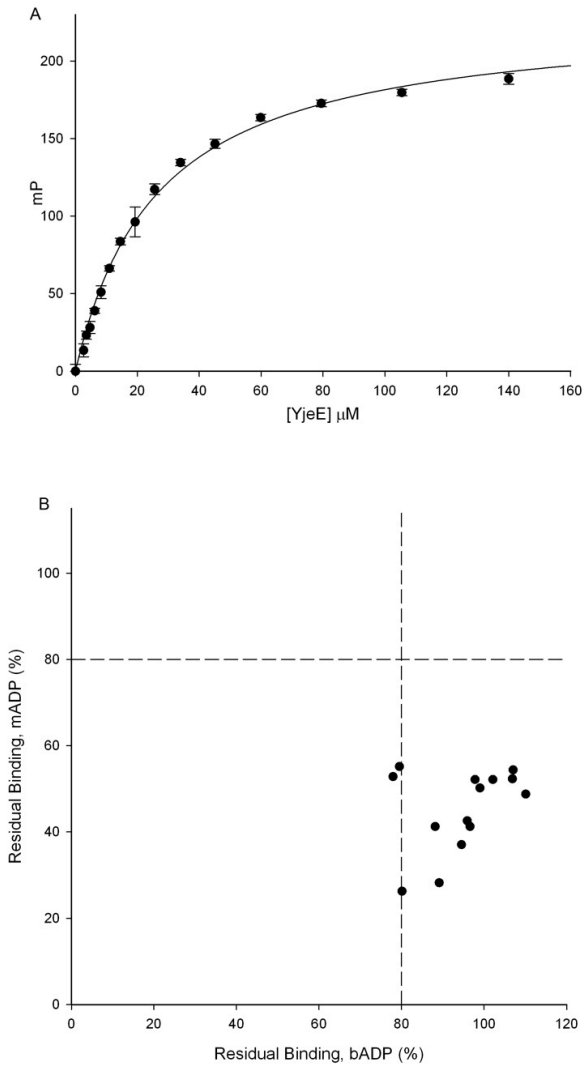

Figure 2-5. The activity of DTT-resistant compounds with bADP.

(A) Determination of the K_D of bADP against YjeE. Increasing amounts of YjeE (2.6 – 150 μM) were incubated with a fixed concentration of bADP (0.5 μM) and the fluorescence polarization was read. These data were fit to the hyperbolic function $mP = (mP_{max}+[YjeE])/(K_D+[YjeE])$ using SigmaPlot v. 11.0 (SPSS Science, Chicago, IL, U.S.A) and a K_D of 26 ± 4 μM was obtained. Data represent the average of triplicates. **(B)** The effect of the fluorophores mADP (y-axis) or bADP (x-axis) on the apparent inhibition of binding by the 14 DTT-resistant compounds. Residual binding was calculated using the following equation (s - μL)/(μH - μL) where s, μL and μH represent sample data, the mean of low control data (n=6) and mean of the high control data (n=6), respectively. The hashed line represents the statistical cut-off of three standard deviations below the uninhibited binding reaction.

controls contained 5mM ADP or DMSO, respectively. The statistical cutoff for binding was set to 3 standard deviations below the high controls (n=6), corresponding to 80% residual binding. All compounds had residual binding below 55% when the fluorophore was mADP, however, there was no observed inhibition when bADP was used. Two compounds that only registered marginally below the statistical cut-off, MAC-0000451 (78.0%) and MAC-0000886 (79.5%), were not pursued.

2.4.4 ASMS development and implementation

Another assay was used to probe the binding of ligands to YjeE. ASMS is based on rapid isolation of the protein:ligand complex using SEC. Purified *E. coli* DHFR and compounds of known affinities were used to optimize the assay. We made miniature SEC columns in 96-well filter plates using size-exclusion Sephadex G-50 resin. DHFR (50 μM) and ^{14}C-trimethoprim (25 μM) were pre-incubated. Half of this mixture was layered onto the SEC column and half was used as a reference for the maximum recovery of ligand. The columns were then centrifuged to elute the DHFR:trimethoprim complex into a 96-well receiver plate below.

The amount of C^{14}-trimethoprim in the complex was determined by liquid scintillation counting. The amount of trimethoprim recovered is reported as a percentage of the total added (Table 2-2, "+DHFR"). The column was efficient in retaining unbound trimethoprim, as 67.39% and 0.35% of trimethoprim was recovered in the eluent in the presence and absence of the protein DHFR, respectively (Table 2-2, "-DHFR", condition 1).

Doubling the DHFR concentration did not increase the yield of trimethoprim (data not shown). Five other conditions were tested in order to maximize the sensitivity and reliability of the ASMS assay. In condition 2, when the bed volume was halved, this smaller column was less efficient in retaining free ligand as 6.98% of trimethoprim was found in the eluent (Table 2-2, condition 2). Chromatographic separation can become less efficient in loosely packed resin with a high void volume. In condition 3, the SEC columns were pre-centrifuged to increase packing and the evacuated buffer was replaced (Table 2-2, condition 3). This procedure had the undesired effects of reducing the recovery of trimethoprim in the presence of DHFR by half and reducing the retention of unbound trimethoprim.

A study by Penefsky and others found that partial dehydration of size exclusion columns prior to use increased recovery of protein:ligand complexes and minimized dilution of the sample [208]. In condition 4, partial dehydration of the SEC columns was accomplished by a short centrifugation. Although the pre-spin reduced the recovery of trimethoprim in the presence of DHFR, it increased the retention of unbound ligand on the column so this practice was continued (Table 2-2, condition 4).

Table 2-2. ASMS development.

		+DHFR		-DHFR			
Condition#	Pre-spin (min•g)	Recovery (%)	σ	Recovery (%)	σ	Bed Volume (μL)	Sephadex Resin
1	0	67.39	2.62	0.35	0.11	200	G-50
2	0	63.05	4.95	6.98	3.06	100	G-50
3	4000	27.42	25.58	0.53	0.39	200	G-50
4	4500	11.14	10.86	0.01	0.00	200	G-50
5	300	60.15	2.75	0.11	0.10	200	G-25, fine
6	300	32.25	9.44	2.40E-03	0.00	200	G-25, superfine

To further increase the efficiency of retention of unbound ligand on the column, two finer grades of resin were used, Sephadex G-25 fine and superfine (Table 2-2, conditions 5 and 6). Sephadex G-25 superfine produced a satisfactory recovery of protein:ligand complex (32.25 %) and, importantly, this was the condition with the lowest amount of trimethoprim eluted in the absence of DHFR (0.0024 %) (Table 2-2, condition 6). This condition was used for future assays.

2.4.5 ASMS using DHFR ligands of varying affinity

The ASMS protocol described above was tested for the ability to identify two ligands with lower affinities than trimethoprim. These compounds were identified in an HTS campaign at the McMaster High Throughput Screening Laboratory for inhibitors of *E. coli* DHFR [203]. Trimethoprim and the lower affinity inhibitors were tested against DHFR using the ASMS protocol and were detected by electrospray mass spectrometry. Mass spectra of the three compounds are shown in Figure 2-6, A-C. The extracted ion traces for the three compounds around 5 m/z units are shown in Figure 2-6, D-F. The black and red lines in the ion traces represent the sample pre and post selection on the SEC column. Figure 2-6 shows the results for trimethoprim (K_i = 3.8 nM, Figure 2-6A & 6F), compound 1 (K_i = 190 nM, Figure 2-6B & 6E) and compound 2 (K_i = 2000 nM, Figure 2-6C & 6F). The pre-selection samples ionized robustly with a strong signal of $\sim 10^7$ cps each. Bound trimethoprim and compound 1 were detected in the post-selection samples with similar peak signal intensities of 4.0 X 10^6 and 4.2 X 10^6 cps respectively. The lowest affinity inhibitor, compound 2, was detectable at a signal intensity of 1.3 and 10^6 cps.

2.4.6 ASMS with putative YjeE ligands

The ASMS protocol, in conjunction with detection by mass spectrometry, was used against the 14 mass-confirmed YjeE ligands. A modification was made to the technique whereby the unselected sample was added to the effluent of a mock selection and prepared for mass spectrometry in the same manner as the selected samples. One half of the sample was applied to the SEC column. The other half was used as a positive control and directly injected into the mass spectrometer to represent the maximal recovery of ligand. To increase the low signal, samples were introduced directly into the mass spectrometer at ~50μL/min instead of first subjecting them to reverse phase chromatography. This provided 1 minute of sampling time through the mass spectrometer and was sufficient to detect ligands. The elimination of reverse phase chromatography produced mass spectra that were dominated by buffer components and molecular adducts of sodium. To reduce this effect, HEPES was reduced from 50 mM to 1 mM in the binding reaction and the resin was equilibrated in 10 mM ammonium acetate to remove HEPES from the final

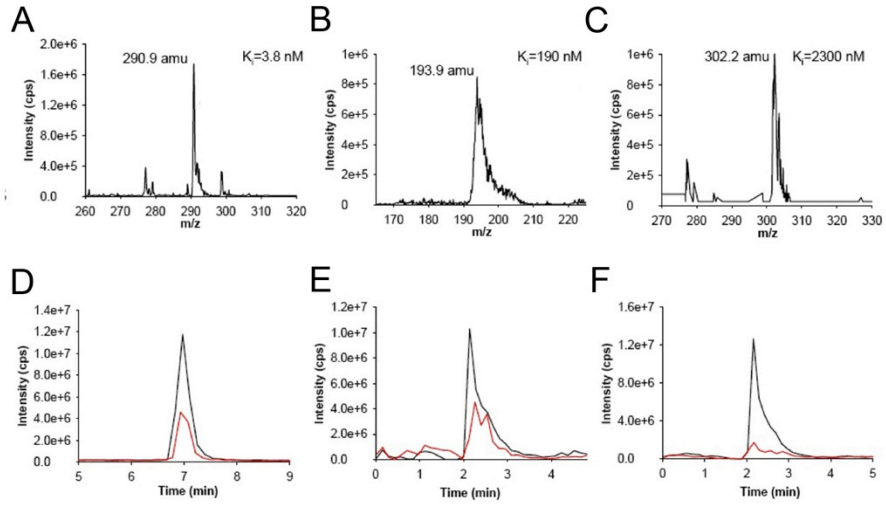

Figure 2-6. ASMS of competitive DHFR inhibitors of varying K_i.

ESI+ spectra of DHFR inhibitors, (A) Trimethoprim, (B) compound 1 and (C) compound 2 to confirm the masses of the ligands. K_i against DHFR is indicated as previously determined [203]. (D-F) Selected Ion Chromatogram (|m/z M+H| ± 2.5 amu) of DHFR inhibitors, (D) trimethoprim, (E) compound 1 and (F) compound 2. The black lines represent the pre-SEC sample containing total ligand while the red lines represent the post-SEC samples containing bound ligand.

sample. Ammonium acetate is volatile and thus compatible with mass spectrometry. These improvements produced satisfactory spectra but no binding of YjeE to putative ligands was observed.

2.5 DISCUSSION

All of the compounds identified in the primary screen turned out to be highly fluorescent or reactive. The first round of compounds selected were potent, but were later found to be reactive. In the second round of selection, compounds were identified that were not reactive but were less potent. These compounds had a low enough intrinsic fluorescence to pass a fluorescence intensity cut-off, but high enough to influence the FP measurements. The cut-off was set to exclude compounds with fluorescence intensity greater than three standard deviations above the high control. The high compound fluorescence was revealed in dose-response assays. At the concentration of compound that was used in the primary assay, the fluorescence intensity was relatively low. As the compound concentration was increased in the dose-response assay, the fluorescence intensity also increased. The intrinsic fluorescence of the compounds likely decreased the measured overall FP of the solution and thus caused false positives.

The ASMS procedure was extensively optimized for measuring the binding of ligand to protein. Quantitative binding of ligands of varying affinities for DHFR was demonstrated. This assay could detect the binding of ligands to DHFR with low micro-molar or higher affinity. The success of the assay was contingent upon the ability to detect ligands by mass spectrometry. The DHFR ligands ionized well and produced a robust signal of 10^7 cps. When the putative YjeE ligands were tested in the ASMS assay, there was a large variability in the ability to detect compounds. Most of the potential YjeE ligands produced signals that were 1 to 2 orders of magnitude less than the DHFR ligands, thus, the detection of ligands has to be optimized individually.

Using an NMR-based approach, Abbott pharmaceuticals screened mixtures of compounds against *H. influenzae* YjeE [209]. They found a biphenyl-substituted molecule that bound YjeE with a K_D of 80 μM, which was then optimized to low micromolar K_D. Four similar molecules were found in the Maybridge compound library that was screened here, however, none were active in the screen. Based on the affinity of mADP for YjeE, the estimated IC_{50} for the active Abbott molecule in the FP assay would be ~200 μM [210]. The concentration of compound used in the FP screen was 10 fold lower so the screen would not have been sensitive to this inhibitor.

Efforts should be continued to develop a small molecule inhibitor of YjeE to achieve quick inhibition of protein function and reduce non-specific pleiotropic effects. YjeE was found to participate in the modification of tRNA, along with YeaZ and YdjD. Many of the other phenotypes that arise from YjeE depletion may be

explained by pleiotropy. For example, depletion of YjeE, YeaZ and YdjD in *E. coli* led to filamentous cells, tiny cells and curved cells with ruffled membranes, respectively [50]. Another unexplained phenotype of depletion of YjeE in *E. coli* was a high level sensitivity to polymyxin B, which is a membrane-active antibiotic [211]. A chemical probe would be useful for testing the importance of the tRNA modification that YjeE helps to carry out and resolving the true function from secondary effects.

3 CHAPTER THREE - KNOWN BIOACTIVE MOLECULES PROBE THE FUNCTION OF YJEE

3.1 Chapter 3 Preface

The follow chapter has been published in:

Mangat, C.S., & E.D. Brown (2008). Known bioactive molecules probe the function of a widely conserved but enigmatic ATPase, YjeE. *Chemistry and Biology*, 15(12), 1287-1295. © Elsevier Ltd.

I wrote the manuscript and edits were contributed by Dr. Eric D. Brown

Permission has been granted by the publisher to reproduce this material here.

3.2 INTRODUCTION

The failure to find a chemical probe of YjeE in the work described in the previous chapter prompted a more direct approach to understanding YjeE's function. Inspiration was drawn from our own group's success with gene reporters that were responsive to lesions in the teichoic acid biosynthetic pathway [212]. In that work, P_{ywac} promoter activity was found to increase in response to lesions in late, but not early, steps of teichoic acid biosynthesis. A screen of bioactive molecules for those that increase P_{ywac} activity identified antibiotics known to affect the recycling of a chemical intermediate common to both teichoic acid and peptidoglycan biosynthesis, which suggested a connectivity between these two pathways. This hypothesis was supported biochemically by the demonstration that peptidoglycan biosynthesis was reduced when late steps of teichoic acid were inhibited.

To better probe the function of YjeE, we took a non-traditional approach of using bioactive molecules of known mechanisms to search for chemical-genetic interactions using a YjeE-responsive promoter. Chemical-genetic refers to the use of small molecules to inhibit biological process, in much the same way that genetics can perturb biology. By measuring the expression of *yjeE* in the presence of these chemically induced perturbations we aimed to uncover a phenotype for *yjeE* that was more informative than lethality, which was the only known phenotype. Recent chemical-genetic approaches have been successful in elucidating new components of the DNA damage response and in discovering new machinery in outer membrane assembly in bacteria [213, 214].

Herein, we have used chemical probes in a directed manner against a protein of unknown function to broadly ascertain its function. This work serves as a proof-of-principle of the potential of chemicals in the discovery of novel biological activities. We constructed a luminescence-based reporter that was up-regulated in response to depletion of YjeE. This promoter-reporter system was used to screen a well-characterized chemical library for compounds that could induce expression of *yjeE*. Norfloxacin, a fluoroquinolone inhibitor of DNA metabolism, was found to be the most profound inducer. Noting the recently uncovered role of norfloxacin in oxidative stress [215, 216], we further characterized the norfloxacin-dependent response of P_{yjeE} in deletion backgrounds of two-component regulatory systems. The latter encompassed some 37 genes responsible for adaptation of *E. coli* to various stresses by controlling diverse aspects of physiology [44]. This experiment uncovered links to central metabolism, stress responses and metal homeostasis. These interactions, along with observations from literature, led us to the hypothesis that YjeE may be involved in respiration. Remarkably, we found that *E. coli yjeE,* a well-known essential gene, was dispensable under anaerobic conditions.

3.3 MATERIALS AND METHODS

All restriction endonucleases and Vent® polymerase were purchased from New England Biolabs Inc. (Beverly, MA). Oligonucleotides were from MOBIX (Hamilton, ON). Viewlux® 96-well plates for luminescence measurements were from Perkin Elmer (Boston, MA). All antibiotics used were purchased from Sigma-Aldrich (Oakville, ON).

Construction of pCS26-*bla*

The β-lactamase resistance cassette (*bla*) from pBluescript (Novagen, Madison, WI) was amplified with Vent polymerase using the primers 5'-GGGGGAGCTCATGAGTAAACTTGGTCTGACAGTTACC-3' and 5'-AAAAGAAGACGAAAGGGCGTGGCACTTTTCGGGGAAATGTGCGCGGAA CCCC-3' where the underlined sequences indicate SacI and BbsI sites respectively. The kanamycin resistance cassette was excised from pCS26-pac by digestion with SacI and BbsI and *bla* was ligated in its place [217]. The resistance cassette is transcribed in the opposite direction as the adjacent *luxCDABE* operon to ensure that it does not influence expression of the reporter.

Construction of pCS26-*bla*-P_{yjeE} and pCS26-*bla*-P_{yjeF}

The 750 bp regions upstream of the *yjeE* and *yjeF* translational start sites were amplified with Vent® polymerase using the primer pairs 5'-CCCCGGATCCGGTTTTTATCAGTCA CTTCCGG-3',5'-GGGCTCGAGCGTATGACGGGGGAAGCGGCG-3' and 5'-GGGGCTCGA GAGCTGGCAGTCATCGCAACCG-3',5'-CCCCGGATCCGTCAGAGCCCCTCGATCTCA ATCAGTTAGCG-3', respectively, where the underlined sequences indicate BamHI and XhoI restriction sites. Each PCR product was digested with BamHI and XhoI and ligated into pCS26-*bla* using standard cloning techniques to yield pCS26-*bla*-P_{yjeE} and pCS26-*bla*-P_{yjeF}.

Promoter profiling

A saturated culture grown overnight at 37°C was diluted 1:400 into fresh Luria Bertani media and incubated in 96-well Viewlux® plates at 37°C with rotation at 250 rpm. Cells were treated with compounds from the Prestwick Chemical Library (Prestwick Chemical Inc., Washington, D.C.) dissolved in dimethylsulfoxide (DMSO) to a maximum final concentration of 1% (*v/v*). Low controls were treated with DMSO alone. The outer wells of the plates were not used to avoid edge effects due to evaporation. Compound addition was carried out by a Biomek FX Liquid Handler (Beckman Coulter, Fullerton, CA) fitted with a 96-channel head. Luminescence was measured in a Perkin Elmer Envision® luminometer with an ultrasensitive luminescence

module (Perkin Elmer, Boston, MA). Data were plotted using SigmaPlot software (San Jose, CA).

Construction of a *gyrA* chromosomal mutant

A Ser83Leu / Asp87Tyr double mutation was introduced into the chromosome of wild-type *E. coli* MG1655 by transforming a 2 Kb linear DNA fragment containing the mutations in the center of the sequence. To create this 2 Kb product, a crossover PCR strategy was used where primers gyrA-A (5'-GATATGCCGCTCTTTTAAACTGG-3') and gyrA-B (5'- TGGCTGCGCCATGCGGACGATCGTGTAATAGACC GCCTGGTCACCATGGGGATGGT ATTTACC -3') were used to amplify 1 kb upstream of the gyrA mutation site and primers gyrA-C (5'-GGTAAATACCATCCCCATGGTGACCAGGCGGTCTATTACACGATCGTCCGCAT GGCGCAGCCA-3') and gyrA-D (5'-CGTCCGGAATGGCTGGAGCCAGAG-3') amplified 1 kb downstream. Primers gyrA-B and gyrA-C were complementary to each other and both contained base substitutions to introduce the mutations (underlined in sequence). Primers gyrA-A and gyrA-D were used to join these two overlapping 1 kb products by crossover PCR. The 2 kb product was purified and transformed into electrocompetent *E. coli* MG1655 cells. Colonies containing the chromosomal mutations were selected on 20 μg/mL of nalidixic acid.

Deletions of two-component systems

All single deletions were obtained from the Keio deletion collection [218]. Only deletions of the transcriptional activator of each two-component system, as identified by Oshima *et al*, were tested. Where the transcriptional activator was not known, the deletion of the sensor histidine kinase was used instead [44].

Growth under anaerobic conditions

All strains were picked from a single colony and grown overnight in LB media supplemented with 50 μg/mL kanamycin. Cultures were diluted 1:400 into fresh LB and grown to an OD_{600} ~ 0.3 before diluting again to a final OD_{600} of 0.1. Cultures were then subjected to 10-fold serial dilutions and 1 μL of each dilution was spotted onto LB-agar (1.5% *w/v*) supplemented with 50 μg/mL kanamycin. Plates were grown under anaerobic conditions using the GasPak™ EZ Anaerobe container system (Becton Dickenson, Oakville, ON) according to the manufacturer's instructions for 4 days at 37°C.

3.4 RESULTS

3.4.1 Reporter validation

Wildtype *E. coli* MG1655 contains two promoters upstream of *yjeE* which may influence its expression [219]. The promoter proximal to *yjeE* (P_{yjeE}) is located within the upstream gene, *yjeF,* whereas the promoter distal to *yjeE* (P_{yjeF}) is located upstream of *yjeF* (Figure 3-1A). The activity of each of these promoters was monitored using the reporter plasmid pCS26-*bla,* which encodes the luciferase operon, *luxCDABE*. This promoter-less plasmid is an ampicillin resistant derivative of pCS26-pac [217]. The 750 bp regions upstream of the start sites of *yjeE* and *yjeF* were cloned into pCS26-*bla* to generate pCS26-*bla*-P_{yjeE} and pCS26-*bla*-P_{yjeF}, respectively.

In order to determine whether expression from either P_{yjeE} or P_{yjeF} is regulated by the intracellular concentration of YjeE, the activities of the promoters were tested in a strain where the level of YjeE could be modulated. In this conditional null, native *yjeE* was replaced by a chloramphenicol resistance cassette while an ectopic copy of *yjeE* was placed at the *araBAD* locus under the control of the arabinose-inducible P_{BAD} promoter [34]. Thus, depletion of cellular YjeE can be achieved by growth in the absence of arabinose. To counter leaky expression of *yjeE* from the P_{BAD} promoter, cells were subjected to three rounds of growth and dilution into media lacking arabinose. This resulted in almost no growth during the fourth round of growth in the absence of arabinose (Figure 3-1B, closed symbols), while cells grown in the presence of arabinose grew robustly (Figure 3-1B, open symbols). The presence of plasmids pCS26-*bla*-P_{yjeE} (Figure 3-1B, triangles) or pCS26-*bla*-P_{yjeF} (Figure 3-1B, circles) did not affect the growth of cells. Under these conditions, pCS26-*bla*-P_{yjeF} showed a modest 3-fold induction of expression upon depletion of the YjeE protein (Figure 3-1C, circles), whereas, pCS26-*bla*-P_{yjeE} exhibited a 73-fold induction (Figure 3-1C, triangles). This large increase in the activity of P_{yjeE} in response to YjeE depletion suggested that this promoter is subject to regulation in the cell by the level of YjeE and is thus likely to be the physiologically relevant promoter for *yjeE*.

In order to test if the promoter activity of P_{yjeE} was only influenced by the addition of arabinose by some trivial mechanism, expression from the promoter was monitored in the presence or absence of arabinose in a strain diploid for *yjeE*. The diploid strain contains a copy of *yjeE* at its native locus as well as a copy at the *araBAD* locus. In this strain, addition of arabinose only caused a small 3-fold change in the activity of P_{yjeE} (Figure 3-2). Furthermore, promoter activity was similar in the *yjeE* conditional null grown in the presence of arabinose as it was in wildtype

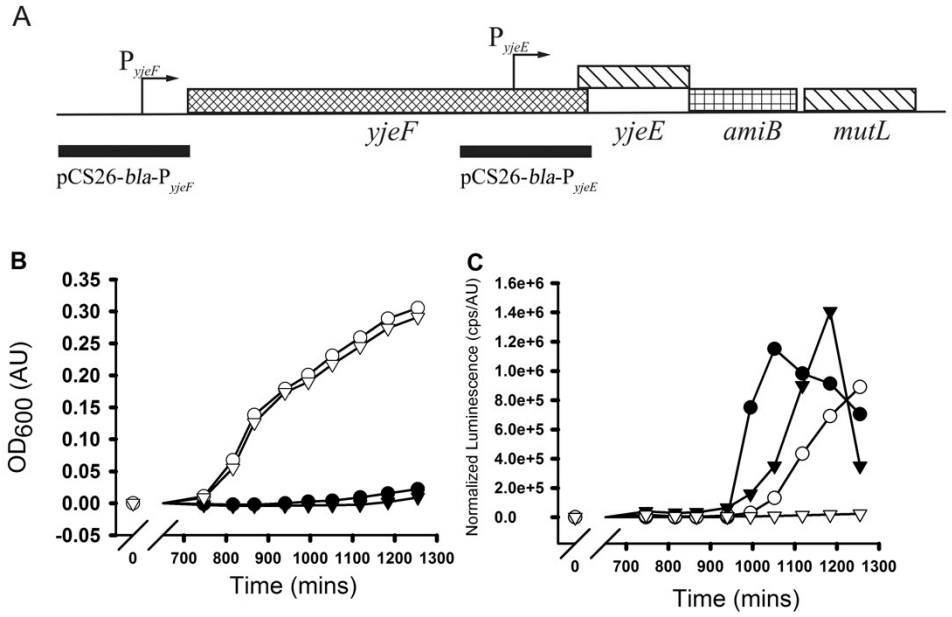

Figure 3-1. Identification of a promoter that responds to the intracellular levels of YjeE.

(A) The *yjeE* chromosomal locus of *E. coli* MG1655. Black bars represent the upstream regions, termed P_{yjeF} and P_{yjeE}, which were cloned into the luminescence reporter plasmid to produce either pCS26-*bla*-P_{yjeF} or pCS26-*bla*-P_{yjeE} respectively. **(B,C)** Growth and luminescence produced by an arabinose-inducible *yjeE* conditional null harboring either pCS26-*bla*-P_{yjeE} (triangles) or pCS26-*bla*-P_{yjeF} (circles). The conditional null was grown under YjeE-deplete (closed symbols) or YjeE-replete (open symbols) conditions. **(B)** OD_{600} and **(C)** density-normalized luminescence are shown.

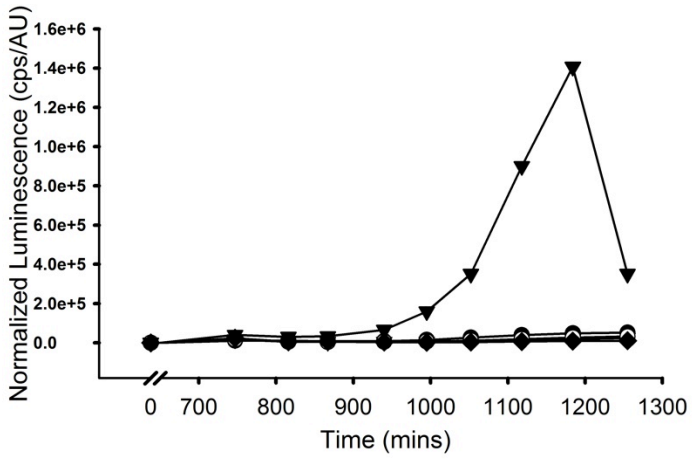

Figure 3-2. Control promoter activity.

Luminescence normalized by OD_{600} of strains harboring the pLux-P_{yjeE} plasmid grown in the presence (open symbols) or absence (closed symbols) of arabinose. Shown are the *yjeE* diploid (circles), wildtype *E. coli* (diamonds) and the *yjeE* complemented knock-out (triangles). Values represent the average of duplicates.

E. coli MG1655 (Figure 3-2). These data suggest that induction of P_{yjeE} activity was not an artifact of arabinose treatment or the consequence of polar effects on genes downstream of *yjeE*.

3.4.2 Development of the P_{yjeE} reporter for HTS

Preliminary tests using a small set of antibiotics revealed that spectinomycin and tetracycline were both able to induce expression from P_{yjeE}. These two antibiotics determine the optimal culture density and concentration to carry out the HTS. It was found that addition of compound at OD_{600} of ~ 0.1 produced an optimal promoter response (Figure 3-3). For both compounds, induction was maximal near their published minimum inhibitory concentrations (MIC) but significant induction was observed within a range of 4-fold above or below the MIC (Figure 3-4). To reduce false negatives, the screen was carried out at two concentrations of compound, 1 μM and 10 μM, which is within 4-fold of the MIC of the majority of antibiotics in the library.

3.4.3 Screen for small molecules with known biological activity that influence the expression of P_{yjeE}

Wildtype *E. coli* MG1655 harboring pCS26-*bla*-P_{yjeE} was used to query the Prestwick Chemical Library (Prestwick Chemical Inc., Washington, D.C.). This library contains a variety of FDA approved drugs and bioactive compounds, including 172 antibiotics. The screen was performed in duplicate. Cell density (OD_{600}) and luminescence were measured hourly for 8 hours after addition of compound and for each time point, luminescence was normalized by cell density.

The maximum fold-increase in normalized luminescence between treated and untreated cells was plotted for each compound (Figure 3-5A & 3-5B). The hit zone was defined as those compounds that caused an increase in normalized luminescence that was more than 6 standard deviations above the untreated controls. Black circles represent the compounds that were defined as hits, open circles represent the compounds that did not affect the activity of P_{yjeE} while gray circles represent untreated controls. Figures 3-5C & 5D show the densities of compound-treated cultures, normalized by the density of the untreated controls. These data revealed that compounds that had an impact on growth also caused stimulation of P_{yjeE}. For example, at 1 μM, all of the compounds that decreased growth rate also induced P_{yjeE}.

3.4.4 Dose dependence of six representative hit compounds

Antibiotics with well-characterized mechanisms of action that caused stimulation of P_{yjeE} were chosen for further study of the function of YjeE. Of 26 hits,

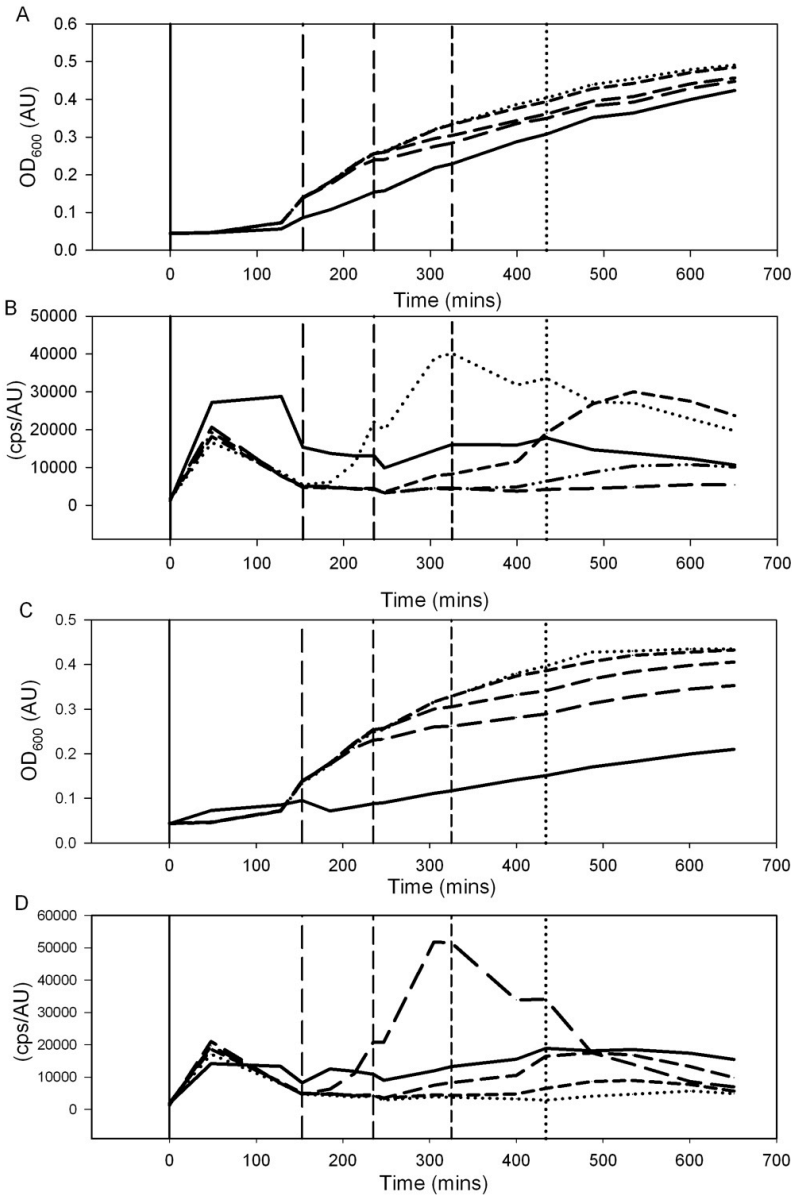

Figure 3-3. Influence of culture density on P_{yjeE} sensitivity to tetracycline and spectinomycin.

E. coli cells harboring pCS26-bla-PyjeE were grown overnight and diluted in 1:250 into fresh media. Cultures were then treated with 8 μg/mL of **(A & B)** streptomycin and **(C & D)** tetracycline at various culture densities, (solid) 0, (long dash) 0.1, (medium dash) 0.2, (short dash) and 0.4 (dotted). Vertical lines indicate when antibiotics were added and are coordinated with the above scheme. Luminescence and OD_{600} were read approximately every hour for 10 hours following dilution. Data represent the average of duplicates

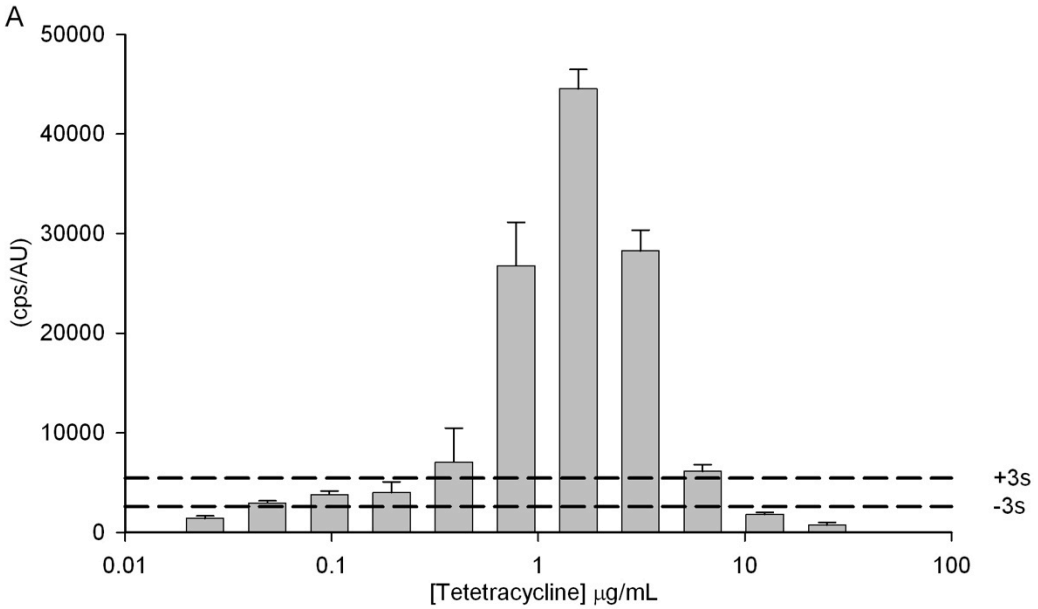

Figure 3-4. Influence of tetracycline concentration of P_{yjeE} activity.

P_{yjeE} activity was monitored as in Figure 3-2 with increasing concentrations of tetracycline added at an OD_{600} = 0.1. Luminescence and optical density were monitored and the peak OD_{600} normalized luminescence is presented above. Hashed lines represent three standard deviations above and below the normalized luminescence of untreated cells. Data are the average of triplicates and error represent one standard deviation.

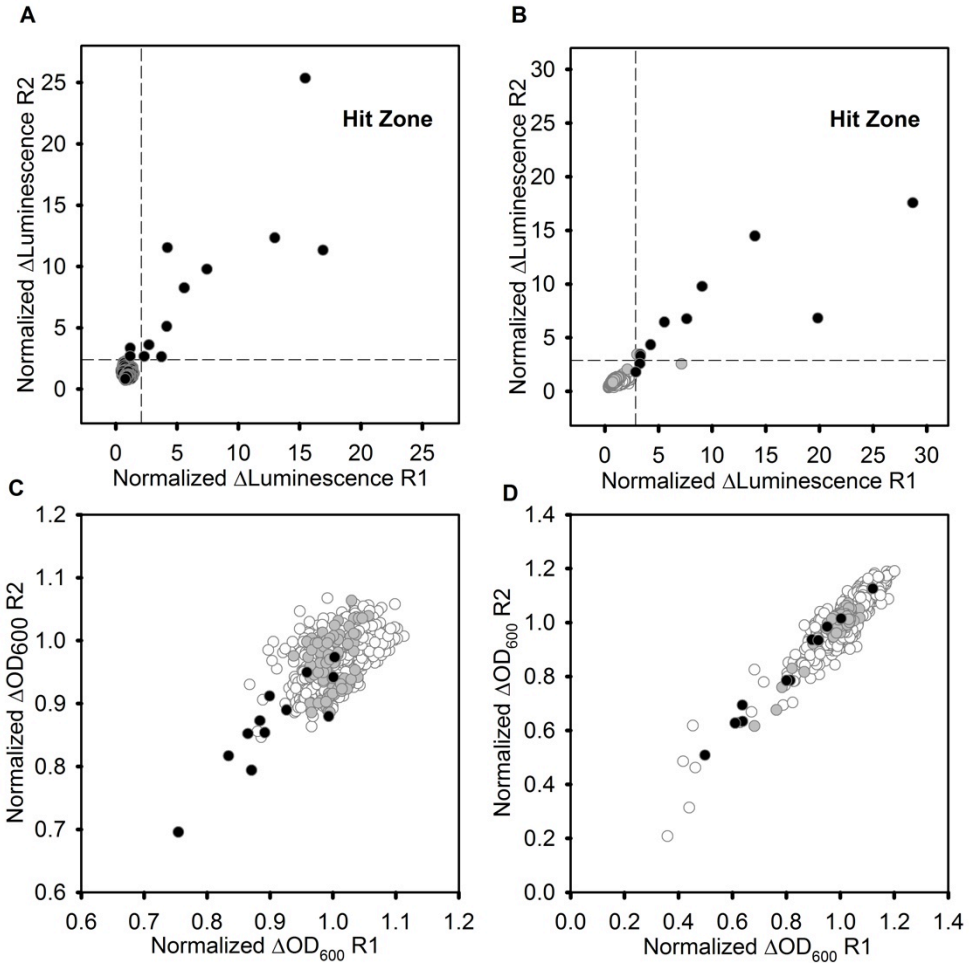

Figure 3-5. Screen of 1121 bioactive molecules with known mechanism of action for stimulation of P_{yjeE}.

E. coli MG1655 harboring pCS26-*bla*-P_{yjeE} were treated with 1 μM **(A, C)** or 10 μM **(B, D)** of compound at an OD_{600} ~ 0.1 and luminescence and OD_{600} was monitored for 8 hours. **(A, B)** Plots of replicate 1 (R1) vs. replicate 2 (R2) showing the maximal fold change in OD_{600}-normalized luminescence of treated vs. untreated cells. **(C, D)** maximal OD_{600} of treated cells normalized by the OD_{600} of the untreated controls. Hashed lines represent 6 standard deviations away from the mean activity of untreated cells. Compounds outside of this area were defined as hits. Shown are the hits (red circles), non-hits (open grey circles) and untreated controls (blue circles). Values represent the average of duplicates.

20 were known antibiotics and these fell into six different chemical classes (Table 3-1). Six compounds had no known target in *E. coli* and were not further characterized. Experiments were carried out with a representative probe from each class of antibiotics, namely, chloramphenicol, dirithromycin, norfloxacin, spectinomycin, streptozotocin and tetracycline. Norfloxacin was found to cause the strongest stimulation of promoter P_{yjeE}.

The concentration dependence of the response of P_{yjeE} to these six representative antibiotics was tested. The response of the constitutively expressed sigma70-16 synthetic promoter [220] was also tested to determine if the observed change in luminescence was specific to P_{yjeE} (Figure 3-6). The maximal induction of P_{yjeE} caused by dirithromycin, chloramphenicol, spectinomycin, streptozotocin or tetracycline was less than 5-fold more than the induction observed for the control sigma70-16 promoter (Figure 3-6A, 6B, 6D - 6F). Norfloxacin, on the other hand, generated a massive 50-fold induction of P_{yjeE} compared to the sigma70-16 control (Figure 3-6C). The ability of norfloxacin to stimulate a transcriptional response from P_{yjeE} suggested that this molecule could inform on the physiological role of YjeE.

Growth and luminescence profiles of wildtype *E. coli* harboring pCS26-bla-P_{yjeE} was measured (Figure 3-7C). The activity of P_{yjeE} increased continuously over the growth cycle (Figure 3-7C – solid line, closed circles). Treatment with norfloxacin at an OD_{600} of 0.15 resulted in similar activity of P_{yjeE} through log phase growth compared to untreated cells, however activity of P_{yjeE} was greatly increased by norfloxacin treatment as cells progressed into stationary phase (Figure 3-6C – solid line, open circles).

3.4.5 Determination of the mechanism of stimulation of P_{yjeE} by norfloxacin

Norfloxacin has four known cellular targets in *E. coli*, which are ParC, ParE, GyrA and GyrB. The Par proteins are responsible for the active partitioning of sister chromosomes and plasmids [221-223] while the Gyr proteins encode DNA gyrase which introduces negative supercoils into DNA [224, 225]. In *E. coli*, the principal target of norfloxacin is thought to be *gyrA* since mutations in *gyrA* alone can give rise to a high level of quinolone resistance [226, 227]. To determine if the observed stimulation of P_{yjeE} by norfloxacin occurred through its target, GyrA, or by some other mechanism, mutations in *gyrA* (Ser83Leu, Asp87Tyr) which give rise to norfloxacin resistance were created [228]. When this double mutation was introduced into *gyrA* on the chromosome, norfloxacin was no longer able to stimulate P_{yjeE} (Figure 3-7A). The DNA alkylating agent streptozotocin, which is

Table 3-1. Compounds that induce P_{yjeE}

	Class, Compound
Antibiotics	
	Chloramphenicols
	Chloramphenicol
	Thiamphenicol
	Florfenicol
	Macrolides
	Dirithromycin
	Tetracyclines
	Doxycycline
	Oxytetracycline
	Meclocycline
	Methacycline
	Demeclocycline
	Aminoglycosides
	Spectinomycin
	Fluoroquinolones
	Norfloxacin
	Ofloxacin
	Lomefloxacin
	Enoxacin
	Cinoxacin
	Glucosamine-nitrosoureas
	Streptozotocin
No Known Bacterial Target	
	Testosterone Analogue
	Danazol
	Acetylcholine Analogue
	Methacholine
	Dihydroindolone
	Molindone
	Morphinan
	Naloxone
	Arylalkanoic acid
	Zomepirac

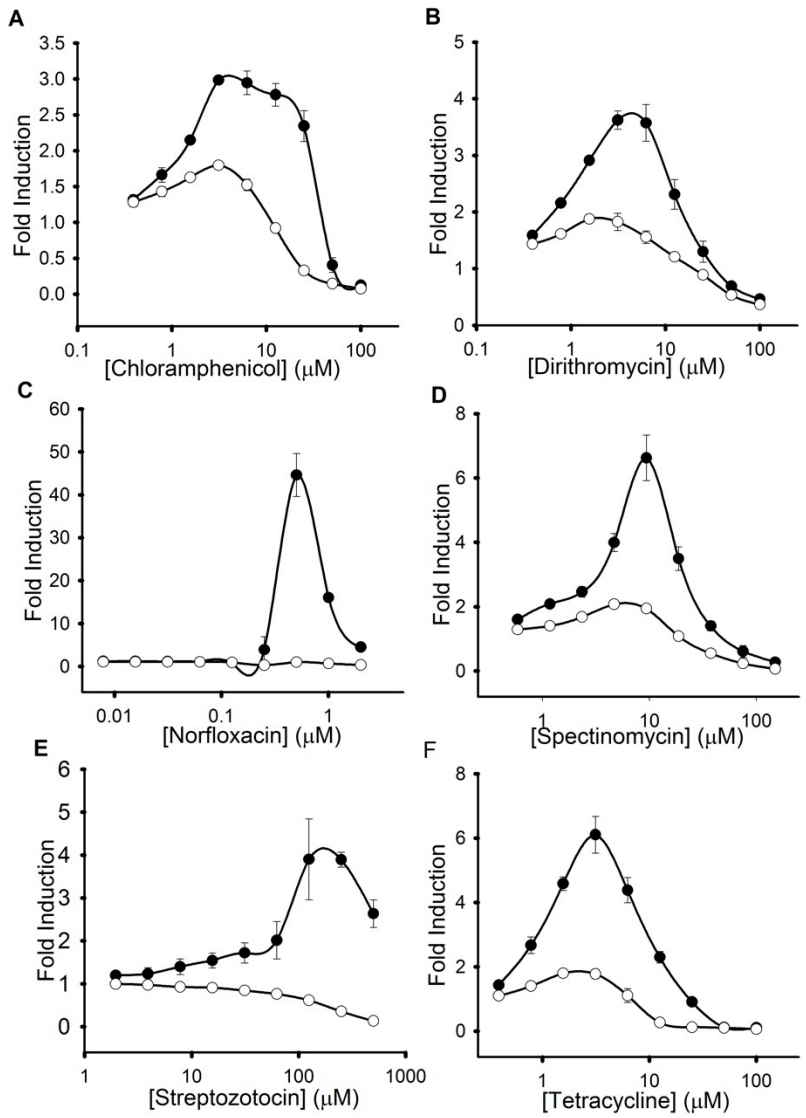

Figure 3-6. Dose response of stimulation of P_{yjeE} by representative antibiotics.

Wildtype *E. coli* harboring the reporter plasmid containing P_{yjeE} (closed circles) or the synthetic constitutive promoter sigma70-16 (open circles) were treated with various concentrations of **(A)** chloramphenicol, **(B)** dirithromycin, **(C)** norfloxacin, **(D)** spectinomycin, **(E)** streptozotocin or **(F)** tetracycline. Fold induction, which is the ratio of OD_{600}-normalized luminescence of treated compared to untreated cells, 8 hours post addition of drug is shown. Error bars represent the standard deviation of triplicates.

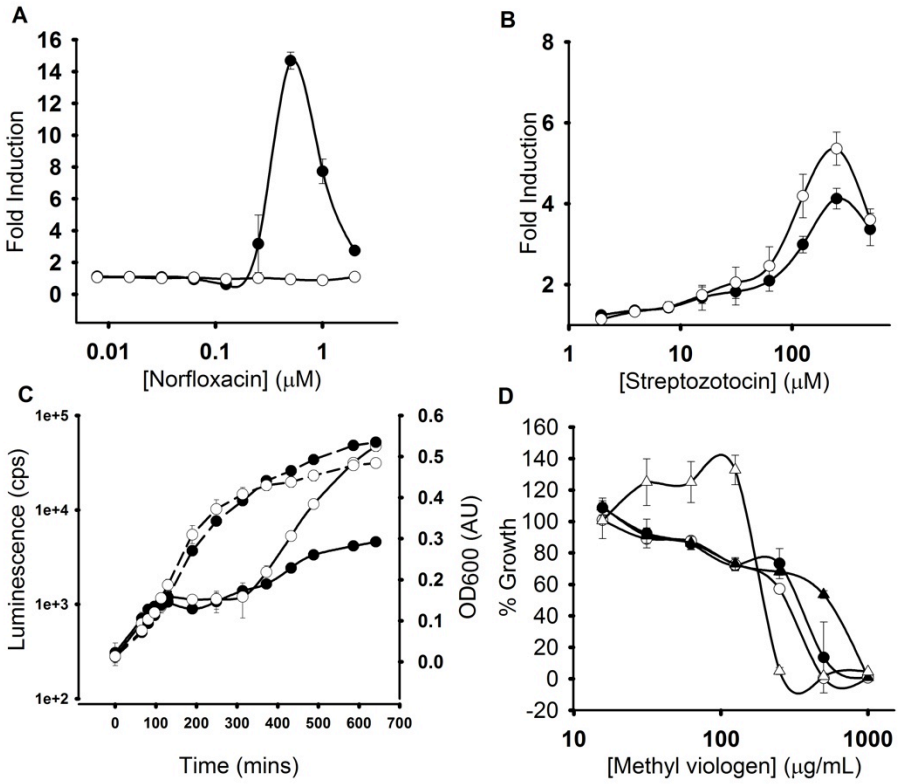

Figure 3-7. Characterization of the mechanism of stimulation of P_{yjeE}.

(A,B) Norfloxacin resistant (open circles) or wild-type (closed circles) *E .coli* MG1655 were treated with **(A)** norfloxacin or **(B)** streptozotocin and fold induction of OD_{600}-normalized luminescence of treated cells over untreated cells was plotted against compound concentration. **(C)** Growth profiles (hashed lines) and promoter response (solid lines) of *E. coli* MG1655 treated with 0.5 μM norfloxacin (open circles) or untreated (closed circles). Drug was added at 120 minutes. **(D)** Percentage growth of the *yjeE* complemented null (triangles) and *yjeE* diploid strain (circles) treated with methyl viologen. Cells were grown in the presence (closed symbols) or absence (open symbols) of arabinose. Error bars represent the standard deviation of triplicates.

known to damage DNA directly, [229] was still able to induce P_{yjeE} in the *gyrA* mutant strain confirming that induction of luminescence in this strain is still possible (Figure 3-7B). These data suggested that the mechanism of norfloxacin stimulation of P_{yjeE} involves its cellular target, GyrA.

Recently, norfloxacin and other bactericidal antibiotics were found to generate toxic oxygen radicals *in vivo*, which was important for their bactericidal activity [216]. Thus, we tested if such a mechanism could explain the chemical-genetic interaction between norfloxacin and P_{yjeE}. The sensitivity of YjeE-depleted and YjeE-replete cells treated with methyl viologen, a chemical which produces reactive oxygen species was measured (Figure 3-7D). The *yjeE* complemented null (Figure 3-7D – triangles) and diploid strain (Figure 3-7D – circles) was grown in the absence (Figure 3-7D – open symbols) or presence (Figure 3-7D - closed symbols) of arabinose. YjeE-depleted cells exhibited a modest 2 fold sensitization to methyl viologen compared to YjeE-replete cells.

3.4.6 Using deletions of two-component response regulators to further characterize the mechanism of norfloxacin stimulation of P_{yjeE}

Two-component systems are regulatory mechanisms which consist of a sensor kinase and a transcriptional activator. These systems have widely characterized roles in diverse cellular processes, thus, deletions in two-component systems were used to shed light on the function of YjeE. The activity of the P_{yjeE} promoter was tested in a panel of 37 strains, each containing a single deletion of the transcriptional activator of a two-component system. If the transcriptional activator was not known, a deletion of the sensor kinase was tested instead [44]. The ability of 0.1 μM norfloxacin to induce P_{yjeE} was either increased or decreased in a number of the deletion strains compared to the isogenic parental strain. Gene deletions that had the greatest impact on norfloxacin stimulation of P_{yjeE} are shown in Figure 5. These chemical- genetic interactions occurred in deletions of regulators of respiration and central metabolism (*torR, narL, arcB, hydG* and *uhpA*), ion or metal responses (*cusR, rcsD*) and oxidative stress responses (*cpxR* and *soxS*) (Figure 3-8).

3.4.7 Growth of the *yjeE* conditional null under anaerobic stress

We reasoned that the abundance of interactions with two-component systems involved in aerobic and alternative respiration might reflect the physiological role of YjeE. Previously, we reported that the indispensability of *yjeE* could be partially suppressed by overexpression of *rstA,* an uncharacterized response regulator [43]. Interestingly, Oshima and co-workers found that deletion of *rstA* affected the expression of genes involved in alternate respiratory pathways in *E. coli* (*narL* and *dmsA*) [44]. In addition, Cabeza *et al* found that overexpression

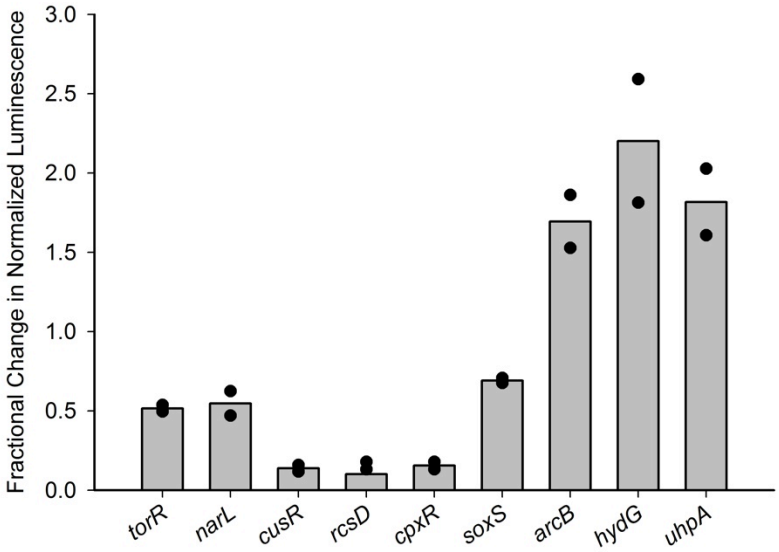

Figure 3-8. Norfloxacin stimulation of P_{yjeE} in various deletions of two-component response regulators.

Cells carrying a single deletion of either the response regulator or the histidine kinase of all known, non-essential two-component systems in *E. coli* were tested for the effect of the deletion on norfloxacin stimulated activity of P_{yjeE}. Shown here are the genes whose deletions had the highest impact on norfloxacin induction of P_{yjeE} Luminescence was measured 8 and 12 hours post addition of drug and the maximal fractional change in luminescence of the deletion strain compared to the isogeneic wildtype strain was plotted. Values represent the average of duplicates.

of the homologue of *rstA* in *Salmonella* also affected the transcription of the alternative respiratory factor *narZ* [230]. These observations, together with the results of the two-component deletion experiment, suggested a role for *yjeE* in respiratory control.

To test this hypothesis, the dispensability of *yjeE* was examined under anaerobic conditions. The conditionally complemented *yjeE* null was grown in the presence or absence of arabinose (which induces expression of the complementing copy of *yjeE*) under both anaerobic and aerobic conditions. As previously reported for aerobic conditions [34], the conditional null was unable to grow in the absence of arabinose (Figure 3-9C & 9D). Remarkably, under anaerobic conditions, cells depleted of YjeE were able to survive and form single colonies (Figure 3-9I & 9J). *E. coli yjeE* has never been shown to be dispensable under any conditions. To ensure that the activity of the P_{BAD} promoter was not simply increased under anaerobic stress, a complemented null of a gene thought to be involved in ribosome biogenesis, *engA,* was tested. The *engA* conditional null was constructed in a manner identical to the *yjeE* conditional null [156], however, this strain did not grow in the absence of arabinose under anaerobic conditions.

3.5 DISCUSSION

Herein, a chemical-genetic approach was used to probe the function of a widely conserved but uncharacterized bacterial ATPase in *E. coli,* YjeE. A library of well-characterized bioactive small molecules was used to explore the transcriptional activity of the promoter of *yjeE*. The discovery of a profound norfloxacin-induced transcriptional activity led us to investigate a role for YjeE in a variety *E. coli* stress responses that are mediated by two-component signal transduction systems. This approach led to the elucidation of significant phenotypic information for this protein, namely anaerobic gene dispensability.

The fluoroquinolone antibiotic norfloxacin, which is an inhibitor of DNA gyrase, was by far the most potent activator of P_{yjeE} and served as a useful chemical probe of the function of YjeE. Mutations in *gyrA,* which abrogate the binding of norfloxacin to DNA gyrase, abolished the stimulation of P_{yjeE} and suggested a possible role for YjeE in the recently elaborated oxidative stress response of bacteria to fluoroquinolones [215, 216]. A survey of deletions of two-component regulatory genes for those that influenced norfloxacin stimulation of P_{yjeE}, revealed that the majority have roles in respiration and central metabolism.

We found that the norfloxacin-stimulated activity of P_{yjeE} was augmented by a deletion in the aerobic respiratory regulator, *arcB,* and was negatively impacted by regulators of alternative respiratory pathways, *narL* and *torR*. Given that aerobic metabolism is known to negatively regulate alternative respiration in *E. coli* [231], our findings suggested that YjeE has a role at the interface between these two

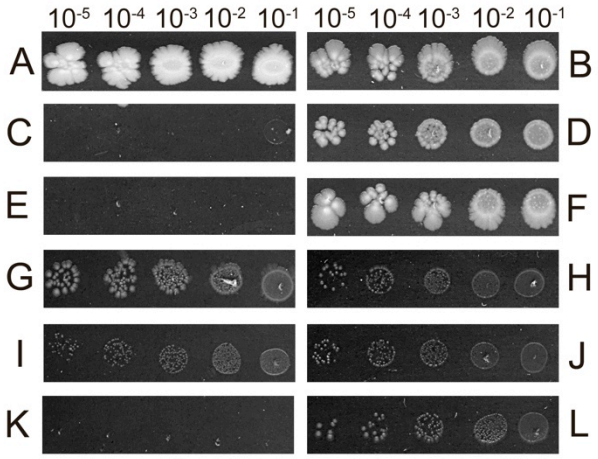

Figure 3-9. Growth phenotype of YjeE-depleted cells in the absence or presence of oxygen.

The *yjeE* diploid (A, B, G, H), *yjeE* complemented null (C,D,I,J) and *engA* complemented null (E, F, K, L) were grown in the presence (A – F) or absence (G - L) of oxygen. In addition, all strains were grown in the presence (right panels) or absence (left panels) of arabinose. The dilutions, relative to an OD_{600} of 0.1, are indicated.

pathways. SoxS is a response regulator whose regulon can lessen the effects of lethal oxygen radicals [232]. Deletion of *soxS* negatively affected the ability of norfloxacin to stimulate P_{yjeE}, suggesting that YjeE may be involved in an oxidative stress response. Methyl viologen, a redox cycling agent that generates reactive oxygen species, was tested for its ability to activate P_{yjeE}, however, no increase in luminescence was observed (data not shown). Further, there was only a slight sensitization to methyl viologen when cells were depleted of YjeE. These results suggested that if YjeE is involved in oxidative stress, its role may be in preventing the formation of toxic oxygen species, as opposed to shielding the cell from the effects of oxygen radicals.

The interaction discovered here between norfloxacin stimulation of P_{yjeE} and *narL*, a controller of nitrate reduction, is likewise supportive of the hypothesis that YjeE has a role in respiration. Further, *rstA,* the high-copy suppressor of the lethality of YjeE depletion, has a known interaction with nitrate respiration in Gram-negative organisms [44, 230]. This represents another phenotypic link between *yjeE* and alternate respiratory pathways in *E. coli*.

We found that bacteriostatic compounds (chloramphenicols, tetracyclines and spectinomycin) could induce P_{yjeE}, albeit 10-fold less than norfloxacin. The previous work by Kohanski *et al* found that only bactericidal antibiotics lead to the production of toxic oxygen radicals while bacteriostatic antibiotics did not [216]. We tested kanamycin, a bactericidal antibiotic, specifically for its ability to influence the expression of P_{yjeE} and did not find any stimulation (data not shown). These observations suggested that the activity of P_{yjeE} may be more intimately linked to the specific mechanism of the fluoroquinolone antibiotics e.g. alteration of DNA topology or regulation of DNA replication by inhibition of DNA gyrase.

Recently, YjeE was found to be an important for the enzymatic steps required for the modification of tRNA but the addition of a threonyl-carbamoyl moiety to the 37^{th} position of a subset of tRNAs (discussed in Chapter 1). Here, the P_{yjeE} promoter was found to interact with two component systems involved in central metabolism and respiration, which led to the discovery that *yjeE* is dispensable in anaerobic conditions. We can reconcile these findings by examining the known interactions of tRNA modifications with central metabolism. These include the modifications carried out by MiaE and TrmD, which act at the same position as YjeE on the tRNA (A37) but they modify different tRNAs (See [233] and references therein).

In *S. typhimurium,* MiaA adds an isopentyl group to the N6 position of A37 in certain tRNAs and MiaE subsequently hydroxylates this group. Loss of MiaE led to the inability of cells to grow on the carbon sources succinate, fumarate and malate. This phenotype was not due to loss of uptake of these carbon sources, enzymatic deficiency or loss of the respiratory chain. Instead, the phenotype was attributed to the loss of iron siderophores. Suppressors were found in transcription factors, suggesting that MiaE activity can regulate transcription. These studies illustrate the ability of tRNA modifications to govern aspects of central metabolism.

The second and more pertinent example is the effect of tRNA modification on purine and thiamine metabolism. PurF is responsible for the first committed step of both purine and thiamine biosynthesis [234]. A *purF* mutant requires supplementation with adenine and thiamine for growth. The combination of mutations of *purF* and a tRNA methylation factor, *trmD,* resulted in thiamine, but not adenine, independent growth. Thus, TrmD, like MiaA, is responsible for the modification of the 37th position of tRNA and controls an aspect of central metabolism. One hypothesis is that this modification of this 37th nucleoside of tRNA has broad effects on metabolism. Further, the activity of P_{yjeE} is altered by deletions of carbon and central metabolism two-component response regulators.

PurF physically interacted with YjeE [235] and suppressed depletion of YjeE at high copy [50], which suggest that these proteins are functionally related. Further, under anaerobic conditions or growth with non-glucose carbon sources, an alternative pyrimidine biosynthetic pathway was induced and there was no longer a requirement for thiamine supplementation in *purF* mutants. Thus, *purF* and *yjeE* both became dispensable under anaerobic conditions. These observations support the hypothesis that the tRNA modification governed by YjeE can control purine biosynthesis.

In summary, the promoter proximal to *yjeE* (P_{yjeE}) was shown to be responsive to the depletion of intracellular YjeE. Profiling of the response of this promoter to bioactive molecules revealed that norfloxacin was a potent stimulator of transcription. This chemical-genetic interaction was used to uncover genetic relationships with two-component regulatory systems. Genes involved in respiration and oxidative stress responses were found to positively or negatively influence the stimulation of the *yjeE* promoter by norfloxacin. YjeE was found to be dispensable in *E. coli* under anaerobic conditions. These findings are among the first phenotypes for this mysterious and widely conserved bacterial ATPase.

4 CHAPTER FOUR- A SCREEN FOR NOVEL RIBOSOME BIOGENESIS FACTORS BY EXPLORING COLD-SENSITIVE PHENOTYPES

4.1 CHAPTER FOUR PREFACE

I performed all the experiments described in this chapter.

I wrote this chapter and edits were contributed by Dr. Eric D. Brown.

4.2 INTRODUCTION

Prokaryotic ribosome synthesis involves the coordinated assembly of 54 ribosomal proteins and 3 ribosomal RNAs as well as 46 known modifications of the protein and rRNA in *E. coli* [122, 123]. Ribosomal subunit assembly is a complex molecular feat and while it can be accomplished *in vitro* with purified ribosomal RNAs and proteins, the conditions and time required are far from physiological [71, 80, 123, 124]. Indeed, a growing set of *trans*-acting factors, termed ribosome biogenesis factors, are thought to be critical for the assembly of ribosomal subunits to occur at a rate that meets the protein synthesis demands of the cell.

Ribosome biogenesis factors often have enigmatic roles in ribosomal subunit assembly [141, 236, 237]. To further our understanding of the repertoire of ribosome biogenesis factors, and ultimately their roles in ribosomal subunit assembly, this work aimed to find new ribosome biogenesis factors. The common phenotypes associated with biogenesis defects, such as ribosomal subunit profile anomalies and aberrant rRNA processing, are not suited to systematic screens of genome-scale clone sets as is done in this work. Nevertheless, early work by Nomura and Ingraham found that cold sensitivity is a more easily tested phenotype that is often associated with ribosome biogenesis defects [238, 239].

The response of the cell to a large and sudden decrease in temperature is termed the cold shock response, where the cell adapts its membranes, DNA and RNA to the effects of low temperature (See [240] for a review on the cold shock). With a drop in temperature, there is an increase in RNA secondary structure and kinetic traps that inhibit ribosome assembly (See Chapter 1). A decrease in temperature also selectively inhibits translation initiation compared to other steps [241]. The cell has a two-stage response to alleviate these effects; the first relieves the increase in RNA secondary structure and the second allows for long term tolerance to growth at low temperatures.

The first response is to produce a set of nucleic acid chaperones termed cold shock proteins (Csp). In *E. coli* there are nine Csps but only four of these are induced upon low temperature shock (See [240] and references therein). Csps have been found to modulate the structure of both mRNA and rRNA [240]. Csps are small and basic proteins, which are features of catalysts that may aid in the folding of RNA ribozymes by disrupting trapped RNA intermediates [88]. The production of Csps immediately following cold shock relieves translation inhibition and allows production of proteins required for long-term survival at low temperature, termed cold acclimatization proteins (Caps). Three Caps are associated with ribosome assembly in *E. coli*: the helicases *rhlE* and *csdA* and the 30S biogenesis factor *rbfA*. Indeed, cold sensitive mutants have been identified in rRNA, ribosomal structural proteins and every class of *trans*-acting ribosome biogenesis factors [171, 242-245]. The direct participation of ribosome assembly factors in the cold shock response and the frequency of cold-sensitivity in ribosome assembly factors emphasize the

fundamental and deleterious effect that low temperature stress has on the biogenesis of the ribosome.

Nomura and Nierhaus studied *in vitro* ribosome assembly by studying the pair-wise interactions between r-proteins. To develop an understanding of the *in vivo* process we must similarly have a comprehensive understanding of all extra-ribosomal assembly factors. Further, to develop ribosome assembly as a drug target, this knowledge is important to finding the most fruitful targets. In this work we aimed to discover new factors by exploiting a nearly universal phenotype of mutants of ribosome assembly, cold-sensitive growth. This phenotype was used to screen the Keio library of non-essential gene deletions in *E. coli* [218] for novel ribosome biogenesis factors. From this analysis, two putative factors were identified that had many of the hallmark phenotypes of ribosome assembly, however, their possible roles in ribosome assembly are still ambiguous.

4.3 MATERIALS AND METHODS

General methods

All growth experiments were performed in Luria Bertani (LB) media. Antibiotics were purchased from Sigma-Aldrich (Oakville, ON). All enzymes were purchased from New England Biolabs (Ipswich, MA).

Primary screen for cold-sensitivity

The screen was performed in duplicate without shaking. Overnight cultures were diluted 400-fold into LB media in deep-well plates (Phoenix Research Products, Candler, NC) using a Biomek FX® liquid handler (Beckman Coulter Inc., Fullerton, CA). 200 μL of diluted culture was dispensed into each of four 96-well Costar #3370 microtiter plates (Corning, Lowell, MA). For each set of 4 plates, two were incubated at 15°C and two were incubated at 37°C. There were no more than 4 plates in a stack to minimize temperature variation within the stack. Optical density at 600 nm (OD_{600}) was measured after 33 hours of growth at 15°C and after 8 hours and 33 hours of growth at 37°C using an EnVision® plate reader (Perkin Elmer, Boston, MA). A growth sensitivity factor was calculated for each clone by dividing OD_{600} at 37°C for 8 hours or 33 hours by the OD_{600} at 15°C for 33 hours. This generated two datasets that had good correspondence with each other. To normalize the data between plates, the mean of the middle two quartiles of data from a plate was set to a value of one and all data on that plate was adjusted by this amount. Each plate was treated independently this way to equalize small growth inconsistencies from plate to plate that were due to plate location during incubation of cultures. After visual inspection of the distribution of growth sensitivities at 33

hours, the top 3.5% of cold-sensitive genes, which corresponded to 158 mutants, was chosen.

Bioinformatic analysis

To eliminate genes unlikely to be novel ribosome biogenesis factors, functional annotations of the 158 genes selected from the primary screen were examined using the Ecocyc online database (http://ecocyc.org) [246]. Genes that had previously characterized biological functions or a known role in ribosome biogenesis were excluded from further analysis. Genes were also excluded that had potential signal sequences or known membrane association by accessing UniprotKB database available online at (http://uniprot.org) [247]. The 10 candidate clones selected by these criteria were picked from the Keio collection and stored in 15 % glycerol at -80°C.

Construction of plasmids for complementation.

The *prfC* and *ychF* genes were amplified from *E. coli* MG1655 DNA using Phusion polymerase and cloned into vector pCA24N [248]. Gene *ychF* was amplified using primers ychF-Forward (5'-ccggatgaggagaaattaaactATGGGATTCAAATGCGGTAT CGTC) and ychF-Reverse (cacctgcaagcttTTAGACGTTGAAAAGGAAGTTCATC) while *prfC* was amplified using primers prfC-Forward (5'-ccggatgaggagaaattaaactATGA CGTTGTCTCCTTATTTGCAA) and prfC-Reverse (cacctgcaagcttTTAATGCTCGCG GGTCTGGTGGAAC), where uppercase represents gene specific sequences and underlined sequences represent BseRI and HindIII restriction sites in the forward and reverse primers, respectively. PCR products were cloned into plasmid pCA24N using standard cloning protocols [249].

16S rRNA analysis

250 μL of cells were grown overnight to saturation in 96 well microtiter plates and diluted 100-fold into fresh LB media. 400 μL of diluted overnight cultures were grown in deep well plates for 24 hours at 20°C. Cells were harvested and RNA was extracted using a Qiagen RNeasy kit (Valencia, CA) according to manufacturer's instructions. Ribosomal RNA was separated by electrophoresis on a 2.25% (*w/v*) agarose gel electrophoresed at 95 V in Buffer R (40 mM Tris-acetate, 1 mM EDTA) for four hours. Buffer R was exchanged with fresh buffer after two hours. Gels were stained with SYBR® Green II and gels were photographed using an AlphaImager HP gel documentation system (ProteinSimple, Santa Clara, CA). 16S and 17S rRNA were identified by comparison to an RNA ladder and comparison to RNA purified from a Δ*yjeQ* deletion strain, which has been previously shown to accumulate 17S rRNA. RNA was quantified by using ImageQuant® v5.2 software

(Molecular Devices, Sunnyvale, CA) and background corrected signal intensities for the 17S rRNA were divided by the 16S rRNA signal intensity. This ratio is reported as a percentage.

Analysis of ribosome profiles.

Wild-type *E. coli* and mutants Δ*ychF* and Δ*prfC* were transformed with either empty pCA24N or pCA24N encoding untagged protein. The cells were grown in the presence of 20 μg/mL chloramphenicol in the absence of inducer. A high level of leaky expression provided complementation from the T5 promoter on the plasmid. 1 L of LB media was inoculated with an overnight culture to an initial OD_{600} of 0.005. The cells were grown at 20°C to a final OD_{600} of 0.2, harvested by centrifugation at 6200 x g for 15 minutes and cell pellets were stored at -80°C for later analysis. Cell pellets were thawed on ice and resuspended in 5.5 mL of ice cold Buffer A (10 mM Tris-Base, 10 mM $MgCl_2$, 100 mM NH_4Cl and 3 mM 2-mercaptoethanol). Cells were lysed by passage through a B-series Cell Disruptor (Constant Systems, Kennesaw, GA) at 15 kpsi. Lysates were clarified by centrifugation at 30, 000 x g for 45 minutes. 40 A_{260} units of the clarified lysate ribosomes was overlaid on a 35 mL 10% – 30% (*w/v*) linear sucrose gradient in Buffer A. Gradients were resolved by centrifugation in a 630 rotor in a Sorvall WX floor ultracentrifuge at 45, 000 x g for 15 hours. Gradients were fractionated by upward displacement with 60% (*v/v*) glycerol using an AKTA Prime chromatography system (GE Life Sciences, Piscataway, NJ) in conjunction with a fractionator (Brandel, Gaithersberg, MD). Absorbance of the fractions was monitored at 254 nm.

4.4 RESULTS

4.4.1 Primary screen

To search for new ribosome biogenesis factors, a screen of a library of deletions of non-essential genes was carried out to identify strains that were sensitized to growth at 15°C compared to 37°C. Replicate plots of growth for 33 hours at 37°C (Figure 4-1A) or at 15°C (Figure 4-1B) showed good correspondence of replicates and suggest that this cold-sensitive screen was reproducible and of high quality. Plate by plate normalization of the data as described in the Methods section was found to be critical to reduce the effect of the position of the plate in the incubator or its location in the stack of plates. Normalized growth sensitivity factors are shown in Figure 4-1C, where growth for 33 hours at 37°C was divided by growth for 33 hours at 15°C to obtain a growth sensitivity factor. These time points were chosen to allow cells to reach their maximum growth at both temperatures in order

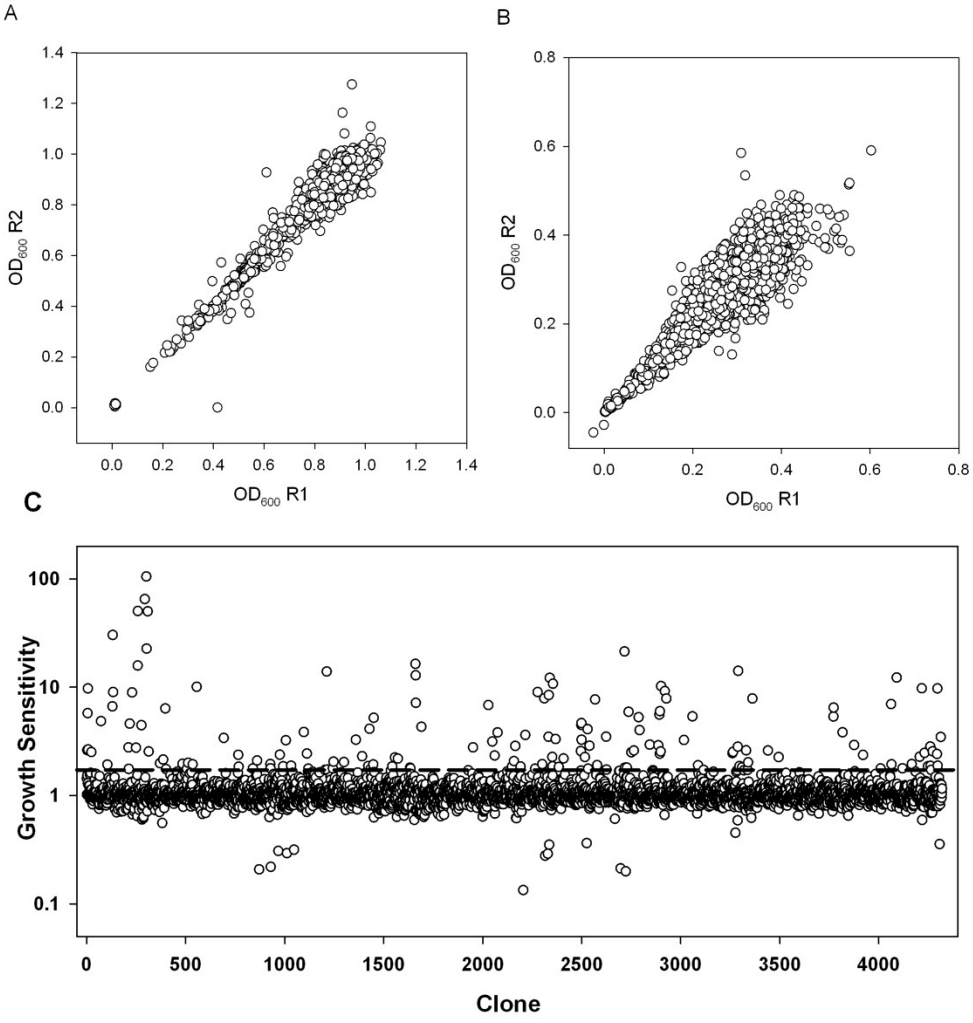

Figure 4-1. Primary screen for cold-sensitivity in a library of deletions.

The Keio library of 4320 deletions of non-essential genes in *E. coli* BW25113 was grown in LB media at two temperatures. Replicate plots depicting OD_{600} of deletion strains grown for 33 hours at **(A)** 37°C or **(B)** 15°C are shown. **(C)** Plot of growth sensitivity of strains grown at 15°C for 33 hours compared to cells grown at 37°C for 33 hours. Data represent the average of the two replicates. The 3.5% most cold-sensitive mutants (158 strains), whose growth sensitivities are shown above the hashed line, were chosen for further analysis.

to highlight slower growing cold-sensitive strains. A cold-sensitive mutant was defined as a strain that displayed growth sensitivity that was in the top 3.5%. This yielded a set of 158 cold-sensitive strains for further study (see Supplemental Data for detailed results from the primary screen). An overview of the screen and the subsequent analysis is provided in Figure 4-2.

4.4.2 Distribution of cellular function of cold-sensitive strains

To understand the functional distribution of cold-sensitive genes, each gene was assigned to a category according to annotations from the clusters of orthologous groups (COG) [26, 250]. This analysis contained multiple functional assignments of some genes and some reassignments of function that were made based on new publications. The genes fell into 4 broad categories: (i) information storage and transfer, (ii) cellular processes, (iii) metabolism and (iv) genes of unknown function (Figure 4-3A). Each of these categories was further divided into functional classes. Some 13% of assignments were related to ribosome function, which was the largest class of genes found (Table A-2 and Figure 4-3A), while 9% of mutants were related to energy production, principally subunits of ATP synthase. Another 8% were related to outer membrane and envelope biogenesis, particularly lipopolysaccharide biosynthesis. Amino acid and carbohydrate transport and metabolism accounted for 7% and 6%, respectively. Some 14% of cold-sensitive genes were not annotated or had only a general functional prediction.

To gain perspective on the relative importance of each of these functional categories on the proliferation of *E. coli* at low temperature, the number of cold-sensitive genes in each category was divided by the total number of non-essential genes in that category in the genome (Figure 4-3B). Ribosome related functions were most prominent as 20% of the mutants in this class of genes were found to be cold-sensitive. This was followed by co-enzyme metabolism, with 10% of genes in this class, mostly ubiquinone biosynthetic genes, exhibiting cold-sensitive phenotypes. Nucleotide metabolism was also prominent, with 7% of genes in this class displaying cold-sensitivity.

4.4.3 Biogenesis factors with known cold-sensitive phenotypes

The list of ribosome biogenesis factors identified here was compared to previously published information for known ribosome biogenesis factors to assess the sensitivity and accuracy of the methodology. Of the ribosome biogenesis factors tested in this screen, 12 were previously described to have slow growth phenotypes below 37°C (*rsmH*, *ksgA*, *deaD*, *rsgA*, *bipA*, *rbfa*, *rimP, yhbY, rluB*, *rluC, rlmF* and *srmB*, see Table 4-1). Of these 12 mutants, the first 8 were identified as cold-sensitive in this work while the latter four were not. The Δ*rluB* mutant was previously found to be cold-sensitive on solid media [146] but not in liquid media [251], which may

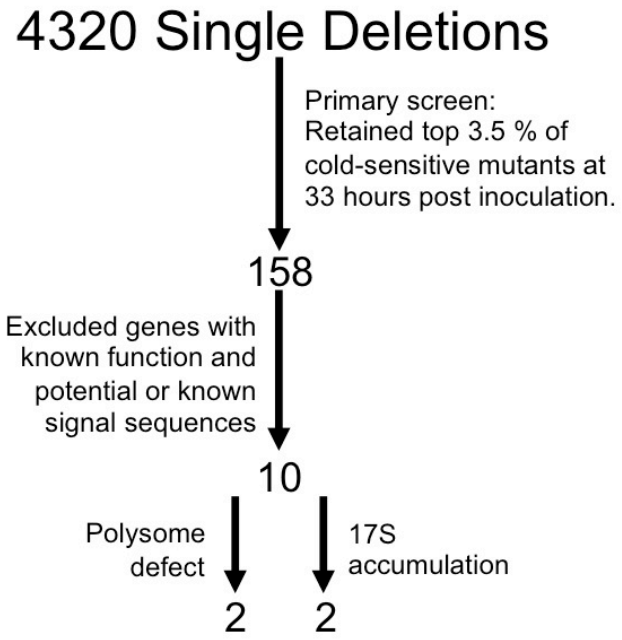

Figure 4-2. Workflow of cold-sensitivity screen.

The primary screen included 4320 mutants, of which 158 were identified as cold-sensitive. After the bioinformatic analysis, 10 strains were chosen for rRNA and ribosome analysis.

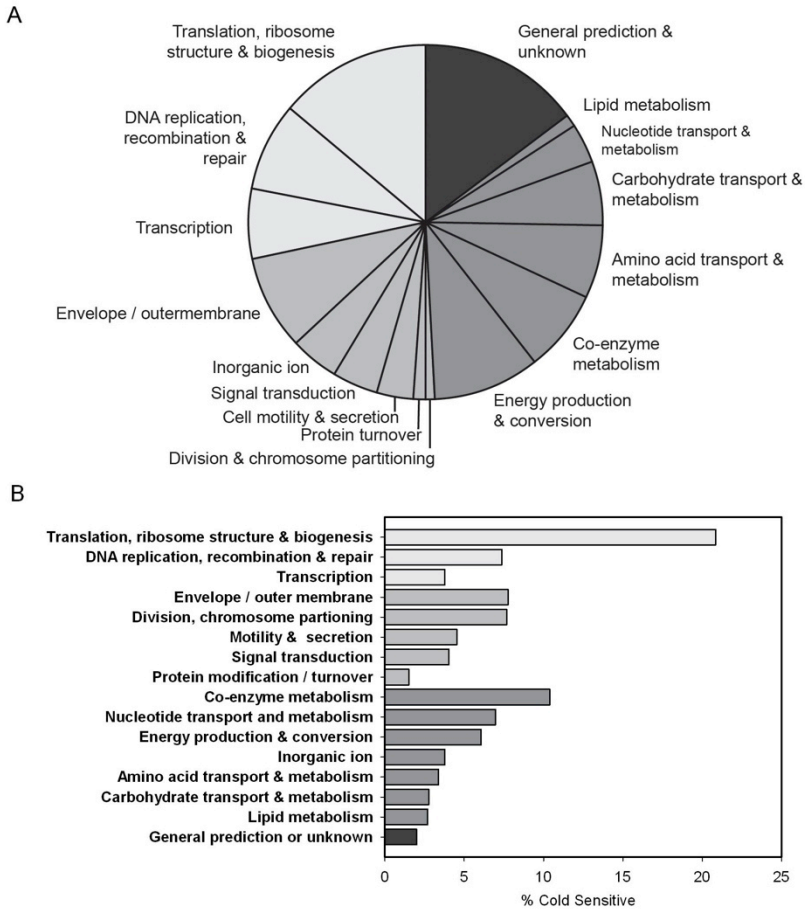

Figure 4-3. Distribution of functional classes amongst the top 3.5% of mutants identified in the primary screen.

Functional classes were assigned according to [26, 250]. **(A)** Distribution of functional classes of the top 3.5% most cold-sensitive mutants. Classes are grouped into the following categories: information storage and transfer (light grey), cellular process (medium grey), metabolism (dark grey) and genes of unknown function (very dark grey). **(B)** Normalization of the hits in each class by the size of the class in the genome. The cold-sensitive mutants in each functional class were divided by the total number of non-essential genes in the genome for that functional class. Shading is the same as panel A.

Table 4-1. Growth phenotypes of non-essential *E. coli* ribosome biogenesis factors deletions.

Blattner number	Gene [a]	Function / Target	Growth phenotype [b]	Reference
16S modifications				
B0082	***rsmH***	m^4C1402	Mild growth defect at 33 °C	[252]
B0051	***ksgA***	$m^6{}_2A1518/m^6{}_2A1519$	CS at 22 °C and 25 °C	[171]
23S modifications				
B0859	***rlmC***	m^5U747		
B0807	*rlmF*	m^6A1618	Slow growth at 30 °C & 37 °C	[253]
B1086	rluC	Ψ955/Ψ2505/Ψ2580	CS at 18 °C	[146]
B2594	***rluD***	Ψ1911/Ψ1915/Ψ1917	Slow growth at 37 °C	[174]
B3179	*rrmJ*	Um2552	CS at 10 °C	[254]
B1269	*rluB*	Ψ2685	No growth defect at 25°C, CS 18°C	[146, 251]
R-protein modifications				
B0852	***rimK***	S6 glutamination		
RNA helicases				
B3162	***deaD***	50S	CS at 15 °C	[255]
B2576	*srmB*	50S	CS at 30 °C	[256]
GTPases				
B4161	***rsgA***	30S	CS at 30 °C	[257]
B3871	***bipA***	30S	CS at 20 °C	[258]
Maturation Factors				
B3167	***rbfA***	30S	CS at 26 °C	[242]
B3170	***rimP***	30S	Mild growth defect at 30 °C	[259]
B2608	***rimM***	30S	Slow growth at 37 °C	[153]
B3180	***yhbY***	50S	CS at 18 °C	[146]

[a] genes indicated in bold were found to be cold-sensitive in this work.
[b] CS means cold sensitive.

explain why it was not identified here in this screen in liquid media. It is not clear why Δ*srmB,* Δ*rlmF* and Δ*rluC* did not display cold-sensitivity in this work. Incidentally, the Δ*rrmJ* mutant is also known to be cold-sensitive but was not tested because this strain was not present in our copy of the Keio collection. In addition to confirming known cold-sensitive phenotypes of ribosome biogenesis factors, two factors with previously unknown cold-sensitive phenotypes, *rluD* and *rimM* (Table 4-1), were also identified. These two factors were previously only known to have growth defects at 37°C. In all, the screen reproduced 8 of the 11 known cold-sensitive phenotypes for non-essential ribosome biogenesis factors suggesting that an assay for growth sensitivity at low temperature is a fairly reliable method for uncovering new ribosome biogenesis factors.

4.4.4 Bioinformatic analysis of primary screening data

The 158 hits from the primary screen were shortlisted using bioinformatics databases to eliminate genes that were unlikely to be novel ribosome biogenesis factors. Functional annotations and known or predicted membrane spanning domains and signal sequences were examined. Functional information was derived from the Ecocyc database (http://ecocyc.org) while information about potential signal sequences and structural motifs was derived from the Swiss Institute of Bioinformatics website (http://expasy.ch/sprot). Genes predicted to be secreted, inserted into a membrane or had a known function that was orthogonal to ribosome biogenesis were not considered further. The conservation of these genes was also taken into account, where genes that were unique to *E. coli* or a limited number of γ-proteobacteria were eliminated. This process reduced the list of hits from 158 genes to 10 genes (Table 4-2).

4.4.5 Survey for immature 16S rRNA

A block in ribosome biogenesis is associated with accumulation of precursors of 16S rRNA [171, 259]. Thus, incomplete rRNA processing was used as a marker to test the 10 cold-sensitive mutants for a possible role in ribosome biogenesis. Immature 16S rRNA (also known as pre-16S or 17S) is slightly larger and thus migrates slower than the 16S rRNA on an agarose gel. Initial tests revealed that two mutants, Δ*prfC* and Δ*ychF,* were found to have an increased amount of pre-16S rRNA compared to wild type (data not shown). These mutants were confirmed by PCR (data not shown). A third mutant, Δ*yjfO*, also exhibited increased 17S rRNA but the deletion could not be confirmed by PCR (data not shown) and thus was not further considered.

Table 4-2. Cold-sensitive mutants chosen for analysis of rRNA and ribosome profiles.

Blattner number	Gene	Growth Sensitivity	Annotation
B2530	*iscS*	1.72	Cysteine desulfurase
B0082	*rsmH*	1.78	16S rRNA methyltransferase
B4375	*prfC*	2.26	Peptide chain release factor
B1203	*ychF*	3.27	Predicted GTP binding protein
B3470	*sirA*	4.31	tRNA modification
B4172	*hfq*	5.21	RNA binding protein
B0214	*rnhA*	12.19	DNA-RNA hybrid degradation
B3344	*yheM*	12.88	tRNA modification
B0631	*ybeD*	13.95	Predicted nuclease domain
B0253	*ykfA*	15.83	Predicted GTP binding protein

We then measured the accumulation of 17S immature rRNA over the course of the growth cycle of wildtype cells or the Δ*prfC* and Δ*ychF* mutants harboring either empty pCA24N or vector encoding the respective gene (Figure 4-4). For wildtype cells, in the early log phase, the amount of immature 17S rRNA was 20% compared to the amount of 16S rRNA (which is set at 100%) (Figure 4-4A & 4B, black lines). The amount of immature 17S rRNA decreased over the course of the growth curve to undetectable levels during stationary phase. Δ*prfC* and Δ*ychF* mutants had markedly increased levels of 17S rRNA compared to wildtype cells and continued to increase during early log phase then decrease during late log phase (Figure 4-4A & 4B, light grey lines). The Δ*prfC* mutant exhibited peak accumulation of 17S rRNA that was 120% compared to the amount of 16S rRNA (Figure 4-4A, grey hashed lines). The Δ*ychF* mutant accumulated 17S rRNA to a lesser degree but still reached a maximum amount of 17S rRNA that was 50% of the amount of 16S (Figure 4-4B, grey hashed lines). 17S rRNA was also measured in complemented Δ*prfC* and Δ*ychF* mutants harboring pCA24N plasmids encoding their respective genes (Figure 4-4A & 4B, dark grey lines). The complemented Δ*prfC* mutant had about 20% 17S rRNA, which is similar to wild-type (Figure 4-4A, black and dark grey line). The complemented Δ*ychF* strain exhibited a peak 17S accumulation of 33% but this decreased to wild type levels as cells entered stationary phase.

4.4.6 Ribosome profiles of cold-sensitive mutants

The distributions of the ribosomal subunits in the 10 candidate ribosome biogenesis factors listed in (Table 4-2) were analyzed by separation of ribosomal species by sucrose density gradient centrifugation. After growth at 20 °C, two mutants were found to have altered ribosome profiles, *ΔprfC* and *ΔychF* (Figure 4-5, light grey lines). The Δ*prfC* mutant accumulated excess 50S subunits compared to wild type and a distinct species accumulated that sedimented slower than mature 30S subunits (Figure 4-5A, light grey line). The *ΔychF* mutant showed a slight increase in 30S and 50S ribosomal subunits (Figure 4-5B, light grey line). The defective ribosome profiles of Δ*prfC* and Δ*ychF* could be corrected by expression of the respective genes from the plasmid pCA24N [248] expressing untagged protein (Figure 4-5, dark grey lines).

4.5 DISCUSSION

Herein we have exploited cold sensitivity to screen the Keio collection of *E. coli* gene deletions to identify new factors involved in ribosome biogenesis. Among the cold-sensitive genes discovered, the category of ribosome related functions (translation, ribosome structure and biogenesis) was the most highly represented. Some 8 of 11 known ribosome biogenesis factors with growth phenotypes were identified in this screen. Together, these findings suggest that our screen was

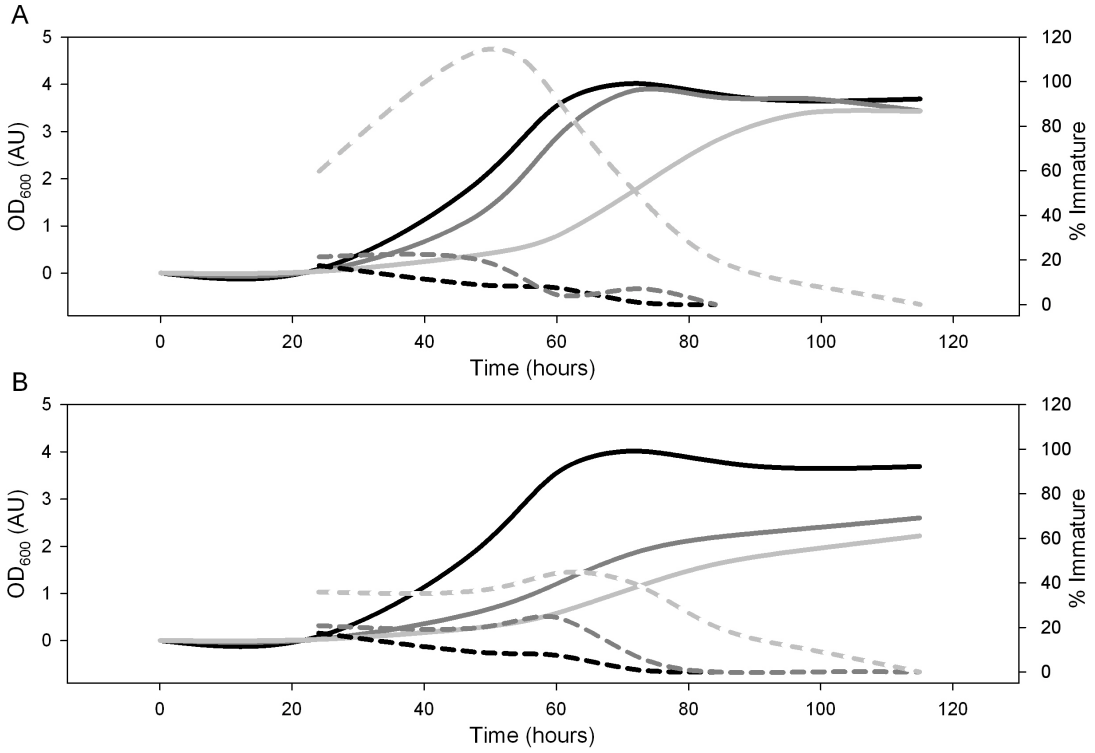

Figure 4-4. Phenotypes of the wildtype, Δ*prfC* and Δ*ychF* mutants.

Cell growth and 17S accumulation is presented for (A) Δ*prfc* and (B) Δ*ychF*. Cell growth (solid lines) and 17S rRNA accumulation (dashed lines) is compared for wild type (black lines) or the deletion strains harboring and empty pCA24N plasmid (light grey lines) or cognate gene (dark grey lines). Cells were grown in baffled flasks grown at 15 ˚C and aerated at 250 rpm. Growth and RNA was measured approximately every 8 hours.

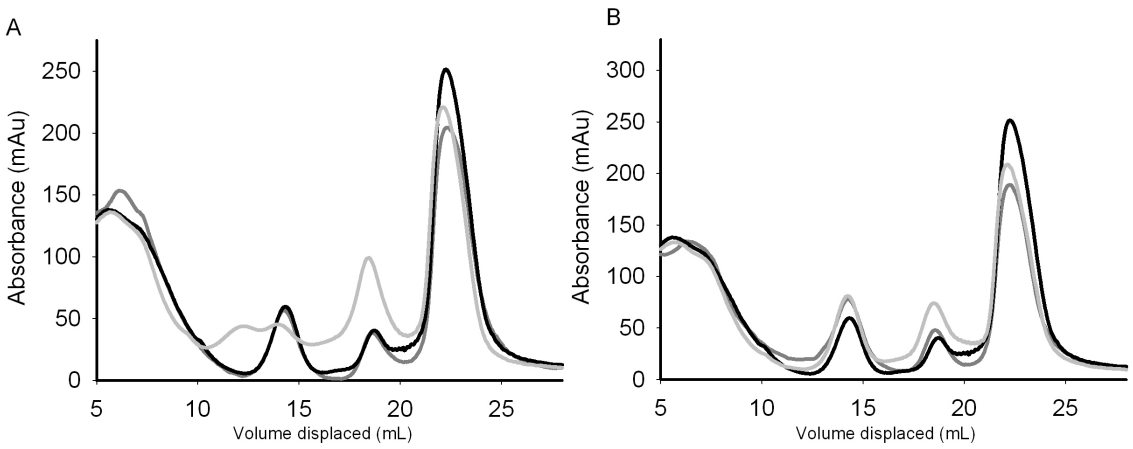

Figure 4-5. Ribosome profiles of cold-sensitive Δ*prfC* and Δ*ychF* mutants.

The ribosome profiles of the Δ*prfC* (A) and Δ*ychF* (B) mutants are compared to wild-type. From left to right, the peaks represent 30S, 50S and 70S. For each panel, black, dark grey and light grey lines represent the wild type, complemented mutant and mutant profiles, respectively. Cells were grown at 20°C and resolved by ultracentrifugation on a sucrose density gradient. Gradients were fractionated by upward displacement and absorbance was monitored at 260 nm. Complementation was achieved by expressing the respective gene from plasmid pCA24N.

effective in searching for new ribosome biogenesis factors. Indeed, an examination of the nature of known ribosome biogenesis factors may provide clues about the number of undiscovered factors in each class and the utility of cold-sensitivity in detecting these factors. Ribosomal modifications (protein and rRNA) are poorly conserved and mutants infrequently show growth phenotypes or ribosome profile defects. Of the protein modifications only one is conserved in both *E. coli* and *B. subtilis*, which is methylation of L11 [159, 260]. Further, of the 36 rRNA modifications in *E. coli*, only methylation by KsgA and pseudouridylation by RluD are universally conserved activities. Thirty-six rRNA modifications of the *E. coli* ribosome have been identified but only 4 of these modifications have yet to be assigned to a gene, which means that there are few unidentified rRNA modification enzymes. Since the majority of mutants in r-proteins and rRNA modifications are not associated with a growth phenotype, cold-sensitivity may not be a good method of identifying new factors in this class. Having come to this conclusion, it appears nevertheless that the cold-sensitive screen may have been very successful in identifying cold-sensitive phenotypes among well-known GTPases and RNA binding proteins thought to have roles in ribosomal subunit assembly.

All of the non-essential GTPases and RNA binding proteins with a previously reported growth phenotype were identified in our screen. Compared to the rRNA and r-protein modification enzymes, GTPases and RNA-binding proteins tend to have strong growth and ribosome assembly phenotypes. Perhaps it is not surprising that these genes also displayed stronger cold-sensitivity phenotypes. Taken together, the results of the genetic screen in the context of known biogenesis factors suggests that our search may have been relatively comprehensive with respect to assembly GTPases and RNA-binding proteins.

There are two reasons why this screen for cold-sensitivity of deletion mutants may not be able to detect certain unknown ribosome biogenesis factors. The first is that mutation of a ribosome biogenesis factor has sometimes produced a stronger phenotype than deletion of the entire gene [171, 261, 262]. One example of this is deletion of the RNA helicase, *dpbA*, which did not produce a growth phenotype but a point mutation produced immature 50S subunits that stimulated the ATPase activity of DbpA. Similarly, the Δ*prmB* deletion mutant did not display cold- sensitivity in this screen even though a mutant of *prmB* is associated with cold-sensitivity and ribosomal defects [183]. These *prmB* phenotypes were attributed to a mutant allele whose mechanism has not been clearly assigned. Significant efforts were made in the 1970s and 1980s to generate cold-sensitive mutants that produce ribosome assembly defects, however, some of these mutations have not been mapped. Thus, it might prove useful to make use of modern genomic information and to map and characterize these mutants, some of which may be novel ribosome biogenesis factors. The second reason why this screen may not detect a novel factor is the possibility of functional redundancy. For example, a mutant in the non-essential RNA nuclease, RNase T, did not show a growth phenotype until other RNases were simultaneously deleted [263] and, as expected, this mutant did not

show cold-sensitivity in our screen. Thus, systematic pair-wise deletions may be a necessary strategy to find these factors. Indeed, genome-scale methodology for the construction of double deletions in *E. coli* has been described recently and may be very useful for uncovering new ribosome biogenesis factors [264, 265].

The earliest link between cold-sensitivity and ribosome biogenesis was the discovery that mutations in ribosomal proteins S5 and S8 caused cold-sensitivity as well as ribosome assembly defects, including accumulation of precursors and lower incorporation of some ribosomal proteins [266, 267]. Although the mechanism underpinning the relationship remains unclear, a possible explanation is the formation of non-native secondary structures in ribosomal RNA. Similar structures formed in mRNA at low temperatures and inhibited translation [240, 268]. Indeed, cold temperature is known to induce a variety of RNA helicases and chaperones that are believed to help in unwinding non-native structures to allow translation to proceed. If rRNA secondary structures form during ribosome biogenesis at low temperatures, this is likely to yield non-productive ribosomes or slower assembly. The existence of non-native rRNA structures has been shown *in vitro* when studying the effects of ribosomal proteins on the formation of rRNA secondary structure [78, 269]. Small subunit ribosomal proteins reduced the amount of non-native rRNA conformations thus facilitating proper ribosome assembly. These observations suggest that changes in rRNA conformation may be the mechanism by which cold-sensitivity is associated with ribosome biogenesis defects. Perhaps the deletion of ribosome biogenesis factors exacerbates difficulties associated with proper rRNA folding at low temperature.

In this work, 158 cold-sensitive mutants were identified and an analysis of their functions revealed that ribosome related functions featured strongly. Functional annotations were used to produce a shortlist of 10 potential ribosome biogenesis factors. Two mutants from this pool of 10, Δ*prfC* and Δ*ychF,* showed an accumulation of pre-16S rRNA and were found to have altered ribosome profiles.

In this work, the Δ*ychF* deletion was found to have an aberrant ribosomal subunit profile but did not accumulate pre-16S rRNA. The lack of accumulation of pre-16S implies that YchF acts very late in the assembly pathway after the pre-16S rRNA is trimmed. YchF is a universally conserved P-loop GTPase of the Obg family of proteins [270] . The crystal structure of the *H. influenzae* orthologue was recently solved [271]. It contained an N-terminal GTPase domain, next to a central mixed α–β domain of the ubiquitin-like superfamily of proteins and a C-terminal coiled coil motif, found in some RNA binding proteins. Indeed, the protein was found to bind GTP and RNA. A protozoan YchF-like protein was found to bind both the ribosome and the proteasome, although this protein showed a preference for ATP [272].

PrfC (also known as RF3) encodes a GTPase with similarity to the translation elongation factor, EF-Tu. PrfC has previously been implicated in the release of two peptide chain release factors (RF), RF1 and RF2, following translation termination [273-275]. It was also suggested to have a related role in release factor mediated quality control of protein synthesis, a newly described mechanism of translation

fidelity control [276]. Here, a Δ*prfC* mutant was found to accumulate pre-16S rRNA as well as 30S and 50S subunits. Further, the ribosome profile of Δ*prfC* contained a peak sedimenting more slowly than 30S of equal intensity, which may be attributed to an immature 30S ribosomal species. We suggest that gene *prfC* may have an alternative or dual role in the cell as a biogenesis factor.

We outline some findings that support a role for PrfC as a biogenesis factor. PrfC (RF3) is distinct in many respects from the other two release factors, RF1 and RF2. While, RF1 and RF2 are both essential and highly conserved in bacteria, *prfC* is non-essential. RF1 and RF2 both recognize specific codons [277, 278]; however, PrfC is not codon-specific [279]. Biochemical evidence for the assignment of PrfC as a release factor may be a non-specific effect of ribosome binding since it happens in the absence of a stop codon [280]. Further, in experiments where the PrfC concentration was quantified, the enzyme PrfC was used in 4-6 fold excess of its ribosome substrate [275, 281]. *In vivo*, PrfC is found at a copy number that is sub-stoichiometric to the ribosome, more consistent with the small fraction of the ribosomal pool that is undergoing synthesis [282]. In contrast, RF1 and RF2 concentrations are 10 and 100 times more than PrfC concentrations at similar growth rates [283].

Three structures are reported with PrfC bound to the 70S ribosome [284-286], which suggest a role as a translation factor, however, 70S binding has been observed in some biogenesis factors. Ribosome biogenesis factors RhlE and RsgA are noted to bind the 70S ribosome. Further, it has been noted in a number of studies that the last steps of ribosome assembly occur on polysomes or pre-translating ribosomes. These data suggest that 70S binding does not exclude PrfC from a role in ribosome biogenesis.

The reported release factor activity of PrfC can be explained by a non-specific inhibition of protein translation due to ribosome binding, similar to that observed for the ribosome biogenesis factor RsgA. When RsgA was incubated with 70S ribosomes it caused dissociation into free subunits. A stoichiometry greater than 1:1 (RsgA:ribosome) inhibited protein synthesis *in vitro* [149, 211]. The likely mechanism is that RsgA binds on the interface side of the 30S subunit at a site that overlaps with inter-subunit bridges, which would inhibit initiation of translation [148]. A similar mechanism could explain the release factor activity observed with PrfC.

While this screen was aimed at discovering new biogenesis factors, it also provided new information about genes in *E. coli* that are important for growth at low temperature. One quarter of functional annotations belonged to the classes of proteins involved in the metabolism and transport of carbohydrates and amino acids and the production and conversion of energy. Interestingly, these classes of genes were highly represented in a study of the transcriptional response to cold temperature in *E. coli* [287] and also in the closely related *Yersinia pestis* [288]. The contribution by transporters such as *proW* to fitness of the cell at low temperature may be due to the uptake of molecules known as compatible solutes which act as

cryoprotectants [289]. A number of genes involved in the production of ubiquinone were found to be cold-sensitive. Ubiquinone is an important co-factor in the shuttling of protons in the electron transport chain during aerobic growth. Recent studies have found that the respiratory capacity of cells in cold-shock was diminished [290] and that the ubiquinone utilizing enzyme NADH dehydrogenase was significantly down regulated upon cold-shock [288]. These results suggest that ubiquinone is important for low temperature growth. Perhaps its importance could be related to membrane fluidity, which is reduced at cold temperature, as ubiquinone was found to increase the fluidity of phospholipid membranes [291]. A number of mutants involved in the biosynthesis of the polysaccharide portion of lipopolysaccharide (LPS) were found to be cold-sensitive in this assay. Two reports have found evidence for adaptation of lipid A to low temperature by modification of acyl chain length and saturation, which is the lipid anchor of LPS [292, 293].

In summary, the screen has provided insight into how bacteria survive cold by identifying deletions that caused a growth disadvantage at low temperature. A significant portion of the genes identified were related to ribosome function and biogenesis. Two genes were identified, *prfC* and *ychF*, which may be novel ribosome biogenesis factors.

5 CHAPTER FIVE

CONCLUSION

The goal of this work was to understand poorly characterized areas of bacterial physiology that are promising as antimicrobial drug targets. Below I review the results of this thesis and how they relate to future drug discovery efforts.

5.1 YjeE AS AN ANTIMICROBIAL DRUG TARGET

In Chapter 2, we found that *yjeE* was dispensable under anaerobic conditions. This suggests that YjeE would serve as a useful antimicrobial target for infections where aerobic pathogens dominate. Its effectiveness in treatment of mixed microbial infections is less clear. Commensal anaerobic bacteria are found in 10 – 1000 fold excess on the mucosal surfaces of the body such as the oral cavity and lower and upper gastrointestinal tract [294]. These commensal bacteria serve as a reservoir for subsequent infection at other sites in the body [295]. A twelve-year survey of infection sites at a U.S. hospital found that anaerobes were prevalent in the following infection sites: abdomen, blood, central nervous system, chest, abscess, cysts and obstetrical / gynecological locations [296]. Anaerobic pathogens can exist as the sole isolate in an infection or as a part of poly-microbial communities [297]. Synergistic interactions between aerobes and anaerobes have been demonstrated in a number of models of infection [298, 299]. Aerobes are also thought to lower the local concentration of oxygen, which facilitates the growth of anaerobes in microenvironments at the infection site [300]. In mixed infections of anaerobes and aerobes, treatment directed against anaerobes are partially effective in animal models, yet complete clearance requires therapies directed at both types of organisms [301-303]. Whether an inhibitor of YjeE directed at bacteria living an aerobic lifestyle in this context would be effective is unclear. To our knowledge, there has been no systematic survey of essential genes in anaerobic pathogens, which would be a useful next step to the further study YjeE as a drug target.

5.2 RIBOSOME ASSEMBLY AS AN ANTIMICROBIAL DRUG TARGET

In Chapter 4, we added two new potential ribosome biogenesis factors to the list of approximately 50 trans-acting assembly factors by using the cold-sensitive phenotype as the search criteria. Mutants of the two genes, *prfC* and *ychF,* were cold sensitive and accumulated precursor rRNA and ribosomal subunits. These phenotypes are consistent with a role in ribosome assembly. In eukaryotes, hundreds of ribosome assembly factors have been identified but there are probably far fewer in prokaryotes because of their simpler physiology. Have we now identified all the ribosome assembly factors in prokaryotes? Phenotypic screens, such as the one used here, have perhaps identified most of the ribosome assembly factors with strong phenotypes. Growth phenotype appears to correlate with the severity of the assembly defect so any remaining assembly factors will likely have more subtle phenotypes than those identified to date.

Ribosome assembly factors identified in the future will likely resemble the helicase *rhlE*, whose phenotypes are subtle and context-dependent. For instance, Δ*rhlE* does not have a growth phenotype, but when it is combined with Δ*deaD,* there is synergistic slow growth [304]. Further, RhlE protein will only strongly bind free subunits that were purified from a Δ*deaD* mutant. These observations may inform two potential approaches for future identification of assembly factors. The first is the exploration of gene-gene interactions, through systematic combination of deletions of known biogenesis factors with non-essential genes. The production of double deletions has recently been simplified by the development of rapid high throughput cloning techniques [305]. The second approach is directly surveying the proteins bound to ribosomal subunits, which was previously used to identify the 50S biogenesis factor *ycbY* [146].

Ribosome assembly is a complex cascade of interdependent protein binding and rRNA folding, which are mediated by r-proteins and *trans*-acting assembly factors. Each of the microscopic events of assembly is a potential point of therapeutic intervention by an antibiotic. Further characterization of ribosome biogenesis is necessary to determine the most worthwhile targets. It follows that the next steps in the development of this therapeutic area are an understanding of which factors are most important for *in vivo* virulence.

5.3 CONCLUSION

In 2004 the Koonin group published a list of the top 10 most widely conserved genes for which only general functional predictions could be made [25]. Four out of ten of these genes were subsequently found to act in translation [306]. In 2006 a systematic study of *E. coli* essential genes identified 15 genes of poorly characterized function and 6 of these were subsequently found to have a function at the ribosome [218]. Ribosome biogenesis, translation and transcription constitute most of the universally conserved and widespread genes found in nature [306, 307]. Bioinformatic analyses has found that a core set of translation related genes is present in all bacteria regardless of their complexity [307]. While bacteria have a remarkable diversity in cell wall composition and life-style, protein translation serves as a universal drug target. Fittingly, YjeE, which was first identified as a gene of unknown function, has now been implicated in protein translation. Here, I have emphasized that YjeE has idiosyncratic interactions with central metabolism and respiration. I have tentatively assigned *prfC* and *ychF* as two new ribosome biogenesis factors. There are approximately 50 ribosome biogenesis factors. The work here has incrementally increased the total number of known factors, which may suggest that we are approaching a comprehensive list of ribosome assembly factors. Future work will come from validating these targets and directing chemical inhibitors against their function.

6 REFERENCES

1. Shanahan, F., *The host-microbe interface within the gut.* Best practice & research. Clinical gastroenterology, 2002. **16**(6): p. 915-31.
2. Costello, E.K., et al., *Bacterial community variation in human body habitats across space and time.* Science, 2009. **326**(5960): p. 1694-7.
3. Grice, E.A., et al., *Topographical and temporal diversity of the human skin microbiome.* Science, 2009. **324**(5931): p. 1190-2.
4. Koch, R. and W.W. Cheyne, *Investigations into the etiology of traumatic infective diseases*. The New Sydenham society Publications1880, London,: The New Sydenham society. xiii, 74 p.
5. Koch, R., *Classics in infectious diseases. The etiology of tuberculosis: Robert Koch. Berlin, Germany 1882.* Reviews of infectious diseases, 1982. **4**(6): p. 1270-4.
6. Brock, T.D., *Milestones in microbiology*1961, London: Prentice-Hall International. xii, 275 p.116-118.
7. Kaufmann, S.H. and U.E. Schaible, *100th anniversary of Robert Koch's Nobel Prize for the discovery of the tubercle bacillus.* Trends in microbiology, 2005. **13**(10): p. 469-75.
8. Gao, Z., et al., *Substantial alterations of the cutaneous bacterial biota in psoriatic lesions.* PloS one, 2008. **3**(7): p. e2719.
9. Turnbaugh, P.J., et al., *An obesity-associated gut microbiome with increased capacity for energy harvest.* Nature, 2006. **444**(7122): p. 1027-31.
10. Berer, K., et al., *Commensal microbiota and myelin autoantigen cooperate to trigger autoimmune demyelination.* Nature, 2011.
11. Marshall, B.J. and J.R. Warren, *Unidentified curved bacilli in the stomach of patients with gastritis and peptic ulceration.* Lancet, 1984. **1**(8390): p. 1311-5.
12. Nobelprize.org. *"Press Release: The 2005 Nobel Prize in Physiology or Medicine".* 2005 [cited 2012 March 1st 2012]; "Press Release: The 2005 Nobel Prize in Physiology or Medicine".]. Available from: http://www.nobelprize.org/nobel_prizes/medicine/laureates/2005/press.html.
13. Brock, T.D., *Milestones in microbiology*1961, London: Prentice-Hall International. xii, 275 p.176-177.
14. Brock, T.D., *Milestones in microbiology*1961, London: Prentice-Hall International. xii, 275 p.195-199.
15. Walsh, C., *Antibiotics : actions, origins, resistance*2003, Washington, D.C.: ASM Press. x, 335 p.
16. D'Costa, V.M., et al., *Sampling the antibiotic resistome.* Science, 2006. **311**(5759): p. 374-7.
17. Simor, A.E., et al., *Methicillin-resistant Staphylococcus aureus colonization or infection in Canada: National Surveillance and Changing Epidemiology, 1995-*

2007. Infection control and hospital epidemiology : the official journal of the Society of Hospital Epidemiologists of America, 2010. **31**(4): p. 348-56.
18. Klevens, R.M., et al., *Invasive methicillin-resistant Staphylococcus aureus infections in the United States.* JAMA : the journal of the American Medical Association, 2007. **298**(15): p. 1763-71.
19. Gyssens, I.C., *Antibiotic policy.* International journal of antimicrobial agents, 2011. **38 Suppl**: p. 11-20.
20. Fischbach, M.A. and C.T. Walsh, *Antibiotics for emerging pathogens.* Science, 2009. **325**(5944): p. 1089-93.
21. Silver, L.L., *Challenges of antibacterial discovery.* Clinical microbiology reviews, 2011. **24**(1): p. 71-109.
22. Butler, M.S. and M.A. Cooper, *Antibiotics in the clinical pipeline in 2011.* The Journal of antibiotics, 2011. **64**(6): p. 413-25.
23. Payne, D.J., et al., *Drugs for bad bugs: confronting the challenges of antibacterial discovery.* Nature reviews. Drug discovery, 2007. **6**(1): p. 29-40.
24. Projan, S.J., *Whither antibacterial drug discovery?* Drug discovery today, 2008. **13**(7-8): p. 279-80.
25. Galperin, M.Y. and E.V. Koonin, *'Conserved hypothetical' proteins: prioritization of targets for experimental study.* Nucleic acids research, 2004. **32**(18): p. 5452-63.
26. Tatusov, R.L., et al., *The COG database: an updated version includes eukaryotes.* BMC Bioinformatics, 2003. **4**: p. 41.
27. Hanson, A.D., et al., *'Unknown' proteins and 'orphan' enzymes: the missing half of the engineering parts list--and how to find it.* The Biochemical journal, 2010. **425**(1): p. 1-11.
28. Schaffer, A.A., et al., *Improving the accuracy of PSI-BLAST protein database searches with composition-based statistics and other refinements.* Nucleic Acids Res, 2001. **29**(14): p. 2994-3005.
29. Kobayashi, K., et al., *Essential Bacillus subtilis genes.* Proc Natl Acad Sci U S A, 2003. **100**(8): p. 4678-83.
30. Winterberg, K.M., et al., *Phenotypic screening of Escherichia coli K-12 Tn5 insertion libraries, using whole-genome oligonucleotide microarrays.* Appl Environ Microbiol, 2005. **71**(1): p. 451-9.
31. Gerdes, S.Y., et al., *Experimental determination and system level analysis of essential genes in Escherichia coli MG1655.* J Bacteriol, 2003. **185**(19): p. 5673-84.
32. Salama, N.R., B. Shepherd, and S. Falkow, *Global transposon mutagenesis and essential gene analysis of Helicobacter pylori.* J Bacteriol, 2004. **186**(23): p. 7926-35.
33. Freiberg, C., et al., *Identification of novel essential Escherichia coli genes conserved among pathogenic bacteria.* J Mol Microbiol Biotechnol, 2001. **3**(3): p. 483-9.

34. Allali-Hassani, A., et al., *Probing the active site of YjeE: a vital Escherichia coli protein of unknown function.* Biochem J, 2004. **384**(Pt 3): p. 577-84.
35. Teplyakov, A., et al., *Crystal structure of the YjeE protein from Haemophilus influenzae: a putative Atpase involved in cell wall synthesis.* Proteins, 2002. **48**(2): p. 220-6.
36. Walker, J.E., et al., *Distantly related sequences in the alpha- and beta-subunits of ATP synthase, myosin, kinases and other ATP-requiring enzymes and a common nucleotide binding fold.* Embo J, 1982. **1**(8): p. 945-51.
37. Leipe, D.D., et al., *Classification and evolution of P-loop GTPases and related ATPases.* J Mol Biol, 2002. **317**(1): p. 41-72.
38. Koretke, K.K., R.B. Russell, and A.N. Lupas, *Fold recognition from sequence comparisons.* Proteins, 2001. **Suppl 5**: p. 68-75.
39. Drummond AJ, A.B., Buxton S, Cheung M, Cooper A, Duran C, Field M, Heled J, Kearse M, Markowitz S, Moir R, Stones-Havas S, Sturrock S, Thierer T, Wilson A. *Geneious v 5.5*. 2012 [cited 2012; Available from: http://www.geneious.com.
40. *The PyMOL Molecular Graphics System, Version 1.2r3pre, Schrödinger, LLC.* 2012 [cited 2012; Available from: http://pymol.sourceforge.net.
41. Kolker, E., et al., *Initial proteome analysis of model microorganism Haemophilus influenzae strain Rd KW20.* J Bacteriol, 2003. **185**(15): p. 4593-602.
42. Yoon, H.S., et al., *Anabaena sp. strain PCC 7120 hetY gene influences heterocyst development.* J Bacteriol, 2003. **185**(23): p. 6995-7000.
43. Campbell, T.L., et al., *Isolation of the rstA gene as a multicopy suppressor of YjeE, an essential ATPase of unknown function in Escherichia coli.* J Bacteriol, 2007. **189**(8): p. 3318-21.
44. Oshima, T., et al., *Transcriptome analysis of all two-component regulatory system mutants of Escherichia coli K-12.* Mol Microbiol, 2002. **46**(1): p. 281-91.
45. Chang, D.E., et al., *Carbon nutrition of Escherichia coli in the mouse intestine.* Proc Natl Acad Sci U S A, 2004. **101**(19): p. 7427-32.
46. Pathania, R., et al., *Chemical genomics in Escherichia coli identifies an inhibitor of bacterial lipoprotein targeting.* Nature chemical biology, 2009. **5**(11): p. 849-56.
47. Powers, D.M. and A. Peterkofsky, *The presence of N-(purin-6-ylcarbamoyl)threonine in transfer ribonucleic acid species whose codons begin with adenine.* The Journal of biological chemistry, 1972. **247**(20): p. 6394-401.
48. El Yacoubi, B., et al., *The universal YrdC/Sua5 family is required for the formation of threonylcarbamoyladenosine in tRNA.* Nucleic acids research, 2009. **37**(9): p. 2894-909.
49. El Yacoubi, B., et al., *A role for the universal Kae1/Qri7/YgjD (COG0533) family in tRNA modification.* The EMBO journal, 2011. **30**(5): p. 882-93.

50. Handford, J.I., et al., *Conserved network of proteins essential for bacterial viability.* Journal of bacteriology, 2009. **191**(15): p. 4732-49.
51. Deutsch, C., et al., *Biosynthesis of Threonylcarbamoyl Adenosine (t6A), a Universal tRNA Nucleoside.* The Journal of biological chemistry, 2012. **287**(17): p. 13666-73.
52. Blanchard, S.C., B.S. Cooperman, and D.N. Wilson, *Probing translation with small-molecule inhibitors.* Chemistry & biology, 2010. **17**(6): p. 633-45.
53. Moller, A.K., et al., *An Escherichia coli MG1655 lipopolysaccharide deep-rough core mutant grows and survives in mouse cecal mucus but fails to colonize the mouse large intestine.* Infect Immun, 2003. **71**(4): p. 2142-52.
54. Campbell, T.L., et al., *The yjeQ gene is required for virulence of Staphylococcus aureus.* Infect Immun, 2006. **74**(8): p. 4918-21.
55. Chang, J., et al., *Identification of novel attenuated Salmonella Enteritidis mutants.* FEMS Immunol Med Microbiol, 2008. **53**(1): p. 26-34.
56. Wimberly, B.T., et al., *Structure of the 30S ribosomal subunit.* Nature, 2000. **407**(6802): p. 327-39.
57. Schluenzen, F., et al., *Structure of functionally activated small ribosomal subunit at 3.3 angstroms resolution.* Cell, 2000. **102**(5): p. 615-23.
58. Ban, N., et al., *The complete atomic structure of the large ribosomal subunit at 2.4 A resolution.* Science, 2000. **289**(5481): p. 905-20.
59. Nobelprize.org. *The Nobel Prize in Chemistry 2009 - Press Release*. 2009 [cited 2012 14 Feb 2012]; Available from: http://www.nobelprize.org/nobel_prizes/chemistry/laureates/2009/press.html.
60. Schuwirth, B.S., et al., *Structures of the bacterial ribosome at 3.5 A resolution.* Science, 2005. **310**(5749): p. 827-34.
61. Agalarov, S.C., et al., *In vitro assembly of a ribonucleoprotein particle corresponding to the platform domain of the 30S ribosomal subunit.* Proceedings of the National Academy of Sciences of the United States of America, 1998. **95**(3): p. 999-1003.
62. Samaha, R.R., et al., *Independent in vitro assembly of a ribonucleoprotein particle containing the 3' domain of 16S rRNA.* Proceedings of the National Academy of Sciences of the United States of America, 1994. **91**(17): p. 7884-8.
63. Adilakshmi, T., P. Ramaswamy, and S.A. Woodson, *Protein-independent folding pathway of the 16S rRNA 5' domain.* Journal of molecular biology, 2005. **351**(3): p. 508-19.
64. McCutcheon, J.P., et al., *Location of translational initiation factor IF3 on the small ribosomal subunit.* Proceedings of the National Academy of Sciences of the United States of America, 1999. **96**(8): p. 4301-6.
65. Frank, J., et al., *The process of mRNA-tRNA translocation.* Proceedings of the National Academy of Sciences of the United States of America, 2007. **104**(50): p. 19671-8.

66. Horan, L.H. and H.F. Noller, *Intersubunit movement is required for ribosomal translocation.* Proceedings of the National Academy of Sciences of the United States of America, 2007. **104**(12): p. 4881-5.
67. Noller, H.F., et al., *Secondary structure model for 23S ribosomal RNA.* Nucleic acids research, 1981. **9**(22): p. 6167-89.
68. Steitz, T.A. and P.B. Moore, *RNA, the first macromolecular catalyst: the ribosome is a ribozyme.* Trends in biochemical sciences, 2003. **28**(8): p. 411-8.
69. Traub, P. and M. Nomura, *Structure and function of E. coli ribosomes. V. Reconstitution of functionally active 30S ribosomal particles from RNA and proteins.* Proceedings of the National Academy of Sciences of the United States of America, 1968. **59**(3): p. 777-84.
70. Held, W.A., S. Mizushima, and M. Nomura, *Reconstitution of Escherichia coli 30 S ribosomal subunits from purified molecular components.* The Journal of biological chemistry, 1973. **248**(16): p. 5720-30.
71. Culver, G.M. and H.F. Noller, *Efficient reconstitution of functional Escherichia coli 30S ribosomal subunits from a complete set of recombinant small subunit ribosomal proteins.* Rna, 1999. **5**(6): p. 832-43.
72. Held, W.A., et al., *Assembly mapping of 30 S ribosomal proteins from Escherichia coli. Further studies.* The Journal of biological chemistry, 1974. **249**(10): p. 3103-11.
73. Mizushima, S. and M. Nomura, *Assembly mapping of 30S ribosomal proteins from E. coli.* Nature, 1970. **226**(5252): p. 1214.
74. Powers, T., G. Daubresse, and H.F. Noller, *Dynamics of in vitro assembly of 16 S rRNA into 30 S ribosomal subunits.* Journal of molecular biology, 1993. **232**(2): p. 362-74.
75. Holmes, K.L. and G.M. Culver, *Analysis of conformational changes in 16 S rRNA during the course of 30 S subunit assembly.* Journal of molecular biology, 2005. **354**(2): p. 340-57.
76. Adilakshmi, T., D.L. Bellur, and S.A. Woodson, *Concurrent nucleation of 16S folding and induced fit in 30S ribosome assembly.* Nature, 2008. **455**(7217): p. 1268-72.
77. Agalarov, S.C., et al., *Structure of the S15,S6,S18-rRNA complex: assembly of the 30S ribosome central domain.* Science, 2000. **288**(5463): p. 107-13.
78. Ramaswamy, P. and S.A. Woodson, *Global stabilization of rRNA structure by ribosomal proteins S4, S17, and S20.* J Mol Biol, 2009. **392**(3): p. 666-77.
79. Ramaswamy, P. and S.A. Woodson, *S16 throws a conformational switch during assembly of 30S 5′ domain.* Nature structural & molecular biology, 2009. **16**(4): p. 438-45.
80. Nierhaus, K.H. and F. Dohme, *Total reconstitution of functionally active 50S ribosomal subunits from Escherichia coli.* Proc Natl Acad Sci U S A, 1974. **71**(12): p. 4713-7.
81. Roth, H.E. and K.H. Nierhaus, *Assembly map of the 50-S subunit from Escherichia coli ribosomes, covering the proteins present in the first*

reconstitution intermediate particle. European journal of biochemistry / FEBS, 1980. **103**(1): p. 95-8.
82. Rohl, R. and K.H. Nierhaus, *Assembly map of the large subunit (50S) of Escherichia coli ribosomes.* Proceedings of the National Academy of Sciences of the United States of America, 1982. **79**(3): p. 729-33.
83. Herold, M. and K.H. Nierhaus, *Incorporation of six additional proteins to complete the assembly map of the 50 S subunit from Escherichia coli ribosomes.* The Journal of biological chemistry, 1987. **262**(18): p. 8826-33.
84. Spillmann, S., F. Dohme, and K.H. Nierhaus, *Assembly in vitro of the 50 S subunit from Escherichia coli ribosomes: proteins essential for the first heat-dependent conformational change.* Journal of molecular biology, 1977. **115**(3): p. 513-23.
85. Williamson, J.R., *After the ribosome structures: how are the subunits assembled?* Rna, 2003. **9**(2): p. 165-7.
86. Woodson, S.A., *RNA folding and ribosome assembly.* Current opinion in chemical biology, 2008. **12**(6): p. 667-73.
87. Talkington, M.W., G. Siuzdak, and J.R. Williamson, *An assembly landscape for the 30S ribosomal subunit.* Nature, 2005. **438**(7068): p. 628-32.
88. Herschlag, D., *RNA chaperones and the RNA folding problem.* The Journal of biological chemistry, 1995. **270**(36): p. 20871-4.
89. Treiber, D.K. and J.R. Williamson, *Exposing the kinetic traps in RNA folding.* Current opinion in structural biology, 1999. **9**(3): p. 339-45.
90. Semrad, K., R. Green, and R. Schroeder, *RNA chaperone activity of large ribosomal subunit proteins from Escherichia coli.* Rna, 2004. **10**(12): p. 1855-60.
91. Coetzee, T., D. Herschlag, and M. Belfort, *Escherichia coli proteins, including ribosomal protein S12, facilitate in vitro splicing of phage T4 introns by acting as RNA chaperones.* Genes & development, 1994. **8**(13): p. 1575-88.
92. Treiber, D.K. and J.R. Williamson, *Beyond kinetic traps in RNA folding.* Current opinion in structural biology, 2001. **11**(3): p. 309-14.
93. Mangeol, P., et al., *Probing ribosomal protein-RNA interactions with an external force.* Proceedings of the National Academy of Sciences of the United States of America, 2011. **108**(45): p. 18272-6.
94. Paul, B.J., et al., *rRNA transcription in Escherichia coli.* Annual review of genetics, 2004. **38**: p. 749-70.
95. Sarmientos, P. and M. Cashel, *Carbon starvation and growth rate-dependent regulation of the Escherichia coli ribosomal RNA promoters: differential control of dual promoters.* Proceedings of the National Academy of Sciences of the United States of America, 1983. **80**(22): p. 7010-3.
96. Sarmientos, P., et al., *Differential stringent control of the tandem E. coli ribosomal RNA promoters from the rrnA operon expressed in vivo in multicopy plasmids.* Cell, 1983. **32**(4): p. 1337-46.

97. Gaal, T., et al., *Transcription regulation by initiating NTP concentration: rRNA synthesis in bacteria.* Science, 1997. **278**(5346): p. 2092-7.
98. Murray, H.D., D.A. Schneider, and R.L. Gourse, *Control of rRNA expression by small molecules is dynamic and nonredundant.* Molecular cell, 2003. **12**(1): p. 125-34.
99. Nikolaev, N., L. Silengo, and D. Schlessinger, *A role for ribonuclease 3 in processing of ribosomal ribonucleic acid and messenger ribonucleic acid precursors in Escherichia coli.* The Journal of biological chemistry, 1973. **248**(22): p. 7967-9.
100. Ginsburg, D. and J.A. Steitz, *The 30 S ribosomal precursor RNA from Escherichia coli. A primary transcript containing 23 S, 16 S, and 5 S sequences.* The Journal of biological chemistry, 1975. **250**(14): p. 5647-54.
101. Li, Z., S. Pandit, and M.P. Deutscher, *RNase G (CafA protein) and RNase E are both required for the 5' maturation of 16S ribosomal RNA.* The EMBO journal, 1999. **18**(10): p. 2878-85.
102. Young, R.A. and J.A. Steitz, *Complementary sequences 1700 nucleotides apart form a ribonuclease III cleavage site in Escherichia coli ribosomal precursor RNA.* Proceedings of the National Academy of Sciences of the United States of America, 1978. **75**(8): p. 3593-7.
103. Hayes, F. and M. Vasseur, *Processing of the 17-S Escherichia coli precursor RNA in the 27-S pre-ribosomal particle.* European journal of biochemistry / FEBS, 1976. **61**(2): p. 433-42.
104. King, T.C., R. Sirdeshmukh, and D. Schlessinger, *RNase III cleavage is obligate for maturation but not for function of Escherichia coli pre-23S rRNA.* Proceedings of the National Academy of Sciences of the United States of America, 1984. **81**(1): p. 185-8.
105. Sirdeshmukh, R. and D. Schlessinger, *Ordered processing of Escherichia coli 23S rRNA in vitro.* Nucleic acids research, 1985. **13**(14): p. 5041-54.
106. Li, Z., S. Pandit, and M.P. Deutscher, *Maturation of 23S ribosomal RNA requires the exoribonuclease RNase T.* Rna, 1999. **5**(1): p. 139-46.
107. Roy, M.K., et al., *Maturation of 5-S rRNA: ribonuclease E cleavages and their dependence on precursor sequences.* European journal of biochemistry / FEBS, 1983. **131**(1): p. 119-27.
108. Li, Z. and M.P. Deutscher, *The tRNA processing enzyme RNase T is essential for maturation of 5S RNA.* Proceedings of the National Academy of Sciences of the United States of America, 1995. **92**(15): p. 6883-6.
109. Zengel, J.M. and L. Lindahl, *Diverse mechanisms for regulating ribosomal protein synthesis in Escherichia coli.* Progress in nucleic acid research and molecular biology, 1994. **47**: p. 331-70.
110. Lemke, J.J., et al., *Direct regulation of Escherichia coli ribosomal protein promoters by the transcription factors ppGpp and DksA.* Proceedings of the National Academy of Sciences of the United States of America, 2011. **108**(14): p. 5712-7.

111. Pardon, B. and R. Wagner, *The Escherichia coli ribosomal RNA leader nut region interacts specifically with mature 16S RNA.* Nucleic acids research, 1995. **23**(6): p. 932-41.
112. Besancon, W. and R. Wagner, *Characterization of transient RNA-RNA interactions important for the facilitated structure formation of bacterial ribosomal 16S RNA.* Nucleic acids research, 1999. **27**(22): p. 4353-62.
113. Balzer, M. and R. Wagner, *Mutations in the leader region of ribosomal RNA operons cause structurally defective 30 S ribosomes as revealed by in vivo structural probing.* Journal of molecular biology, 1998. **276**(3): p. 547-57.
114. Schaferkordt, J. and R. Wagner, *Effects of base change mutations within an Escherichia coli ribosomal RNA leader region on rRNA maturation and ribosome formation.* Nucleic acids research, 2001. **29**(16): p. 3394-403.
115. Srivastava, A.K. and D. Schlessinger, *Escherichia coli 16S rRNA 3'-end formation requires a distal transfer RNA sequence at a proper distance.* The EMBO journal, 1989. **8**(10): p. 3159-66.
116. Szymkowiak, C., et al., *The tRNAGlu2 gene in the rrnB operon of E. coli is a prerequisite for correct RNase III processing in vitro.* Nucleic acids research, 1988. **16**(16): p. 7885-99.
117. Liiv, A., et al., *Multiple functions of the transcribed spacers in ribosomal RNA operons.* Biological chemistry, 1998. **379**(7): p. 783-93.
118. de Narvaez, C.C. and H.W. Schaup, *In vivo transcriptionally coupled assembly of Escherichia coli ribosomal subunits.* Journal of molecular biology, 1979. **134**(1): p. 1-22.
119. Lindahl, L., *Intermediates and time kinetics of the in vivo assembly of Escherichia coli ribosomes.* J Mol Biol, 1975. **92**(1): p. 15-37.
120. Dennis, P.P., et al., *Varying rate of RNA chain elongation during rrn transcription in Escherichia coli.* Journal of bacteriology, 2009. **191**(11): p. 3740-6.
121. Lewicki, B.T., et al., *Coupling of rRNA transcription and ribosomal assembly in vivo. Formation of active ribosomal subunits in Escherichia coli requires transcription of rRNA genes by host RNA polymerase which cannot be replaced by bacteriophage T7 RNA polymerase.* Journal of molecular biology, 1993. **231**(3): p. 581-93.
122. Kaczanowska, M. and M. Ryden-Aulin, *Ribosome biogenesis and the translation process in Escherichia coli.* Microbiol Mol Biol Rev, 2007. **71**(3): p. 477-94.
123. Traub, P. and M. Nomura, *Structure and function of Escherichia coli ribosomes. VI. Mechanism of assembly of 30 s ribosomes studied in vitro.* J Mol Biol, 1969. **40**(3): p. 391-413.
124. Nomura, M. and V.A. Erdmann, *Reconstitution of 50S ribosomal subunits from dissociated molecular components.* Nature, 1970. **228**(5273): p. 744-8.
125. Shajani, Z., M.T. Sykes, and J.R. Williamson, *Assembly of bacterial ribosomes.* Annual review of biochemistry, 2011. **80**: p. 501-26.

126. Pan, C. and R. Russell, *Roles of DEAD-box proteins in RNA and RNP Folding.* RNA biology, 2010. **7**(6): p. 667-76.
127. Iost, I. and M. Dreyfus, *DEAD-box RNA helicases in Escherichia coli.* Nucleic acids research, 2006. **34**(15): p. 4189-97.
128. Jagessar, K.L. and C. Jain, *Functional and molecular analysis of Escherichia coli strains lacking multiple DEAD-box helicases.* Rna, 2010. **16**(7): p. 1386-92.
129. Charollais, J., M. Dreyfus, and I. Iost, *CsdA, a cold-shock RNA helicase from Escherichia coli, is involved in the biogenesis of 50S ribosomal subunit.* Nucleic acids research, 2004. **32**(9): p. 2751-9.
130. Charollais, J., et al., *The DEAD-box RNA helicase SrmB is involved in the assembly of 50S ribosomal subunits in Escherichia coli.* Molecular microbiology, 2003. **48**(5): p. 1253-65.
131. Peil, L., K. Virumae, and J. Remme, *Ribosome assembly in Escherichia coli strains lacking the RNA helicase DeaD/CsdA or DbpA.* The FEBS journal, 2008. **275**(15): p. 3772-82.
132. Beckmann, R.P., L.E. Mizzen, and W.J. Welch, *Interaction of Hsp 70 with newly synthesized proteins: implications for protein folding and assembly.* Science, 1990. **248**(4957): p. 850-4.
133. Gaitanaris, G.A., et al., *Successive action of Escherichia coli chaperones in vivo.* Molecular microbiology, 1994. **14**(5): p. 861-9.
134. Alix, J.H. and M.F. Guerin, *Mutant DnaK chaperones cause ribosome assembly defects in Escherichia coli.* Proceedings of the National Academy of Sciences of the United States of America, 1993. **90**(20): p. 9725-9.
135. Al Refaii, A. and J.H. Alix, *Ribosome biogenesis is temperature-dependent and delayed in Escherichia coli lacking the chaperones DnaK or DnaJ.* Molecular microbiology, 2009. **71**(3): p. 748-62.
136. El Hage, A., M. Sbai, and J.H. Alix, *The chaperonin GroEL and other heat-shock proteins, besides DnaK, participate in ribosome biogenesis in Escherichia coli.* Molecular & general genetics : MGG, 2001. **264**(6): p. 796-808.
137. Maki, J.A., D.J. Schnobrich, and G.M. Culver, *The DnaK chaperone system facilitates 30S ribosomal subunit assembly.* Molecular cell, 2002. **10**(1): p. 129-38.
138. Maki, J.A., D.R. Southworth, and G.M. Culver, *Demonstration of the role of the DnaK chaperone system in assembly of 30S ribosomal subunits using a purified in vitro system.* Rna, 2003. **9**(12): p. 1418-21.
139. Alix, J.H. and K.H. Nierhaus, *DnaK-facilitated ribosome assembly in Escherichia coli revisited.* Rna, 2003. **9**(7): p. 787-93.
140. Rene, O. and J.H. Alix, *Late steps of ribosome assembly in E. coli are sensitive to a severe heat stress but are assisted by the HSP70 chaperone machine.* Nucleic acids research, 2011. **39**(5): p. 1855-67.
141. Britton, R.A., *Role of GTPases in bacterial ribosome assembly.* Annu Rev Microbiol, 2009. **63**: p. 155-76.

142. Verstraeten, N., et al., *The universally conserved prokaryotic GTPases.* Microbiology and molecular biology reviews : MMBR, 2011. **75**(3): p. 507-42, second and third pages of table of contents.
143. Daigle, D.M. and E.D. Brown, *Studies of the interaction of Escherichia coli YjeQ with the ribosome in vitro.* Journal of bacteriology, 2004. **186**(5): p. 1381-7.
144. March, P.E., et al., *The Escherichia coli Ras-like protein (Era) has GTPase activity and is essential for cell growth.* Oncogene, 1988. **2**(6): p. 539-44.
145. Roy-Chaudhuri, B., et al., *Suppression of a cold-sensitive mutation in ribosomal protein S5 reveals a role for RimJ in ribosome biogenesis.* Molecular microbiology, 2008. **68**(6): p. 1547-59.
146. Jiang, M., et al., *Identification of novel Escherichia coli ribosome-associated proteins using isobaric tags and multidimensional protein identification techniques.* J Bacteriol, 2007. **189**(9): p. 3434-44.
147. Sharma, M.R., et al., *Interaction of Era with the 30S ribosomal subunit implications for 30S subunit assembly.* Molecular cell, 2005. **18**(3): p. 319-29.
148. Jomaa, A., et al., *Cryo-electron microscopy structure of the 30S subunit in complex with the YjeQ biogenesis factor.* Rna, 2011. **17**(11): p. 2026-38.
149. Guo, Q., et al., *Structural basis for the function of a small GTPase RsgA on the 30S ribosomal subunit maturation revealed by cryoelectron microscopy.* Proceedings of the National Academy of Sciences of the United States of America, 2011. **108**(32): p. 13100-5.
150. Datta, P.P., et al., *Structural aspects of RbfA action during small ribosomal subunit assembly.* Molecular cell, 2007. **28**(3): p. 434-45.
151. Ogle, J.M., A.P. Carter, and V. Ramakrishnan, *Insights into the decoding mechanism from recent ribosome structures.* Trends in biochemical sciences, 2003. **28**(5): p. 259-66.
152. Goto, S., et al., *RsgA releases RbfA from 30S ribosome during a late stage of ribosome biosynthesis.* The EMBO journal, 2011. **30**(1): p. 104-14.
153. Lovgren, J.M., et al., *The PRC-barrel domain of the ribosome maturation protein RimM mediates binding to ribosomal protein S19 in the 30S ribosomal subunits.* Rna, 2004. **10**(11): p. 1798-812.
154. Bunner, A.E., et al., *The effect of ribosome assembly cofactors on in vitro 30S subunit reconstitution.* Journal of molecular biology, 2010. **398**(1): p. 1-7.
155. Jomaa, A., et al., *Understanding ribosome assembly: the structure of in vivo assembled immature 30S subunits revealed by cryo-electron microscopy.* Rna, 2011. **17**(4): p. 697-709.
156. Bharat, A., et al., *Cooperative and critical roles for both G domains in the GTPase activity and cellular function of ribosome-associated Escherichia coli EngA.* J Bacteriol, 2006. **188**(22): p. 7992-6.
157. Hwang, J. and M. Inouye, *The tandem GTPase, Der, is essential for the biogenesis of 50S ribosomal subunits in Escherichia coli.* Molecular microbiology, 2006. **61**(6): p. 1660-72.

158. Kobayashi, G., S. Moriya, and C. Wada, *Deficiency of essential GTP-binding protein ObgE in Escherichia coli inhibits chromosome partition.* Molecular microbiology, 2001. **41**(5): p. 1037-51.
159. Arnold, R.J. and J.P. Reilly, *Observation of Escherichia coli ribosomal proteins and their posttranslational modifications by mass spectrometry.* Anal Biochem, 1999. **269**(1): p. 105-12.
160. Arigoni, F., et al., *A genome-based approach for the identification of essential bacterial genes.* Nature biotechnology, 1998. **16**(9): p. 851-6.
161. Hwang, J. and M. Inouye, *A bacterial GAP-like protein, YihI, regulating the GTPase of Der, an essential GTP-binding protein in Escherichia coli.* Journal of molecular biology, 2010. **399**(5): p. 759-72.
162. Schaefer, L., et al., *Multiple GTPases participate in the assembly of the large ribosomal subunit in Bacillus subtilis.* Journal of bacteriology, 2006. **188**(23): p. 8252-8.
163. Cooper, E.L., J. Garcia-Lara, and S.J. Foster, *YsxC, an essential protein in Staphylococcus aureus crucial for ribosome assembly/stability.* BMC microbiology, 2009. **9**: p. 266.
164. Sato, A., et al., *The GTP binding protein Obg homolog ObgE is involved in ribosome maturation.* Genes Cells, 2005. **10**(5): p. 393-408.
165. Jiang, M., et al., *The Escherichia coli GTPase CgtAE is involved in late steps of large ribosome assembly.* Journal of bacteriology, 2006. **188**(19): p. 6757-70.
166. Rodnina, M.V., W. Wintermeyer, and R. Green, *Ribosomes : structure, function, and dynamics*2011, Wien ; New York: Springer. ix, 442 p.97-110.
167. Decatur, W.A. and M.J. Fournier, *rRNA modifications and ribosome function.* Trends in biochemical sciences, 2002. **27**(7): p. 344-51.
168. Krzyzosiak, W., et al., *In vitro synthesis of 16S ribosomal RNA containing single base changes and assembly into a functional 30S ribosome.* Biochemistry, 1987. **26**(8): p. 2353-64.
169. Green, R. and H.F. Noller, *In vitro complementation analysis localizes 23S rRNA posttranscriptional modifications that are required for Escherichia coli 50S ribosomal subunit assembly and function.* Rna, 1996. **2**(10): p. 1011-21.
170. Poldermans, B., L. Roza, and P.H. Van Knippenberg, *Studies on the function of two adjacent N6,N6-dimethyladenosines near the 3' end of 16 S ribosomal RNA of Escherichia coli. III. Purification and properties of the methylating enzyme and methylase-30 S interactions.* The Journal of biological chemistry, 1979. **254**(18): p. 9094-100.
171. Connolly, K., J.P. Rife, and G. Culver, *Mechanistic insight into the ribosome biogenesis functions of the ancient protein KsgA.* Mol Microbiol, 2008. **70**(5): p. 1062-75.
172. Campbell, T.L. and E.D. Brown, *Genetic interaction screens with ordered overexpression and deletion clone sets implicate the Escherichia coli GTPase YjeQ in late ribosome biogenesis.* Journal of bacteriology, 2008. **190**(7): p. 2537-45.

173. Ofengand, J., *Ribosomal RNA pseudouridines and pseudouridine synthases.* FEBS letters, 2002. **514**(1): p. 17-25.
174. Huang, L., et al., *Identification of two Escherichia coli pseudouridine synthases that show multisite specificity for 23S RNA.* Biochemistry, 1998. **37**(45): p. 15951-7.
175. Raychaudhuri, S., et al., *A pseudouridine synthase required for the formation of two universally conserved pseudouridines in ribosomal RNA is essential for normal growth of Escherichia coli.* Rna, 1998. **4**(11): p. 1407-17.
176. Gutgsell, N.S., M.P. Deutscher, and J. Ofengand, *The pseudouridine synthase RluD is required for normal ribosome assembly and function in Escherichia coli.* Rna, 2005. **11**(7): p. 1141-52.
177. Leppik, M., et al., *Substrate specificity of the pseudouridine synthase RluD in Escherichia coli.* The FEBS journal, 2007. **274**(21): p. 5759-66.
178. Caldas, T., et al., *The FtsJ/RrmJ heat shock protein of Escherichia coli is a 23 S ribosomal RNA methyltransferase.* The Journal of biological chemistry, 2000. **275**(22): p. 16414-9.
179. Caldas, T., et al., *Translational defects of Escherichia coli mutants deficient in the Um(2552) 23S ribosomal RNA methyltransferase RrmJ/FTSJ.* Biochemical and biophysical research communications, 2000. **271**(3): p. 714-8.
180. Bugl, H., et al., *RNA methylation under heat shock control.* Molecular cell, 2000. **6**(2): p. 349-60.
181. Tan, J., U. Jakob, and J.C. Bardwell, *Overexpression of two different GTPases rescues a null mutation in a heat-induced rRNA methyltransferase.* J Bacteriol, 2002. **184**(10): p. 2692-8.
182. Cumberlidge, A.G. and K. Isono, *Ribosomal protein modification in Escherichia coli. I. A mutant lacking the N-terminal acetylation of protein S5 exhibits thermosensitivity.* J Mol Biol, 1979. **131**(2): p. 169-89.
183. Lhoest, J. and C. Colson, *Cold-sensitive ribosome assembly in an Escherichia coli mutant lacking a single methyl group in ribosomal protein L3.* Eur J Biochem, 1981. **121**(1): p. 33-7.
184. Vanet, A., et al., *Ribosomal protein methylation in Escherichia coli: the gene prmA, encoding the ribosomal protein L11 methyltransferase, is dispensable.* Mol Microbiol, 1994. **14**(5): p. 947-58.
185. Isono, K. and S. Isono, *Ribosomal protein modification in Escherichia coli. II. Studies of a mutant lacking the N-terminal acetylation of protein S18.* Molecular & general genetics : MGG, 1980. **177**(4): p. 645-51.
186. Anton, B.P., et al., *RimO, a MiaB-like enzyme, methylthiolates the universally conserved Asp88 residue of ribosomal protein S12 in Escherichia coli.* Proceedings of the National Academy of Sciences of the United States of America, 2008. **105**(6): p. 1826-31.
187. Elowitz, M.B., et al., *Stochastic gene expression in a single cell.* Science, 2002. **297**(5584): p. 1183-6.

188. Cai, L., N. Friedman, and X.S. Xie, *Stochastic protein expression in individual cells at the single molecule level.* Nature, 2006. **440**(7082): p. 358-62.
189. O'Connor, C.J., L. Laraia, and D.R. Spring, *Chemical genetics.* Chemical Society reviews, 2011. **40**(8): p. 4332-45.
190. Barker, C.A., M.A. Farha, and E.D. Brown, *Chemical genomic approaches to study model microbes.* Chemistry & biology, 2010. **17**(6): p. 624-32.
191. Falconer, S.B., T.L. Czarny, and E.D. Brown, *Antibiotics as probes of biological complexity.* Nature chemical biology, 2011. **7**(7): p. 415-23.
192. Banks, P., M. Gosselin, and L. Prystay, *Impact of a red-shifted dye label for high throughput fluorescence polarization assays of G protein-coupled receptors.* J Biomol Screen, 2000. **5**(5): p. 329-34.
193. Buchli, R., et al., *Development and validation of a fluorescence polarization-based competitive peptide-binding assay for HLA-A*0201--a new tool for epitope discovery.* Biochemistry, 2005. **44**(37): p. 12491-507.
194. Do, E.U., et al., *Fluorescence polarization assays for high-throughput screening of neuropeptide FF receptors.* Anal Biochem, 2004. **330**(1): p. 156-63.
195. Kim, J., et al., *Development of a fluorescence polarization assay for the molecular chaperone Hsp90.* J Biomol Screen, 2004. **9**(5): p. 375-81.
196. Lokesh, G.L., et al., *High-throughput fluorescence polarization assay to identify small molecule inhibitors of BRCT domains of breast cancer gene 1.* Anal Biochem, 2006.
197. Nakayama, G.R., et al., *A fluorescence polarization assay for screening inhibitors against the ribonuclease H activity of HIV-1 reverse transcriptase.* Anal Biochem, 2006. **351**(2): p. 260-5.
198. Owicki, J.C., *Fluorescence polarization and anisotropy in high throughput screening: perspectives and primer.* J Biomol Screen, 2000. **5**(5): p. 297-306.
199. Rishi, V., et al., *A high-throughput fluorescence-anisotropy screen that identifies small molecule inhibitors of the DNA binding of B-ZIP transcription factors.* Anal Biochem, 2005. **340**(2): p. 259-71.
200. Roehrl, M.H., J.Y. Wang, and G. Wagner, *Discovery of small-molecule inhibitors of the NFAT--calcineurin interaction by competitive high-throughput fluorescence polarization screening.* Biochemistry, 2004. **43**(51): p. 16067-75.
201. Annis, D.A., et al., *A general technique to rank protein-ligand binding affinities and determine allosteric versus direct binding site competition in compound mixtures.* J Am Chem Soc, 2004. **126**(47): p. 15495-503.
202. Davis, J., R. Anderegg, and B. S, *Iterative size-exclusion chromatography coupled with liquid chromatographic mass spectrometry to enrich and identify tight-binding ligands from complex mixtures.* Tetrahedron, 1998. **55**: p. 11653-11667.
203. Zolli-Juran, M., et al., *High throughput screening identifies novel inhibitors of Escherichia coli dihydrofolate reductase that are competitive with dihydrofolate.* Bioorg Med Chem Lett, 2003. **13**(15): p. 2493-6.

204. Hiratsuka, T., *New ribose-modified fluorescent analogs of adenine and guanine nucleotides available as substrates for various enzymes.* Biochimica et biophysica acta, 1983. **742**(3): p. 496-508.
205. Lakowicz, J.R., *Principles of fluorescence spectroscopy*. 2nd ed1999, New York: Kluwer Academic/Plenum. xxiii, 698.
206. McGovern, S.L., et al., *A common mechanism underlying promiscuous inhibitors from virtual and high-throughput screening.* Journal of medicinal chemistry, 2002. **45**(8): p. 1712-22.
207. Shoichet, B.K., *Screening in a spirit haunted world.* Drug discovery today, 2006. **11**(13-14): p. 607-15.
208. Penefsky, H.S., *A centrifuged-column procedure for the measurement of ligand binding by beef heart F1.* Methods Enzymol, 1979. **56**: p. 527-30.
209. Lerner, C.G., et al., *From bacterial genomes to novel antibacterial agents: discovery, characterization, and antibacterial activity of compounds that bind to HI0065 (YjeE) from Haemophilus influenzae.* Chem Biol Drug Des, 2007. **69**(6): p. 395-404.
210. Huang, X., *Fluorescence polarization competition assay: the range of resolvable inhibitor potency is limited by the affinity of the fluorescent ligand.* Journal of biomolecular screening, 2003. **8**(1): p. 34-8.
211. Campbell, T.L., *Investigating the Uncharacterized Proteins IspF and YjeQ*, in *Biochemistry and Biomedical Sciences*2007, McMaster University: Hamilton, ON. p. 138.
212. D'Elia, M.A., et al., *Probing teichoic acid genetics with bioactive molecules reveals new interactions among diverse processes in bacterial cell wall biogenesis.* Chemistry & biology, 2009. **16**(5): p. 548-56.
213. Ruiz, N., et al., *Chemical conditionality: a genetic strategy to probe organelle assembly.* Cell, 2005. **121**(2): p. 307-17.
214. Van Dyk, T.K., E.J. DeRose, and G.E. Gonye, *LuxArray, a high-density, genomewide transcription analysis of Escherichia coli using bioluminescent reporter strains.* J Bacteriol, 2001. **183**(19): p. 5496-505.
215. Dwyer, D.J., et al., *Gyrase inhibitors induce an oxidative damage cellular death pathway in Escherichia coli.* Mol Syst Biol, 2007. **3**: p. 91.
216. Kohanski, M.A., et al., *A common mechanism of cellular death induced by bactericidal antibiotics.* Cell, 2007. **130**(5): p. 797-810.
217. Bjarnason, J., C.M. Southward, and M.G. Surette, *Genomic profiling of iron-responsive genes in Salmonella enterica serovar typhimurium by high-throughput screening of a random promoter library.* J Bacteriol, 2003. **185**(16): p. 4973-82.
218. Baba, T., et al., *Construction of Escherichia coli K-12 in-frame, single-gene knockout mutants: the Keio collection.* Mol Syst Biol, 2006. **2**: p. 2006 0008.
219. Kitagawa, R., et al., *A novel DnaA protein-binding site at 94.7 min on the Escherichia coli chromosome.* Mol Microbiol, 1996. **19**(5): p. 1137-47.

220. Kim, W. and M.G. Surette, *Coordinated regulation of two independent cell-cell signaling systems and swarmer differentiation in Salmonella enterica serovar Typhimurium.* J Bacteriol, 2006. **188**(2): p. 431-40.
221. Adams, D.E., et al., *The role of topoisomerase IV in partitioning bacterial replicons and the structure of catenated intermediates in DNA replication.* Cell, 1992. **71**(2): p. 277-88.
222. Kato, J., et al., *New topoisomerase essential for chromosome segregation in E. coli.* Cell, 1990. **63**(2): p. 393-404.
223. Zechiedrich, E.L. and N.R. Cozzarelli, *Roles of topoisomerase IV and DNA gyrase in DNA unlinking during replication in Escherichia coli.* Genes Dev, 1995. **9**(22): p. 2859-69.
224. Gellert, M., et al., *DNA gyrase: an enzyme that introduces superhelical turns into DNA.* Proc Natl Acad Sci U S A, 1976. **73**(11): p. 3872-6.
225. Nollmann, M., N.J. Crisona, and P.B. Arimondo, *Thirty years of Escherichia coli DNA gyrase: from in vivo function to single-molecule mechanism.* Biochimie, 2007. **89**(4): p. 490-9.
226. Khodursky, A.B., E.L. Zechiedrich, and N.R. Cozzarelli, *Topoisomerase IV is a target of quinolones in Escherichia coli.* Proc Natl Acad Sci U S A, 1995. **92**(25): p. 11801-5.
227. Everett, M.J., et al., *Contributions of individual mechanisms to fluoroquinolone resistance in 36 Escherichia coli strains isolated from humans and animals.* Antimicrob Agents Chemother, 1996. **40**(10): p. 2380-6.
228. Vila, J., et al., *Association between double mutation in gyrA gene of ciprofloxacin-resistant clinical isolates of Escherichia coli and MICs.* Antimicrob Agents Chemother, 1994. **38**(10): p. 2477-9.
229. Fram, R.J., et al., *DNA repair mechanisms affecting cytotoxicity by streptozotocin in E. coli.* Mutat Res, 1989. **218**(2): p. 125-33.
230. Cabeza, M.L., et al., *Induction of RpoS Degradation by the Two-Component System Regulator RstA in Salmonella enterica.* J Bacteriol, 2007. **189**(20): p. 7335-42.
231. Unden, G. and J. Bongaerts, *Alternative respiratory pathways of Escherichia coli: energetics and transcriptional regulation in response to electron acceptors.* Biochim Biophys Acta, 1997. **1320**(3): p. 217-34.
232. Storz, G. and R. Hengge-Aronis, *Bacterial stress responses*2000, Washington, D.C.: ASM Press. xv, 485 p.
233. Bjork, G.R., et al., *Transfer RNA modification: influence on translational frameshifting and metabolism.* FEBS letters, 1999. **452**(1-2): p. 47-51.
234. Messenger, L.J. and H. Zalkin, *Glutamine phosphoribosylpyrophosphate amidotransferase from Escherichia coli. Purification and properties.* The Journal of biological chemistry, 1979. **254**(9): p. 3382-92.
235. Butland, G., et al., *Interaction network containing conserved and essential protein complexes in Escherichia coli.* Nature, 2005. **433**(7025): p. 531-7.

236. Comartin, D.J. and E.D. Brown, *Non-ribosomal factors in ribosome subunit assembly are emerging targets for new antibacterial drugs.* Curr Opin Pharmacol, 2006. **6**(5): p. 453-8.
237. Connolly, K. and G. Culver, *Deconstructing ribosome construction.* Trends Biochem Sci, 2009. **34**(5): p. 256-63.
238. Tai, P.C., D.P. Kessler, and J. Ingraham, *Cold-sensitive mutations in Salmonella typhimurium which affect ribosome synthesis.* J Bacteriol, 1969. **97**(3): p. 1298-304.
239. Guthrie, C., H. Nashimoto, and M. Nomura, *Structure and function of E. coli ribosomes. 8. Cold-sensitive mutants defective in ribosome assembly.* Proc Natl Acad Sci U S A, 1969. **63**(2): p. 384-91.
240. Weber, M.H. and M.A. Marahiel, *Bacterial cold shock responses.* Sci Prog, 2003. **86**(Pt 1-2): p. 9-75.
241. Friedman, H., P. Lu, and A. Rich, *Temperature control of initiation of protein synthesis in Escherichia coli.* Journal of molecular biology, 1971. **61**(1): p. 105-21.
242. Dammel, C.S. and H.F. Noller, *Suppression of a cold-sensitive mutation in 16S rRNA by overexpression of a novel ribosome-binding factor, RbfA.* Genes Dev, 1995. **9**(5): p. 626-37.
243. Lerner, C.G., P.S. Gulati, and M. Inouye, *Cold-sensitive conditional mutations in Era, an essential Escherichia coli GTPase, isolated by localized random polymerase chain reaction mutagenesis.* FEMS Microbiol Lett, 1995. **126**(3): p. 291-8.
244. Kirthi, N., et al., *A novel single amino acid change in small subunit ribosomal protein S5 has profound effects on translational fidelity.* Rna, 2006. **12**(12): p. 2080-91.
245. Iost, I. and M. Dreyfus, *DEAD-box RNA helicases in Escherichia coli.* Nucleic Acids Res, 2006. **34**(15): p. 4189-97.
246. Keseler, I.M., et al., *EcoCyc: a comprehensive database of Escherichia coli biology.* Nucleic Acids Res, 2011. **39**(Database issue): p. D583-90.
247. *The Universal Protein Resource (UniProt) in 2010.* Nucleic Acids Res, 2010. **38**(Database issue): p. D142-8.
248. Kitagawa, M., et al., *Complete set of ORF clones of Escherichia coli ASKA library (a complete set of E. coli K-12 ORF archive): unique resources for biological research.* DNA Res, 2005. **12**(5): p. 291-9.
249. Sambrook, J. and D.W. Russell, *Molecular cloning : a laboratory manual*. 3rd ed2001, Cold Spring Harbor, N.Y.: Cold Spring Harbor Laboratory Press.
250. Tatusov, R.L., E.V. Koonin, and D.J. Lipman, *A genomic perspective on protein families.* Science, 1997. **278**(5338): p. 631-7.
251. Del Campo, M., Y. Kaya, and J. Ofengand, *Identification and site of action of the remaining four putative pseudouridine synthases in Escherichia coli.* Rna, 2001. **7**(11): p. 1603-15.

252. Kimura, S. and T. Suzuki, *Fine-tuning of the ribosomal decoding center by conserved methyl-modifications in the Escherichia coli 16S rRNA.* Nucleic Acids Res, 2010. **38**(4): p. 1341-52.
253. Sergiev, P.V., et al., *The ybiN gene of Escherichia coli encodes adenine-N6 methyltransferase specific for modification of A1618 of 23 S ribosomal RNA, a methylated residue located close to the ribosomal exit tunnel.* Journal of molecular biology, 2008. **375**(1): p. 291-300.
254. Caldas, T., et al., *Translational defects of Escherichia coli mutants deficient in the Um(2552) 23S ribosomal RNA methyltransferase RrmJ/FTSJ.* Biochem Biophys Res Commun, 2000. **271**(3): p. 714-8.
255. Jones, P.G., et al., *Cold shock induces a major ribosomal-associated protein that unwinds double-stranded RNA in Escherichia coli.* Proc Natl Acad Sci U S A, 1996. **93**(1): p. 76-80.
256. Charollais, J., et al., *The DEAD-box RNA helicase SrmB is involved in the assembly of 50S ribosomal subunits in Escherichia coli.* Mol Microbiol, 2003. **48**(5): p. 1253-65.
257. Himeno, H., et al., *A novel GTPase activated by the small subunit of ribosome.* Nucleic Acids Res, 2004. **32**(17): p. 5303-9.
258. Pfennig, P.L. and A.M. Flower, *BipA is required for growth of Escherichia coi K12 at low temperature.* Mol Genet Genomics, 2001. **266**(2): p. 313-7.
259. Nord, S., et al., *The RimP protein is important for maturation of the 30S ribosomal subunit.* J Mol Biol, 2009. **386**(3): p. 742-53.
260. Lauber, M.A., W.E. Running, and J.P. Reilly, *B. subtilis ribosomal proteins: structural homology and post-translational modifications.* J Proteome Res, 2009. **8**(9): p. 4193-206.
261. Sharpe Elles, L.M., et al., *A dominant negative mutant of the E. coli RNA helicase DbpA blocks assembly of the 50S ribosomal subunit.* Nucleic Acids Res, 2009. **37**(19): p. 6503-14.
262. Elles, L.M. and O.C. Uhlenbeck, *Mutation of the arginine finger in the active site of Escherichia coli DbpA abolishes ATPase and helicase activity and confers a dominant slow growth phenotype.* Nucleic Acids Res, 2008. **36**(1): p. 41-50.
263. Kelly, K.O. and M.P. Deutscher, *The presence of only one of five exoribonucleases is sufficient to support the growth of Escherichia coli.* J Bacteriol, 1992. **174**(20): p. 6682-4.
264. Butland, G., et al., *eSGA: E. coli synthetic genetic array analysis.* Nat Methods, 2008. **5**(9): p. 789-95.
265. Typas, A., et al., *High-throughput, quantitative analyses of genetic interactions in E. coli.* Nat Methods, 2008. **5**(9): p. 781-7.
266. Nashimoto, H., et al., *Structure and function of bacterial ribosomes. XII. Accumulation of 21 s particles by some cold-sensitive mutants of Escherichia coli.* J Mol Biol, 1971. **62**(1): p. 121-38.

267. Geyl, D., A. Bock, and H.G. Wittmann, *Cold-sensitive growth of a mutant of Escherichia coli with an altered ribosomal protein S8: analysis of revertants.* Mol Gen Genet, 1977. **152**(3): p. 331-6.
268. Phadtare, S. and K. Severinov, *RNA remodeling and gene regulation by cold shock proteins.* RNA Biol, 2010. **7**(6).
269. Ramaswamy, P. and S.A. Woodson, *S16 throws a conformational switch during assembly of 30S 5' domain.* Nat Struct Mol Biol, 2009. **16**(4): p. 438-45.
270. Brown, E.D., *Conserved P-loop GTPases of unknown function in bacteria: an emerging and vital ensemble in bacterial physiology.* Biochem Cell Biol, 2005. **83**(6): p. 738-46.
271. Teplyakov, A., et al., *Crystal structure of the YchF protein reveals binding sites for GTP and nucleic acid.* J Bacteriol, 2003. **185**(14): p. 4031-7.
272. Gradia, D.F., et al., *Characterization of a novel Obg-like ATPase in the protozoan Trypanosoma cruzi.* Int J Parasitol, 2009. **39**(1): p. 49-58.
273. Freistroffer, D.V., et al., *Release factor RF3 in E.coli accelerates the dissociation of release factors RF1 and RF2 from the ribosome in a GTP-dependent manner.* EMBO J, 1997. **16**(13): p. 4126-33.
274. Pavlov, M.Y., et al., *Fast recycling of Escherichia coli ribosomes requires both ribosome recycling factor (RRF) and release factor RF3.* EMBO J, 1997. **16**(13): p. 4134-41.
275. Zavialov, A.V., R.H. Buckingham, and M. Ehrenberg, *A posttermination ribosomal complex is the guanine nucleotide exchange factor for peptide release factor RF3.* Cell, 2001. **107**(1): p. 115-24.
276. Zaher, H.S. and R. Green, *Quality control by the ribosome following peptide bond formation.* Nature, 2009. **457**(7226): p. 161-6.
277. Scolnick, E., et al., *Release factors differing in specificity for terminator codons.* Proceedings of the National Academy of Sciences of the United States of America, 1968. **61**(2): p. 768-74.
278. Capecchi, M.R., *Polypeptide chain termination in vitro: isolation of a release factor.* Proceedings of the National Academy of Sciences of the United States of America, 1967. **58**(3): p. 1144-51.
279. Freistroffer, D.V., et al., *Release factor RF3 in E.coli accelerates the dissociation of release factors RF1 and RF2 from the ribosome in a GTP-dependent manner.* The EMBO journal, 1997. **16**(13): p. 4126-33.
280. Grentzmann, G., et al., *Function of polypeptide chain release factor RF-3 in Escherichia coli. RF-3 action in termination is predominantly at UGA-containing stop signals.* The Journal of biological chemistry, 1995. **270**(18): p. 10595-600.
281. Pavlov, M.Y., et al., *Release factor RF3 abolishes competition between release factor RF1 and ribosome recycling factor (RRF) for a ribosome binding site.* Journal of molecular biology, 1997. **273**(2): p. 389-401.

282. Holst-Hansen, P., et al., *Immunochemical determination of the cellular content of polypeptide chain release factor RF3 in Escherichia coli.* Biochimie, 1997. **79**(12): p. 725-9.
283. Adamski, F.M., et al., *The concentration of polypeptide chain release factors 1 and 2 at different growth rates of Escherichia coli.* J Mol Biol, 1994. **238**(3): p. 302-8.
284. Zhou, J., et al., *Crystal structure of release factor RF3 trapped in the GTP state on a rotated conformation of the ribosome.* Rna, 2012. **18**(2): p. 230-40.
285. Klaholz, B.P., A.G. Myasnikov, and M. Van Heel, *Visualization of release factor 3 on the ribosome during termination of protein synthesis.* Nature, 2004. **427**(6977): p. 862-5.
286. Gao, H., et al., *RF3 induces ribosomal conformational changes responsible for dissociation of class I release factors.* Cell, 2007. **129**(5): p. 929-41.
287. Phadtare, S. and M. Inouye, *Genome-wide transcriptional analysis of the cold shock response in wild-type and cold-sensitive, quadruple-csp-deletion strains of Escherichia coli.* J Bacteriol, 2004. **186**(20): p. 7007-14.
288. Han, Y., et al., *DNA microarray analysis of the heat- and cold-shock stimulons in Yersinia pestis.* Microbes Infect, 2005. **7**(3): p. 335-48.
289. Ko, R., L.T. Smith, and G.M. Smith, *Glycine betaine confers enhanced osmotolerance and cryotolerance on Listeria monocytogenes.* J Bacteriol, 1994. **176**(2): p. 426-31.
290. Minakami, H. and I. Fridovich, *Alcohols protect Escherichia coli against cold shock.* Proc Soc Exp Biol Med, 1991. **197**(2): p. 168-74.
291. Asai, Y. and S. Watanabe, *The interaction of ubiquinone-3 with phospholipid membranes.* FEBS Lett, 1999. **446**(1): p. 169-72.
292. Carty, S.M., K.R. Sreekumar, and C.R. Raetz, *Effect of cold shock on lipid A biosynthesis in Escherichia coli. Induction At 12 degrees C of an acyltransferase specific for palmitoleoyl-acyl carrier protein.* J Biol Chem, 1999. **274**(14): p. 9677-85.
293. Vorachek-Warren, M.K., et al., *An Escherichia coli mutant lacking the cold shock-induced palmitoleoyltransferase of lipid A biosynthesis: absence of unsaturated acyl chains and antibiotic hypersensitivity at 12 degrees C.* J Biol Chem, 2002. **277**(16): p. 14186-93.
294. Brook, I., *Anaerobic infections : diagnosis and management*2007, New York ; London: Informa Healthcare. x, 417 p.14.
295. Bowler, P.G., B.I. Duerden, and D.G. Armstrong, *Wound microbiology and associated approaches to wound management.* Clinical microbiology reviews, 2001. **14**(2): p. 244-69.
296. Brook, I., *Recovery of anaerobic bacteria from clinical specimens in 12 years at two military hospitals.* Journal of clinical microbiology, 1988. **26**(6): p. 1181-8.
297. Brook, I., *Anaerobic infections : diagnosis and management*2007, New York ; London: Informa Healthcare. x, 417 p.43.

298. Brook, I., *Enhancement of growth of aerobic and facultative bacteria in mixed infections with Bacteroides species.* Infection and immunity, 1985. **50**(3): p. 929-31.
299. Brook, I., *Enhancement of growth of aerobic, anaerobic, and facultative bacteria in mixed infections with anaerobic and facultative gram-positive cocci.* The Journal of surgical research, 1988. **45**(2): p. 222-7.
300. Brook, I., *Anaerobic infections : diagnosis and management*2007, New York ; London: Informa Healthcare. x, 417 p.45.
301. Brook, I., J.C. Coolbaugh, and R.I. Walker, *Antibiotic and clavulanic acid treatment of subcutaneous abscesses caused by Bacteroides fragilis alone or in combination with aerobic bacteria.* The Journal of infectious diseases, 1983. **148**(1): p. 156-9.
302. Onderdonk, A.B., et al., *Activity of metronidazole against Escherichia coli in experimental intra-abdominal sepsis.* The Journal of antimicrobial chemotherapy, 1979. **5**(2): p. 201-10.
303. Bartlett, J.G., et al., *Therapeutic efficacy of 29 antimicrobial regimens in experimental intraabdominal sepsis.* Reviews of infectious diseases, 1981. **3**(3): p. 535-42.
304. Jain, C., *The E. coli RhlE RNA helicase regulates the function of related RNA helicases during ribosome assembly.* Rna, 2008. **14**(2): p. 381-9.
305. Butland, G., et al., *eSGA: E. coli synthetic genetic array analysis.* Nature methods, 2008. **5**(9): p. 789-95.
306. Galperin, M.Y. and E.V. Koonin, *From complete genome sequence to 'complete' understanding?* Trends in biotechnology, 2010. **28**(8): p. 398-406.
307. Koonin, E.V. and Y.I. Wolf, *Genomics of bacteria and archaea: the emerging dynamic view of the prokaryotic world.* Nucleic acids research, 2008. **36**(21): p. 6688-719.
308. Peil, L., K. Virumae, and J. Remme, *Ribosome assembly in Escherichia coli strains lacking the RNA helicase DeaD/CsdA or DbpA.* FEBS J, 2008. **275**(15): p. 3772-82.
309. Ohmori, H., *Structural analysis of the rhlE gene of Escherichia coli.* Idengaku zasshi, 1994. **69**(1): p. 1-12.
310. Himeno, H., et al., *A novel GTPase activated by the small subunit of ribosome.* Nucleic acids research, 2004. **32**(17): p. 5303-9.
311. Takiff, H.E., et al., *Locating essential Escherichia coli genes by using mini-Tn10 transposons: the pdxJ operon.* Journal of bacteriology, 1992. **174**(5): p. 1544-53.
312. Conrad, J., et al., *16S ribosomal RNA pseudouridine synthase RsuA of Escherichia coli: deletion, mutation of the conserved Asp102 residue, and sequence comparison among all other pseudouridine synthases.* Rna, 1999. **5**(6): p. 751-63.

313. Okamoto, S., et al., *Loss of a conserved 7-methylguanosine modification in 16S rRNA confers low-level streptomycin resistance in bacteria.* Mol Microbiol, 2007. **63**(4): p. 1096-106.
314. Lesnyak, D.V., et al., *Methyltransferase that modifies guanine 966 of the 16 S rRNA: functional identification and tertiary structure.* J Biol Chem, 2007. **282**(8): p. 5880-7.
315. Gu, X.R., et al., *Identification of the 16S rRNA m5C967 methyltransferase from Escherichia coli.* Biochemistry, 1999. **38**(13): p. 4053-7.
316. Andersen, N.M. and S. Douthwaite, *YebU is a m5C methyltransferase specific for 16 S rRNA nucleotide 1407.* J Mol Biol, 2006. **359**(3): p. 777-86.
317. Basturea, G.N., K.E. Rudd, and M.P. Deutscher, *Identification and characterization of RsmE, the founding member of a new RNA base methyltransferase family.* Rna, 2006. **12**(3): p. 426-34.
318. Gustafsson, C. and B.C. Persson, *Identification of the rrmA gene encoding the 23S rRNA m1G745 methyltransferase in Escherichia coli and characterization of an m1G745-deficient mutant.* J Bacteriol, 1998. **180**(2): p. 359-65.
319. Raychaudhuri, S., et al., *Functional effect of deletion and mutation of the Escherichia coli ribosomal RNA and tRNA pseudouridine synthase RluA.* J Biol Chem, 1999. **274**(27): p. 18880-6.
320. Sergiev, P.V., et al., *Identification of Escherichia coli m2G methyltransferases: II. The ygjO gene encodes a methyltransferase specific for G1835 of the 23 S rRNA.* J Mol Biol, 2006. **364**(1): p. 26-31.
321. Persaud, C., et al., *Mutagenesis of the modified bases, m(5)U1939 and psi2504, in Escherichia coli 23S rRNA.* Biochem Biophys Res Commun, 2010. **392**(2): p. 223-7.
322. Lovgren, J.M. and P.M. Wikstrom, *The rlmB gene is essential for formation of Gm2251 in 23S rRNA but not for ribosome maturation in Escherichia coli.* J Bacteriol, 2001. **183**(23): p. 6957-60.
323. Lesnyak, D.V., et al., *Identification of Escherichia coli m2G methyltransferases: I. the ycbY gene encodes a methyltransferase specific for G2445 of the 23 S rRNA.* J Mol Biol, 2006. **364**(1): p. 20-5.
324. Purta, E., et al., *YgdE is the 2'-O-ribose methyltransferase RlmM specific for nucleotide C2498 in bacterial 23S rRNA.* Molecular microbiology, 2009. **72**(5): p. 1147-58.
325. Toh, S.M., et al., *The methyltransferase YfgB/RlmN is responsible for modification of adenosine 2503 in 23S rRNA.* Rna, 2008. **14**(1): p. 98-106.

7 APPENDICES

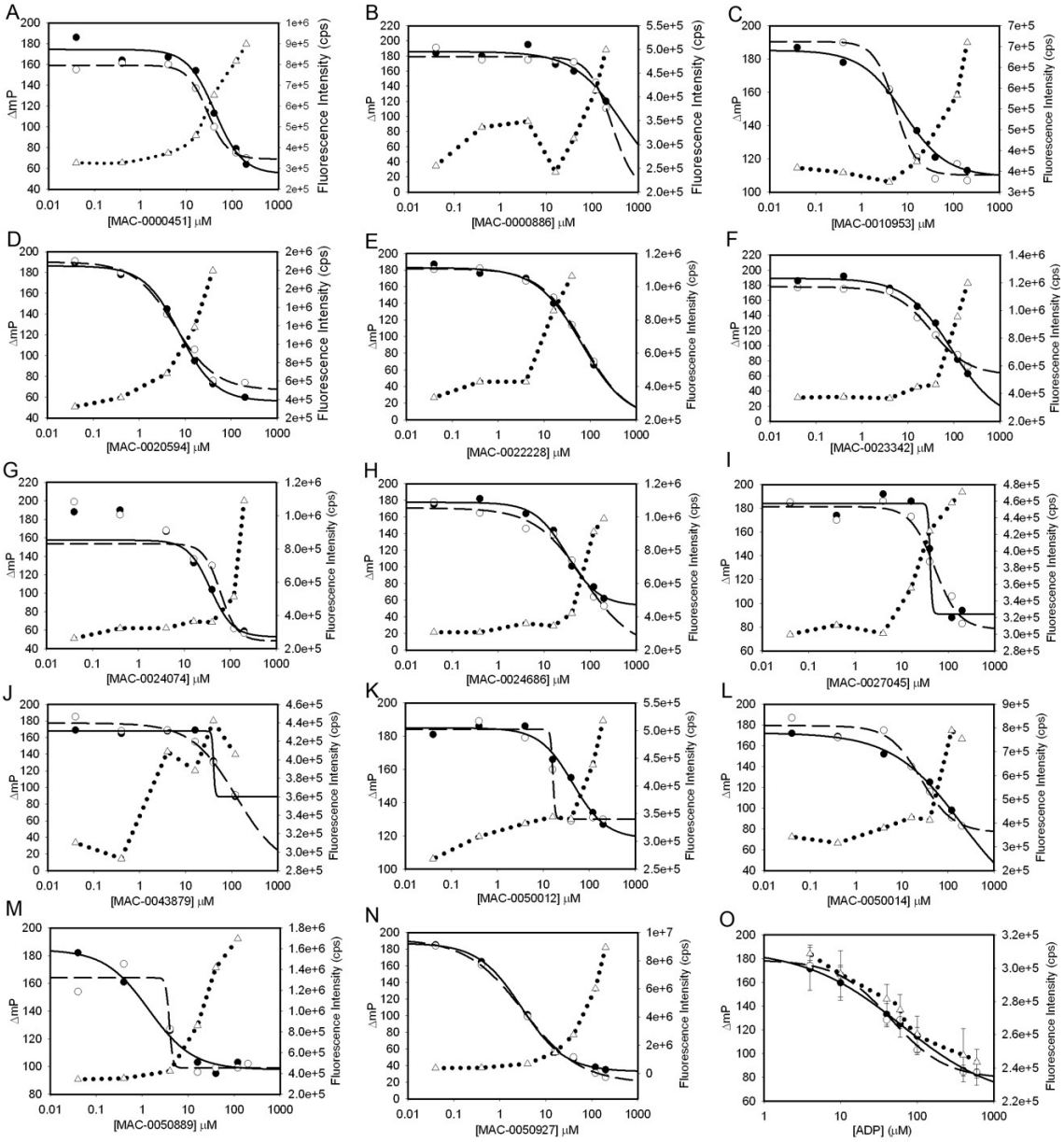

Figure A-1 for Chapter 2. Fluorescence polarization dose-response curves of the 14 DTT-resistant and mass-confirmed compounds.

Assays were performed in the presence (closed circles, solid line) and absence (open circles, long dashed line) of DTT. (A-N) Compound data and (O) ADP. Data were collected and processed as in Figure 2-7. ADP and compound data is the average of triplicates and duplicates respectively, errors bars represent one standard deviation. Fluorescence intensity (triangles, short dashed line) is presented on the second axis.

Table A-1 for Chapter 4. Trans-acting ribosome biogenesis factors in *E. coli.*

Blattner number	Gene	Function / Target	Growth phenotype	Reference
RNA helicases				
B3162	*deaD*	50S	Non-essential	[255]
B1343	*dbpA*	50S	Non-essential	[308]
B2576	*srmB*	50S	Non-essential	[256]
B0797	*rhlE*	50S	Non-essential	[309]
Chaperones				
B0014	*dnaK*		Non-essential	[218]
B4142/3	*groEL*		Non-essential	[218]
Small Subunit Factors				
B4161	*rsgA*	30S	Non-essential	[310]
B3871	*bipA*	30S	Non-essential	[258]
B3167	*rbfA*	30S	Non-essential	[242]
B3170	*rimP*	30S	Non-essential	[259]
B2608	*rimM*	30S	Non-essential	[153]
B3602	*yibL*	30S	Non-essential	[146]
B2566	*era*	30S	Essential	[311]
Large Subunit Factors				
B3180	*yhbY*		Non-essential	[146]
B2511	*der / engA*		Essential	[156]
B3183	*obgE / cgtA*		Essential	[160]
B3866	*yihI*		Non-essential	[31]
B3865	*yihA*		Essential	[160]
16S rRNA modifications				
B2183	*rsuA*	Ψ516	Non-essential	[312]
B3740	*rsmG / gidB*	m^7G527	Non-essential	[313]
B3465	*rsmD*	m^2G966	Non-essential	[314]
B3289	*rsmB*	m^5C967	Non-essential	[315]
B4371	*rsmC*	m^2G1207	Non-essential	[218]
B0082	*rsmH*	m^4C1402	Non-essential	[252]
	*rsmI**	Cm1402	Non-essential	[252]
B1835	rsmF	m^5C1407	Non-essential	[316]
B2946	*rsmE*	m^3U1498	Non-essential	[317]
	unknown	m^2G1516		
B0051	*ksgA*	$m^6{}_2$A1518/$m^6{}_2$A1519	Non-essential	[171]
23S rRNA modifications				
B1822	*rrmA*	m^1G745	Non-essential	[318]
B0058	*rluA*	Ψ746	Non-essential	[319]
B0859	*rlmC*	m^5U747	Non-essential	[218]

B1086	*rluC*	Ψ955/Ψ2504/Ψ2580	Non-essential	[146]
B0807	*rlmF / ybiN*	m^6A1618	Non-essential	[253]
B3084	*rlmG*	m^2G1835	Non-essential	[320]
B2594	*rluD*	Ψ1911/Ψ1915/Ψ1917	Non-essential	[218]
B2785	*rlmD / rumA*	m^5U1939	Non-essential	[321]
	unknown	m^5C1962		
	unknown	m^6A2030		
	unknown	m^7G2069		
B4180	*rlmB*	Gm2251	Non-essential	[322]
B1427	*rlmL*	m^2G2445	Non-essential	[323]
B1135	*rluE*	Ψ2457	Non-essential	[251]
B3179	*rlmE/rrmJ*	Um2552	Non-Essential	[179]
B2806	*rlmM*	Cm2498	Non-essential	[324]
B2517	*rlmN*	m^3A2503	Non-essential	[325]
B4022	*rluF*	Ψ2604	Non-essential	[251]
B1269	*rluB*	Ψ2685	Non-essential	[146, 251]
R-protein modification				
B1066	*rimJ*	S5 acetylation	Non-essential	[182]
B0852	*rimK*	S6 glutamination	Non-essential	[31]
	unknown	S11 methylation		
B0835	*rimO*	S12 methylthiolation	Non-essential	[186]
B4373	*rimI*	S18 acetylation	Non-essential	[31]
B2330	*prmB*	L3 methylation	Non-essential	[183]
	rimL	L7/L12 acetylation	Non-essential	[146]
B3259	prmA	L11 methylation	Non-essential	[184]
	unknown	L16 methylation		
	unknown	L33 methylation		

Table A-2 for Chapter 4. Top 3.5% of cold-sensitive strains identified in the primary screen.

Category	Blattner number	Gene	33 h growth sensitivity	Function
Information Storage and Processing				
Translation, Ribosome structure and biogenesis				
	B3170	*rimP*	1.72	30S biogenesis factor
	B0082	*mraW*	1.78	16S rRNA methyltransferase
	B0859	*rlmC*	1.81	23S methyltransferase
	B2185	*rplY*	1.81	Ribosomal protein L25
	B3180	*yhbY*	1.81	50S binding protein
	B3165	*rpsO*	1.88	Ribosomal protein S15
	B4375	*prfC*	2.26	Peptide chain release factor
	B3065	*rpsU*	2.42	Ribosomal Protein S21
	B1133	*trmU*	2.95	tRNA modification
	B2594	*rluD*	4.10	23S pseudouridine synthase
	B3470	*sirA*	4.31	tRNA modification
	B4161	*rsgA*	5.38	30S biogensis factor
	B3345	*tusD*	7.16	tRNA modification
	B3871	*bipA*	7.85	30S biogenesis factor
	B4129	*lysU*	7.86	lysyl-tRNA synthase
	B0051	*ksgA*	8.46	16S rRNA methyltransferase
	B3984	*rplA*	9.75	Ribosomal protein L1
	B3164	*pnp*	9.75	mRNA degradation factor
	B3167	*rbfA*	12.28	30S binding protein
	B3344	*tusC*	12.88	tRNA modification
	B2608	*rimM*	14.16	Ribosome maturation protein
	B3343	*tusB*	16.42	tRNA modification
	B0852	*rimK*	21.37	S6 protein modification
Transcription				
	B1508	*hipB*	1.72	Transcriptional regulator
	B3261	*fis*	2.52	DNA-binding protein
	B0313	*betI*	2.66	Trancriptional repressor of glycine betaine biosynthesis
	B4172	*hfq*	5.21	RNA binding protein
	B0564	*appY*	5.75	Acid phosphatase transcriptional regulator
	B3067	*rpoD*	7.69	Sigma70
	B3743	*asnC*	9.72	Asparagine dependent transcriptional regulator
	B3190	*yrbA*	10.24	Predicted DNA binding protein

DNA replication, recombination and repair

B2496	*had*	1.71	Regulator of DnaA
B0454	*atl*	1.72	DNA base flipping
B3778	*rep*	1.75	DNA helicase
B2820	*recB*	1.77	DNA helicase
B2002	*yeeS*	1.77	Similar to radC helicase
B0779	*uvrB*	1.86	DNA nucleotide excision repair
B0215	*dnaQ*	1.90	DNA polymerase
B2822	*recC*	1.94	DNA helicase
B0714	*nei*	2.27	DNA base excision repair
B3162	*deaD*	5.37	DEAD box RNA helicase
B2699	*recA*	6.36	SOS response regulatory protein
B0214	*rnhA*	12.19	DNA-RNA hybrid degradation

Cellular Processes

Signal Transduction

B4399	*creC*	1.76	TCS involved in sugar metabolism
B1341	*ydaM*	1.77	c-DiGMP responsive transcriptional regulator
B4398	*creB*	2.78	TCS involved in sugar metabolism
B0049	*apaH*	3.48	Diadenosine tetraphosphatase
B0145	*dksA*	4.12	RNAP-binding transcription factor
B2218	*rcsC*	4.86	TCS Involved in colanic acid biosynthesis

Cell Envelope, outmembrane biogenesis

B2742	*nlpD*	1.75	Putative outermembrane lipoprotein
B3621	*rfaC*	1.77	LPS biosynthesis
B3620	*rfaF*	1.85	LPS biosynthesis
B3035	*tolC*	1.87	Outer membrane channel
B0632	*dacA*	1.98	D-ala-D-ala carboxypeptidase
B0987	*gfcA*	2.05	Capsule production
B3842	*rfaH*	2.87	LPS biosynthesis
B0200	*gmhB*	2.92	LPS biosynthesis
B3052	*rfaE*	3.25	LPS biosynthesis
B0222	*lpcA*	3.32	LPS biosynthesis
B0293	*matB*	3.40	Conserved fimbrillin
B2049	*manC*	4.61	Colanic acid biosynthesis
B3201	*lptB*	5.29	LPS biosynthesis
B3506	*slp*	50.16	Starvation lipoprotein
B0741	*pal*	105.01	Peptidoglycan asscociated OMP

Cell motility and secretion

B1881	*cheZ*	1.71	Chemotaxis regulator

B1884	*cheR*	1.85	Chemotaxis methyltransferase
B1947	*fliO*	2.52	Flagellar biosynthesis
B1885	*tap*	2.76	Chemotaxis protein
B3609	*secB*	3.62	Protein secretion
Protein turnover			
B1829	*htpX*	2.15	Inner membrane heat shock protein
B2269	*elaD*	2.28	Deubiquitniase
Division & chromosome partitioning			
B2213	*mrp*	2.63	DNA damage repair regulator

Metabolism

Energy production and conversion			
B0973	*hyaB*	1.83	Hydrogenase
B0621	*dcuC*	1.86	Dicarboxylate transporter
B1241	*adhE*	1.93	Alchohol dehydrogenase
B2236	*yfaE*	1.95	Fe-S protein
B3732	*atpD*	2.08	ATP synthase
B3115	*tdcD*	2.43	Propionate kinase
B3734	*atpA*	2.57	ATP synthase
B3738	*atpB*	3.27	ATP synthase
B3736	*atpF*	4.48	ATP synthase
B3737	*atpE*	4.66	ATP synthase
B2488	*hyfH*	5.92	Hydrogenase
B0720	*gltA*	8.94	Citrate synthase
B2463	*maeB*	30.36	Malate dehydrogenase
B0306	*ykgE*	50.53	Predicted oxidoreductase
Carbohydrade and metabolism			
B4239	*treC*	1.95	Trehalose-6P hydrolase
B1613	*manA*	2.20	Mannose-6P isomerase
B2739	*ygbM*	2.38	Glyoxylate induced protein
B1280	*yciM*	2.44	Predicted N-acetylglucosaminyl transferase
B2416	*ptsI*	2.51	PTS enzyme I
B2901	*bglA*	2.90	6P-phosphoglucosidase
B2388	*glk*	6.65	Glucokinase
B3176	*mrsA*	9.01	Glucosamine mutase
B2465	*tktB*	9.02	Transketolase II
Amino acid transport and metabolism			
B2530	*iscS*	1.72	Cysteine desulfurase
B1293	*sapB*	1.73	Peptide transporter
B1453	*ansP*	1.78	Asparagine biosynthesis

B2578	*yfiK*	1.86	Integral protein
B2937	*speB*	1.88	Polyamine biosynthesis
B3390	*aroK*	2.48	Amino acid biosynthesis
B2678	*proW*	2.60	Glycine betaine transporter
B1260	*trpA*	2.78	Tryptophan biosynthesis
B1440	*ydcS*	3.23	Periplasmic protein
B1291	*sapD*	3.49	Peptide transporter
B3591	*selA*	9.19	selenocysteine synthase
Co-enzyme metabolism			
B0662	*ubiF*	1.73	Ubiquinone biosynthesis
B3997	*hemE*	1.90	Porphyrin biosynthesis
B0009	*mog*	1.94	Predicted Molybdochelatase
B0613	*citG*	2.03	Predicted feroxin like protein (Fe-S)
B2311	*ubiX*	2.34	Ubiquinone biosynthesis
B3177	*folP*	2.55	Dihydropteroate synthase
B2232	*ubiG*	2.83	Ubiquinone biosynthesis
B1638	*pdxH*	3.14	Pyridoxine biosynthesis
B3833	*ubiE*	3.81	Ubiquinone biosynthesis
B2907	*ubiH*	3.83	Ubiquinone biosynthesis
B3058	*folB*	5.59	THF biosynthesis
B0628	*lipA*	6.84	Lipoate synthase
Nucleotide Transport and Metabolism			
B2065	*dcd*	2.26	dCTP deaminase
B2508	*guaB*	2.82	GMP biosynthesis
B4177	*purA*	2.88	AMP biosynthesis
B2507	*guaA*	6.99	GMP biosynthesis
B0910	*cmk*	10.78	Cytidylate kinase
Inorganic ion transport			
B0585	*fes*	1.71	Enterochelin esterase
B2764	*cysJ*	1.77	Sulfite reductase flavoprotein
B1757	*ynjE*	2.30	Predicted thiosulphate sulphur transferase
B1102	*fhuE*	2.55	Outer membrane receptor for iron uptake
B3290	*trkA*	4.02	K+ transporter
Lipid metabolism			
B3193	*mlaD*	1.77	Phospholipid transporter
B0418	*pgpA*	7.88	Phosphatidylglycerophosphatase
Unknown or uncharacterized			
B2991	*hybF*	1.71	Putative hydrogenase maturation factor
B0965	*yccU*	1.78	Predicted CoA binding protein

B1154	*ycfK*	1.84	Predicted prophage protein
B1234	*ychK*	1.85	Contains lysophospholipase domain
B1668	*ydhS*	1.94	Conserved protein with NAD/FAD binding site
B2117	*molR*	1.95	Molybdate regulator split protein
B2732	*ygbA*	2.00	Predicted protein upregulated by nitrosative stress
B3233	*yhcB*	2.02	Inner membrane protein
B1582	*ynfA*	2.10	Inner membrane protein
B2956	*yggM*	2.19	Predicted protein
B2898	*ygfZ*	2.25	Folate binding protein
B2003	*yeeT*	2.37	Predicted prophage protein
B1128	*ycfD*	2.37	Conserved protein with ACR, cupin superfamily
B1567	*ydfW*	2.56	Predicted prophage protein
B4050	*pspG*	2.60	Phage shock, inner membrane protein
B3085	*ygjP*	2.61	Conserved metal dependent hydrolase
B1203	*ychF*	3.27	Predicted GTP binding protein
B1132	*hflD*	3.48	Lysogenization regulator
B1065	*yceL*	3.85	MFS permease
B2604	*yfiN*	4.45	Predicted diguanylate cyclase, inner membrane protein,
B3120	*yhaB*	6.00	Conserved protein
B186	*yebV*	10.10	Conserved protein
B0631	*ybeD*	13.95	Predicted nuclease domain
B0253	*ykfA*	15.83	Prophage predicted protein
B1664	*ydhQ*	65.23	Predicted protein